Investigating a role of HER3 in anti-HER2 target therapy in breast cancer

Kenji Hashimoto

St. John's College

University of Oxford

A thesis submitted for the degree of

Doctor of Philosophy

Trinity 2014

ABSTRACT

Thesis title:	Investigating a role of HER3 in anti-HER2 target therapy in breast cancer
Author:	Kenji Hashimoto
College:	St. John's College
Submission for degree:	Doctor of Philosophy in Medical Oncology
Term of Submission:	Trinity 2014

Background

HER2-positive breast cancer is a poor prognostic subgroup, even if treated with anti-HER2 directed therapy. Trastuzumab is an important HER2-targeting antibody but only limited patients respond to this drug, and acquired resistance is a common problem. HER3 has been shown to be a key candidate in mediating resistance to trastuzumab and other ErbB inhibitors. The aims of the project are to investigate the resistance mechanisms and the relevant biomarkers in relation to trastuzumab treatment and resistance in HER2-positive breast cancer, in particular, HER3 subcellular localisation and HER3 phosphorylation.

Methods

Effects of trastuzumab on HER3 subcellular localisation and HER3 phosphorylation in relation to MET receptor were studied using western blots, nuclear fractionation, confocal microscopy, and immunoprecipitation in a panel of HER2-positive cell lines, including SKBr3 and BT474 breast cancer cells in which trastuzumab resistance was induced by long-term drug exposure. Effects of drug and knockdown experiments were tested by cell viability and proliferation assays. HER3 and MET expression was assessed by immunohistochemistry in xenograft tumours and human tissue samples, and clinical impact was assessed in different cohorts of HER2-positive breast cancer patients.

Results

Acquired trastuzumab resistant SKBr3 cells showed an increase of nuclear $HER3_{100kD}$, which was derived from C-terminus of HER3. Nuclear $HER3_{100kD}$ could be due to the proteolytic cleavage of HER3 since it was reduced by ADAM17 or γ-secretase inhibitor. In a panel of HER2-positive cell lines and xenograft samples, nuclear HER3 was observed only in the resistant cells. In addition, nuclear HER3 was associated with poor progression-free and overall survivals in HER2-positive breast cancer patients. It was also found that HER3

phosphorylation was maintained in acquired trastuzumab resistant cells, which was contributed by the ligand independent interaction of MET and HER3. Higher MET expression was associated with better overall survival in HER2-positive, breast cancer patients who were not treated with trastuzumab.

Conclusions

Nuclear HER3 was found in trastuzumab resistant cells and appeared to result from HER3 proteolytic cleavage mediated by ADAM17 and γ-secretase. Further studies are required to investigate its mechanism and to identify the HER3 cleavage sites. MET was a key factor in maintaining HER3 phosphorylation during trastuzumab resistance. Lastly, nuclear HER3 and MET could be two potential biomarkers in HER2-positive breast cancer.

ACKNOWLEDGEMENT

First and foremost, I would like to express a great appreciation to Dr. Anthony Kong and Dr. Valentine Macaulay for supervising and supporting me throughout my DPhil. Dr. Kong has great ideas and provides creative inputs on my project. Dr. Macaulay gives me fabulous inputs both technically and theoretically, and keeps me motivated. I would like to say thank you to my laboratory members, Dr. Fenix Leung, Ms. Katahrina Feldinger, Ms. Ashwag Albukari, and Dr. Abul Azad for their technical support. I also appreciate former laboratory members including Ms. Merel Gijsen and Dr. Siti Mohd Nafi, Ms. Amalina Moomin, and past and present laboratory members in the IGF group for their kind advice. It would not be possible to complete my DPhil without them. A big thank you to Dr. Ioannis Roxanis, he is a fantastic pathologist and read more than 3000 samples with me in the last 2 years. My former clinical colleagues Dr. Fumiaki Koizumi, Dr. Mayu Yunokawa, and Ms. Yuka Kitamura should be included here since they kindly sent some cell lines to me. I also would like to say thank you to Prof. Ahmed Ahmed, and Prof. John Crown for providing us some cell lines. I express deep gratitude to Dr. Stéphanie Kermorgant and Mr. Bakouche Bakouche at the Barts

Cancer Institute for their significant insights on MET study and this fantastic collaboration. I also appreciate Dr. Neil O'Brien (UCLA), Dr. Sara Hurvitz (UCLA), Prof. Dennis Slamon (UCLA), Prof. Heikki Joensuu (University of Helsinki), Dr. Daniele Generali (Instituti Ospitalieri di Cremona), Dr. Daniele Andreis (Instituti Ospitalieri di Cremona), and all staff in the Breast Cancer Campaign for kindly providing me the patient tissue samples. A tiny project started from a small laboratory became a big project with these samples. My research goal as a translational researcher is to provide a feedback to patients, and all your supports made this possible at the end. I appreciate the GlaxoSmithKlein, UICC, and Heiwa-Nakajima Foundation for their financial supports throughout my DPhil. I must say "thanks a million" to my family, especially to my wife Dr. Akiko. She quitted her job just to come to Oxford for my DPhil and raised 3 children. I am delighted that she also started her DPhil here at Oxford University in 2013. Finally, special thanks to Umika who always makes me happy and gives me joy right after her birth. I am grateful and joyful to be with 2 more treasures who were born in Oxford, Kai and Keito. They give a bit of spice to my life. My life is shimmering with them and I am content to have my permanent fellows.

TABLE OF CONTENTS

LIST OF FIGURES

Chapter 1

Chapter 3

LIST OF TABLES

ABBREVIATIONS

ADAM	A Disintegrin And Metalloprotease
ADCC	Antibody-Dependent Cellular Cytotoxicity
AKT	Protein kinase-B (PKB)
APH-1	Anterior Pharynx-Defective 1
APP	Amyloid Precursor Protein
ATP	Adenosine triphosphate
BSA	Bovine Serum Albumin
BTC	Betacellulin
cDNA	Complementary DNA
CDK2	Cyclin-Dependent Kinase 2
CI	Confidence Interval
CISH	Chromogenic *In Situ* Hybridization
CK5/6	Cytokeratin 5/6
COX2	Cyclooxygenase-2
Ct	Threshold Cycle value
CXCL16	Chemokine (C-X-C motif) ligand 16
DAPI	4',6-diamidino-2-phenylindole
DMSO	Dimethyl Sulfoxide
DNA	Deoxyribonucleic acid
ECL	Enhanced ChemiLuminescence
EDTA	EthyleneDiamineTetraacetic Acid
EGF	Epidermal Growth Factor
EGFR	Epidermal Growth Factor Receptor
EMT	Epithelial-Mesenchymal Transition
EpCAM	Epithelial Cell Adhesion Molecule
ER	Oestrogen Receptor
FBS	Fetal Bovine Serum
FDA	US Food and Drug Administration
FFPE	Formalin-Fixed Paraffin-Embedded
FISH	Fluorescence *In Situ* Hybridization
FOXo	Forkhead Box o
Gab1	GRB2-associated binding protein 1

Grb2	Growth Factor Receptor Bound 2
HER1	Human Epidermal Growth Factor Receptor-1 (EGFR)
HER2	Human Epidermal Growth Factor Receptor-2 (ErbB2)
HER3	Human Epidermal Growth Factor Receptor-3
HER4	Human Epidermal Growth Factor Receptor-4
HGF	Hepatocyte Growth Factor
HMGB	High-Mobility Group Box
HR	Hazard Ratio
HRG	Heregulin (neuregulin 1)
HRP	Horseradish Peroxidas
HSP	Heat Shock Protein
IC50	Half maximal (50%) Inhibitory Concentration
ICAM	Intercellular Adhesion Molecule
IgG	Immunogloblin G
IGF	Insulin-like Growth Factor
IGF1R	Insulin-like Growth Factor Receptor 1
IHC	Immunohistochemistory
IL6	Interleukin 6
IRS	Immunoreactive Scoring Sysem
JMa/JMb	Juxtamembrane a/b
LDL	Low Density Lipoprotein
LDS	Lithium Dodecyl Sulfate
LR	Lapatinib Resistant
MAPK	Mitogen-Activated Protein Kinase
mRNA	Messenger RNA
NLS	Nuclear Localisation Sequence
NRG	Neuregulin
Opti-MEM	Opti-Minimal Essential Medium
PBS	Phosphate Buffered Saline
PCR	Polymerase Chain Reaction
PEN2	Presenilin Enhancer 2
PFA	Paraformaldehyde
PgR	Progesterone Receptor

PI3K	Phosphatidylinositol-3 Kinase
PTEN	Phosphatase and Tensin Homolog Deleted from Chromosome 10
PVDF	PolyVinylidene DiFluoride
qRT-PCR	Quantitative Real Time PCR
SEM	Standard Erroe Mean
RAS	Rat sarcoma
RET	REarranged during Transfection
RNA	RiboNucleic Acid
SEM	Standard Error of the Mean
Shc	Src homology 2 domain containing
SH2	Src Homology 2
SOS	Son of Sevenless
STAT	Signal Transducer and Activator of Transcription
TGFα	Transforming Growth Factor-α
TNF	Tumour Necrosis Factor
TNBC	Triple Negative Breast Cancer
TR	Trastuzumab Resistant
Tris	Tris (hydroxymethyl) aminomethane
VCAM	Vascular Cell Adhesion Molecule
VEGF	Vascular Endothelial Growth Factor
VLDL	Very Low Density Lipoprotein
ºC	Celcius
Δ	Delta

CHAPTER 1. INTRODUCTION

1.1 Breast cancer

Breast cancer is one of the leading causes of cancer death in women in the US[1]. In the UK, breast cancer is the most common cancer. About 50,000 patients were diagnosed with invasive breast cancer and about 12,000 patients died from invasive breast cancer in 2011 (http://www.cancerresearchuk.org/cancer-info/cancerstats/types/breast/). Due to the improvement of mass screening and treatment, the 5-year survival rate of breast cancer is approximately 85%[2]. Breast cancer is a histopathological diagnosis and is subdivided by tumour morphology into different subtypes such as ductal carcinoma, lobular carcinoma, mucinous carcinoma, and some others[3]. Moreover, tumour grade, tumour size, lymph node and other organ metastases, oestrogen receptor (ER) and progesterone receptor (PgR) expression, human epidermal growth factor receptor-2 (HER2, ErbB2, HER2/neu), and patient age are considered in decision making to plan treatment[4]. Although breast cancer is a heterogeneous disease, some distinctive phenotypic variants are identified due to the recent advance of molecular biology. By using microarray technique, breast cancer is divided into 5 intrinsic subtypes including basal-like, HER2, normal-breast-like, and luminal/epithelial type A and

B[5]. Subsequently, these molecular subtypes have been identified as having prognostic significance[6]. Basal-like and HER2 subtype are identified as poor prognostic subgroups. Although basal-like and triple-negative breast cancer (TNBC: ER-, PgR- and HER2-) have been used interchangeably, not all TNBC are basal-like; and there are also basal-like breast cancers that are not TNBC, which highlights the heterogeneity problem in TNBC[7,8]. In clinical practice, basal-like tumours can be defined using immunohistochemistry (IHC) staining for basal cell markers, e.g. CK5/6 positive and/or EGFR positive[7,8]. Breast cancers with HER2 molecular subtype usually correlate with the HER2 positivity as determined by IHC or FISH (fluorescence *in situ* hybridisation)/CISH(chromogenic *in situ* hybridisation)[5,6], but there are discrepancies and some of these cancers have been found to be TNBC[9].

HER2-positive breast cancer consists of 15-20% of all breast cancer, which is defined as HER2 expression 3+ by IHC or 2+ by IHC and HER2 amplification by FISH[10]. The current FDA approved HER2-directed therapies include trastuzumab (anti-HER2 monoclonal antibody, Herceptin®), lapatinib [epidermal growth factor receptor (HER1 or EGFR) and HER2 dual tyrosine kinase inhibitor,

Tykerb® or Tyverb®], pertuzumab (anti-HER2 dimerisation arm monoclonal antibody, Perjeta®), and T-DM1 (trastuzumab emtansine, Kadcyla®)[11]. The median overall survival for metastatic HER2-positive breast cancer patients has been estimated to be 25-40 months[12,13], and approximately 50% of patients on HER2-directed therapy experience relapse within a year[12,13]. Overcoming resistance of anti-HER2 directed therapy is warranted.

1.2 Trastuzumab

Trastuzumab is a humanised anti-HER2 monoclonal antibody, which binds to domain IV of HER2[14]. Trastuzumab has been in clinical use since 1998. It is well known that only 10-30 % of HER2-positive patients respond to trastuzumab monotherapy, and trastuzumab and chemotherapy combination treatment yields about 50-60 % of response[15-21]. However, the majority of responding patients in the metastatic setting become resistant to trastuzumab within a year[12,17,19]. The mechanism of action by which trastuzumab acts as an anti-tumour agent is not fully understood. The proposed action is that trastuzumab induces Antibody-Dependent Cellular Cytotoxicity (ADCC)[22], inhibits phosphatidyl inositol 3-

kinase/protein kinase-B (PI3K/AKT) signalling[23], induces cell cycle arrest through p27 restoration and CDK2 suppression[23,24], disrupts HER2-HER3 interaction[25], or induces PTEN expression to inhibit AKT signalling[26].

The proposed trastuzumab resistance mechanisms include PI3K pathway activation by mutation or PTEN loss[27], SRC activation[28], Insulin-like growth factor-1 receptor (IGF1R) activation [29], MET receptor activation[30], HER2 extracellular domain shedding to maintain HER2 kinase activation[31]. Previous work from our group suggested that HER ligand shedding by a disintegrin and metalloproteinase (ADAM) 10 and ADAM17 proteases contributes to activate other HER family receptors and leads to trastuzumab resistance[32,33]. Despite these findings, there is no available biomarker in clinical practice to predict trastuzumab response.

1.3 The HER family and ligands

Human epidermal growth factor receptor (ErbB/HER) family comprises four closely related class I transmembrane tyrosine kinase receptors: EGFR/Erb1, HER2/ErbB2, HER3/ErbB3 and HER4/ErbB4[34,35]. All the members of the ErbB

receptor family have a ligand binding extracellular domain, single transmembrane domain, and intracellular domain which has protein tyrosine kinase domain. The extracellular domain of the HER family consists of four domains, domain I, II, III, and IV. Domain II is the dimerisation arm and it is tethered between domain II and domain IV. It can be exposed for dimerisation on ligand stimulation since ligand can bridge domain I and III[14,34-36] (Figure 1.1). Normally, ErbB receptors exist as a monomer to inactivate their tyrosine kinase domain[37]. Upon ligand stimulation, conformational change is initiated to form a stabilised structure to expose the dimerisation arm, which results in homo or hetero dimerisation[34,35] (Figure 1.1).

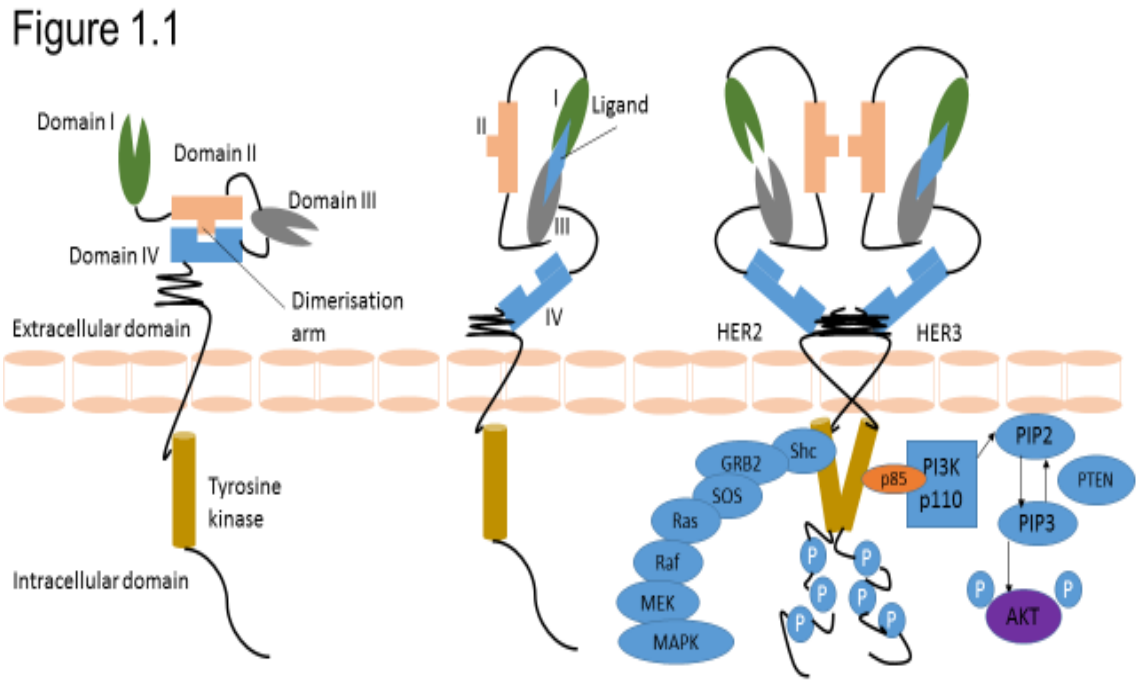

Figure 1.1 Schematic diagram of human epidermal growth factor receptor (HER) conformation change and dimerisation by ligand stimulation (Modified from: Baselga J *et al*., Nat Rev Cancer 2009; 9: 463-475, modified).

HER2 has no known ligand probably because its dimerisation arm is exposed without ligand binding, rendering HER2 constitutively activated[37]. EGFR is regulated by at least 7 known ligands including EGF, transforming growth factor-α, and betacellulin[38]. HER3 and HER4 share 4 neuregulins[37,38]. Heregulin (HRG) is an isoform of splicing variant of neuregulin 1, and is known to promote HER2-HER3 dimerisation[25,39,40]. Dimerisation is essential for phosphorylation of carboxyl-terminus tyrosine residues of ErbB receptors, which results in signal diversification of their downstream pathways, leading to cell proliferation, migration, and differentiation. For example, HER3 is phosphorylated by heterodimerising with HER2, and phosphorylated HER3 is recognised by Src homology 2 (SH2) domain of PI3K subunit p85. As a result, phosphatidylinositol (4,5)-bisphosphate (PIP2) is phosphorylated and is converted to Phosphatidylinositol (3,4,5)-trisphosphate (PIP3) (Figure 1.1). HER2 is able to recruit growth factor receptor bound 2 (GRB2) through Src homology 2 domain containing (Shc). As a result, GRB2 recruits Son of Sevenless (SOS) followed by the activation of Rat sarcoma protein (RAS). These effects result in activations of the mitogen-activated protein kinase (MAPK) and the PI3K-AKT pathways[41-44] (Figure 1.1). A structure based study suggests that asymmetric kinase domain

dimerisation is required for EGFR activation[45]. EGFR, HER2, and HER4 contain catalytic kinase domains and can form heterodimeric pairs with each other, while HER3 has an inactivate kinase domain although it can form heterodimers with other receptors for transphosphorylation[44]. Notably, HER3 cannot homodimerise on HRG stimulation[46]. Interestingly, recent studies have shown that the ligand stimulation is not essential for forming asymmetric kinase domain dimerisation [25,47-49].

1.4 HER3 in normal tissue and cancer

It has been reported that HER3 is expressed in normal gastrointestinal tract, respiratory tract, urinary tract, reproductive, skin, and nervous systems. EGFR is mainly expressed in skin and gastrointestinal tract and HER2 expression is observed in gastrointestinal tract, respiratory, reproductive, urinary tract, skin, placenta, and breast[50-52]. One of the main functions of HER3 in normal tissue is for mammary gland development and neural crest differentiation[53,54]. HER2 and HER3 are the preferential binding partners for each other and HER3 is usually co-expressed with HER2, which results in the oncogenic activity[55,56]. Indeed,

knockdown of HER3 in HER2-positive cells results in rapid tumour regression[56]. Somatic mutations of HER3 have been reported, which render the cells to be HRG independent[57]. The PI3K/Akt pathway is driven predominantly via transphosphorylation of HER3 since HER3 is the only ErbB receptor that has Tyr-X-X-Met motif, the p85 SH2 domain recognition sequence[58-60]. HER3 has at least 6 docking sites recognised by the p85 of PI3K directly while EGFR and HER2 interact with PI3K through Grb2 or GRB2-associated binding protein 1 (Gab1)[34,35]. Thus, PI3K signalling is crucial for HER3-driven cancer cells[60].

HER3 expression is reported in several cancers including colorectal, breast, skin, bladder, cervix, ovarian, laryngeal, oesophageal, gastric, lung, pancreatic, head and neck cancer, and melanoma[61-76]. The meta-analysis covering all cancer types identified that HER3 expression is associated with poor prognosis[77]. However, some studies suggest that HER3 expression in regards to the prognosis is controversial. In uveal melanoma, HER3 has been detected in the nucleus and nuclear HER3 is related to good overall survival, whereas cytoplasmic HER3 has not been indicated as a prognostic factor[72]. The HER2 expression status is not measured in this study. Yoon *et al (2014)* have identified that HER3 expression in cytoplasm is associated with HER2 expression and

there is a trend that HER3 expression is related to better survival[76]. In breast cancer, HER3-positivity is significantly correlated with poor progression-free survival for 125 HER2-positive patients treated with taxane and trastuzumab[78]. In triple-negative breast cancer or non-selected breast cancer subtypes, HER3 expression has been reported to be associated with poor progression-free survival and overall survival[79,80]. Moreover, HER3 gene amplification has been identified in non-selected breast cancer subtypes, which is associated with poor disease-free survival while protein expression of HER3 is not[81]. Recently, HER2-HER3 dimerisation detected by proximity ligation assay as well as EGFR-HER2 and HER2-HER4 dimerisation have been suggested as predictors of poor progression-free survival and overall survival in breast cancer. Although HER2-HER3 dimerisation is measured in this study, it is not identified as a prognostic marker in the limited HER2-positive patient samples[82]. In most of the studies, HER3 has been found in the cytoplasm and membrane, while nuclear HER3 is not fully investigated although it can be observed clearly in several figures[66,73]. Interestingly, HER3 can be detected in the nucleus on human tissue sections by both HER3 antibodies raised against C-terminus and N-terminus, although nuclear positivity is not mentioned by authors[66,74]. Therefore, there is

considerable uncertainty around the existence of nuclear HER3, and the prognostic significance of HER3 expression.

1.5 HER3 as a key player for resistance to HER family targeting drugs

The significance of HER3 in mediating resistance to HER family targeted therapies has been reported in HER2-positive cells. HER3 expression is induced by AKT inhibition via recruiting Forkhead box O (FOXo) to the HER3 promoter, while AKT activation negatively regulates HER3 expression[83]. Similarly, HER3 expression is induced by a PI3K inhibitor and its expression is inhibited by FOXo knockdown[84]. Upregulated HER3 is phosphorylated by HER2, resulting in the maintenance of PI3K/AKT pathway[85]. HER3 feedback via FOX protein is also identified in RAF/MEK inhibitors[86-88].

Trastuzumab is an anti-HER2 monoclonal antibody but it has a minimal effect on HER2 expression and phosphorylation after extensive investigation[25,26,32]. However, trastuzumab can decrease AKT phosphorylation as well as HER3 phosphorylation probably by disrupting ligand-independent HER2-HER3 dimerisation or inducing PTEN expression[25,26]. Narayan *et al.* have reported that long-term trastuzumab treatment increased HER3 and EGFR

expression[89], while others reported that HER3 expression is similar despite a decrease of phosphorylation of HER3[25,28]. In our laboratory, trastuzumab has been reported to decrease HER3 phosphorylation. However, HER3 phosphorylation recovered when cells become resistant to trastuzumab after long exposure to trastuzumab[32]. This may be due to ligand release via proteinase activity. All these previous reports suggest that the HER3/PI3K/AKT pathway activation is involved in trastuzumab treatment, and blockade of PI3K seems to be effective in inhibiting the growth of trastuzumab resistant cell lines[90].

1.6 Crosstalk of HER3 and insulin-like growth factor receptor 1 (IGF1R) in trastuzumab treatment

Aberrant activation of other receptor tyrosine kinases has been reported in response to HER family targeted therapy[35]. Lu *et al.* have identified that forced expression of insulin-like growth factor receptor 1 (IGF1R) in SKBr3 cells renders the cells resistant to trastuzumab. Trastuzumab sensitivity is recovered by addition of IGF binding protein 3, which suppresses IGF1R signaling[29]. In this report, it is mentioned that addition of IGF, a ligand for IGF1R, may reduce sensitivity to trastuzumab in IGF1R overexpressing MCF7/HER2 cells[29]. Indeed,

Huang *et al. (2010)* suggest that enhanced HER2-IGF1R or HER3-IGF1R interaction is observed exclusively in trastuzumab resistant cells and the knockdown of HER3 or IGF1R leads to recovery of the sensitivity to trastuzumab in the resistant cells[91].

1.7 Crosstalk of HER3 and MET in trastuzumab treatment

MET is a receptor tyrosine kinase for hepatocyte growth factor (HGF) and plays a critical role for tumorigenesis in many cancers. MET is synthesized as a precursor (170kD) followed by maturation in the endoplasmic reticulum. The matured heterodimeric MET (190kD) is formed through disulfide bonds, posttranslational glycosylation, and proteolytic cleavage. MET consists of extracellular ligand binding domain α (50kD) and transmembrane domain β (145kD) which has a tyrosine kinase domain[92]. The α and β subunits are bound by disulfide bonds. MET is activated by ligand induced-dimerisation. Phosphorylation of Tyr1234/1235 leads to autophosphorylation of Tyr 1349/1356, which results in recruitment of Gab1, Grb2, and SRC[93]. MET signaling is mainly mediated by the MAPK and the PI3K/AKT pathways. Similar to the ErbB family

receptors, MET is internalised through endocytosis and degraded or recycled. Unbalanced MET recycling sustains MET signaling in cancer[94].

In tissue development, the role of MET is to mediate invasive growth[95]. During placental development, MET is required for the migration of myoblasts, liver construction, and nerve outgrowth[95]. During adult life, MET is essential for liver regeneration and wound healing in the skin[95]. Thus, aberrant MET activation in cancer allows intense cell proliferation, metastasis, and alternation of microenvironment which results in angiogenesis[96]. MET is also important during placental development since HGF-MET signaling directs mesenchymal cells to their final destination[97]. MET expression is associated with triple-negative breast cancer, which potentially has a mesenchymal signature with a poor prognosis[98,99].

MET activation is achieved mainly by 3 routes: HGF autocrine or paracrine loop, MET overexpression, and MET point mutations. HGF autocrine loop has been observed in several cancers including breast[100]. MET overexpression is frequently observed at the transcriptional level rather than gene amplification, and MET expression is induced by various oncogenes including Ras and RET[101]. Overexpression of MET can increase the sensitivity to HGF or promote interaction with other receptors, which results in reciprocal activation

without ligand stimulation[95]. MET point mutations lead to constitutive activation of MET kinase which confers invasive phenotype[102]. MET overexpression or amplification is associated with poor prognosis in several cancers including breast cancer[99,103-113].

MET is reported to be increased by trastuzumab treatment and aberrant MET expression confers trastuzumab resistance[30]. Inhibition of MET increases the sensitivity to trastuzumab[30]. MET and HER3 interaction is also reported in gefitinib (EGFR tyrosine kinase inhibitor) resistant lung cancer cells[114]. MET amplification causes gefitinib resistance by driving HER3-dependent activation of the PI3K/AKT pathway[114]. In addition, MET and HER3 co-expression in Chinese hamster ovary (CHO) cells results in HER3 phosphorylation[114]. MET tyrosine kinase inhibitor decreases the phosphorylation of HER3 as well as phosphorylation of MET although HGF, a putative ligand for MET does not increase HER3 phosphorylation[115]. MET knockdown leads to a decrease of HER3 and AKT phosphorylation[114]. While direct interaction between MET and HER3 is not reported, it is suggested that pre-existing MET amplified cells can be selected by HER family targeted therapy plus HGF stimulation. Therefore, the cells selected by HER targeted therapy and HGF stimulation show MET

overexpression. MET overexpression in these cells contributes to the protection of HER3 phosphorylation from HER family targeted therapy[116]. These results suggest that MET is important for activating the HER3/PI3K/AKT pathway[35].

1.8 The HER family and MET in the nucleus

All HER family receptors are known to exist in the nucleus[117-120]. The HER family receptor internalisation followed by nuclear localisation is mediated by endosome-mediated nuclear translocation of full-length receptors, and also by proteolytic cleavage[118,121]. EGFR[122,123], HER2[124], and HER3[125] are known to exist in the nucleus as full-length receptors. Nuclear EGFR is identified in normal basal cells with high Ki67 index, and EGF ligand stimulation induces nuclear localisation of EGFR and phosphorylated EGFR [123]. Nuclear EGFR can bind directly to the promoter region of cyclin D1, and overexpression of cyclin D1 shortens cell cycle arrest and accelerates cell proliferation[123]. Nuclear HER2 binds to the promoter region of the gene encoding cyclooxygenase enzyme COX-2. COX-2 overexpression enables cells to increase anti-apoptotic and metastatic potential[124,126]. HER4 undergoes two step proteolytic cleavage by ADAM 17 and

γ-secretase upon HRG stimulation, and the cleaved COOH terminus of HER4 translocates into the nucleus[118]. Nuclear HER4 interacts with ER and sensitises the cells to tamoxifen[127]. Nuclear HER4 is also known to be co-localised with STAT5A which activate β-casein promoter[128].

HER3 and HER4 have similar sequences and share the same ligand, HRG[38]. HER3 is known to translocate into the nucleus[119]. HER3 has several fragments below $HER3_{180kD}$, which is full-length HER3[129]. These fragments are identified by C-terminus HER3 antibody. Several HER3 truncated transcripts are identified but all encode part or all of the receptor extracellular domain except one in human; thus they are considered to be secreted and circulate in the serum or stay on the plasma membrane[130-132]. Hence, there might be a truncated nuclear HER3 protein since the majority of HER3 fragments detected by C-terminus antibody are produced by an unknown mechanism. Nuclear HER3 in Schwann cells interacts with promoter region of Ezrin and High Mobility Group Box (HMGB)[129]. Several reports suggest that HER3 has also nuclear variants[129,132], and 80kD HER3 in the nucleus is known to interact with cyclin D1[132].

Nuclear HER4 expression seems to be associated with low tumour grade and low tumour mitosis in breast cancer[133] although our laboratory has shown that nuclear HER4 is correlated with poor prognosis in HER2-positive breast cancer[134]. Nuclear EGFR expression and nuclear HER2 expression in some cancers have been reported as poor prognostic factors[135-139]. Nuclear HER3 in prostate cancer is associated with hormone-refractory status and high Gleason score[140]. Nuclear HER3 expression is shown to be affected by the microenvironment. Tumours from prostate cancer cell lines implanted into the mouse femur have nuclear HER3 expression while the same cell lines implanted in the skin show HER3 mainly in cytoplasm[141]. There is a possibility that HER3 expression in the nucleus can be an alternative pathway for cell proliferation instead of classical signaling pathways including the AKT and the MAPK pathways[141].

Trafficking of ErbB receptors from the cytoplasm to the nucleus is proposed to be through endosome-mediated nuclear translocation and retro-translocation by endoplasmic reticulum-associated trafficking machinery[121]. Indeed, the HER family receptors have nuclear localisation sequences, which are recognised by

nuclear transporter importin proteins[117-120]. It has been reported that HER3 has 3 nuclear localisation sequence (NLS)[119,132] (Figure 1.2). Retro-translocation is the process that the internalised receptors are transported to the endoplasmic reticulum membrane followed by releasing into the cytoplasm. The receptors are stabilised by HSP70 before entering into the nucleus directed by the importin proteins. Furthermore, it is reported that leptomycin B, a drug that blocks nuclear export, can concentrate nuclear expression of HER3, suggesting that HER3 can shuttle from the membrane and cytoplasm to the nucleus, then from the nucleus to the cytoplasm and membrane[125]. HRG has a functional effect on HER3. In the absence of HRG, HER3 accumulates in nucleoli, and exogenous HRG can shift HER3 from nucleoli to the nucleus then to cytoplasm in immortalised non-malignant cells[125]. HRG is known to have an NLS and is transported into the nucleus[142]. Recently, HRG is identified in the nucleus in glial cells[143]. It is possible that HER3 subcellular localisation might bypass the anti-proliferative effect of trastuzumab or other HER family targeted therapy[144].

MET is also known to exist in the nucleus although its role in the nucleus is still unclear. MET is internalised rapidly after HGF stimulation via endocytosis

mediated by dynamin and clathrin, and is localised to the nucleus through importin and Gab1[94,145,146]. In turn, MET in the nucleus initiates calcium signalling[146]. A report suggests that a 60kD fragment from C-terminus localises to the nucleus although the mechanism of the nuclear localisation is unclear[147]. Nuclear MET is often seen in the cells with mesenchymal phenotypes[147] although the clinical significance of nuclear MET expression should be clarified [145,148].

Figure 1.2

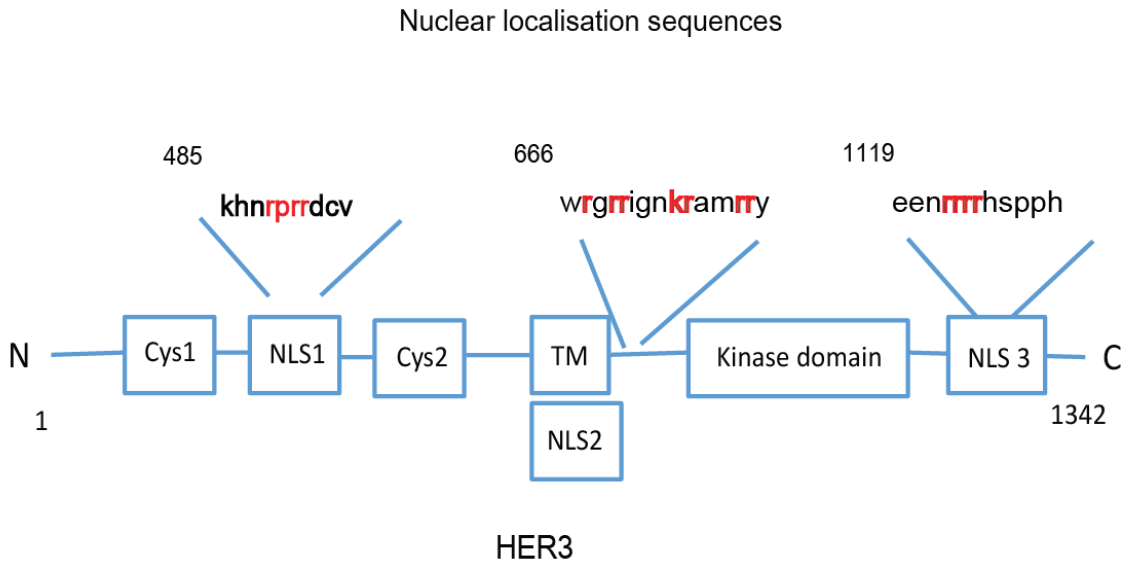

Figure1.2. Domain structure of HER3 showing nuclear localisation sequences (NLS)
Cys: cysteine rich domain, TM: transmembrane domain. NLSs are shown in red.

1.9 Ligand release and ADAM (A Disintegrin And Metalloproteinase) family

The ADAM proteins are a family of metalloproteases that shed membrane-anchored cytokines, growth factors, and receptors[149]. The ADAMs are transmembrane proteins and 21 ADAMs have been identified. Of these 21, only 13 possess proteolytic activity and other proteolytic inactive ADAMs play roles as an intracellular communicator[150,151]. Activation of ADAMs begins with the removal of pro-domain by furin-like protein followed by metalloprotease domain activation. Here, I would like to discus ADAM17, a heavily investigated isoform which is implicated in the shedding of HER4 and HER receptor ligands[118,152]. ADAM17 recognises several different sequences for cleavage and there are no similarities in the sequence near the cleavage sites, however, most cleavages occur at 10-15 amino acids from the plasma membrane[152].

More than 50 ADAM17 substrates such as HER4 and some HER family ligands including pro-HRG, pro-betacellulin, and pro-transforming growth factor-α (TGFα) have been identified[152] (Table 1.1). A soluble form of cleaved ligand is released from the membrane by the ADAMs and, thus the ADAMs regulate autocrine, juxtacrine, and paracrine signalling. Due to the wide variety of substrates that are regulated by ADAM17, its activation is associated with cancer,

inflammatory disease including rheumatoid arthritis, stroke, cardiovascular disease, renal disease, respiratory disease, metabolic disease, and Alzheimer's disease[152]. ADAM17 has been a target for cancer therapy since ADAM17 is involved in the cleavage of HER4 and growth factors[118,152]. In our laboratory, ADAM17 is found to be up-regulated after trastuzumab treatment and, thus it maintains HER family phosphorylation through ligand activation, which results in trastuzumab resistance[32].

HER4 has two different spliced isoforms, JMa and JMb, which have different sequences in juxtamembrane region[153]. Only the JMa isoform can be recognised by ADAM17, which cleaves HER4 between His651 and Ser652 although each protein cleaved by ADAM17 has a different ADAM17 recognition site[152,154]. A HER3 fragment has been reported to exist in the nucleus[129,132]. However, HER3 cleavage by any protease has not been identified, although it is possible that this could have been missed due to technical factors[129,132]. ADAM17 is an attractive target for cancer treatment. Several ADAM17 inhibitors exist, including INCB4298, a highly selective ADAM17 inhibitor used in this project[155], and these are at different stages of clinical trials[152]. A recent study suggests that

co-inhibition of ADAM17 and ADAM10 has clinical activity [156], and suggests that the selection of target patients and proper biomarker (s) are necessary.

1.10 The γ-secretase complex for ligand release and HER4 cleavage

The γ-secretase complex has important roles in ligand shedding and HER4 cleavage. The γ-secretase complex exists in the plasma membrane and is composed of presenilin, nicastrin, anterior pharynx-defective 1 (APH-1), CD147, and presenilin enhancer 2 (PEN2)[157]. The γ-secretase complex cleaves type I transmembrane proteins including HER4, β-amyloid precursor protein, CD44, and Notch in their transmembrane domains[118,158-160] (Table 1.1). Receptor internalisation is required for γ-secretase activation[161]. The γ-secretase complex activity can be higher when the length of the receptor extracellular domain is shorter[161]. It is controversial whether the γ-secretase complex recognises a specific sequence for cleavage[161,162]. Presenilin is the active site of γ-secretase and the other 3 components support catalytic activity of presenilin. Loss of PEN2 activity leads to a reduction of presenilin level[163] and presenilin endoproteolysis which produces an active form of presenilin[164], and loss of proteolytic activities[165],

while overexpression of PEN2 results in an increase of γ-secretase activity[166,167]. Since HER3 and HER4 share the same ligand and have similar sequences, there is a possibility that HER3 can be cleaved by these proteolytic enzymes and that truncated HER3 could translocate into the nucleus.

Table 1.1. Representative ADAM17 and γ-secretase substrates

ADAM17 Substrates	γ-secretase substrates
Cytokines and growth factors	
proTNF-α (tumour necrosis factor)	proNRG1 (neuregulin)
proTGF-β (transforming growth factor)	proNRG2 (neureguliin)
proBTC (betacellulin)	proBTC (betacellulin)
proNRGα-2C (neuregulin, heregulin)	Delta1
proHB-EGF (epidermal growth factor)	
Receptors	
HER4	VEGF-R1
Notch	VLDL receptor
CD30	Notch
CD40	HER4
IL6Rα (interleukin)	IL6Rα (interleukin)
LDL receptor	Insulin receptor
Adhesion molecules	
ICAM-1 (intercellular adhesion molecule)	EpCAM
VCAM-1 (vascular cell adhesion molecule)	CXCL16
CD44	CD44
Others	
APP (amyloid precursor protein)	APP (amyloid precursor protein)
MUC-1	MUC-1

Modified from: Arribas J *et al.*, Curr Pharm Des 2009; 15: 2319-35
Modified from: Haapasalo A *et al.*, J Alzheimers Dis 2011; 25: 3-28

1.11 HER3 and MET as a druggable target

There is some evidence that HER3 signalling is involved in resistance to HER family targeted therapies, and HER3 is a highly interesting target for cancer treatment[25,85,114]. HER3 downregulation in an *in vivo* model clearly suggests anti-proliferative activity[56,168]. However, due to the lack of kinase enzyme activity of HER3, it is challenging to target this protein. Thus, the strategy to target HER3 has mainly utilized various antibodies against the HER3 extracellular domain. Some HER3 antibodies (MM121, LJM716, SGP1) have been generated to bind in the ligand binding site (domain I and III) or to lock HER3 in the tethered conformation, thus theoretically preventing ligand dependent and independent HER3 signalling[168-172]. Other HER3 antibodies generated against the extracellular domain (U3-1287, AV-203) lead to downregulation of HER3 through increased endocytosis[173]. There are also several anti-HER3 antibodies in clinical trials although the mechanism of action is not documented (GSK2849330, RO5479599). AZD8931 is a unique tyrosine kinase inhibitor for EGFR and HER2 and its ability to inhibit HER3 phosphorylation is higher than gefitinib and lapatinib[174].

LJM716, which locks domains I and III of HER3, is shown to decrease the phosphorylation of HER3 and AKT. However, it seems that AKT and HER3 phosphorylation return after 24 hours of treatment[171]. In preclinical study, LJM716 and trastuzumab combination treatment can improve survival in mice[171]. Another HER3 antibody, U3-1287, reduces phosphorylation of HER3, and the combination of trastuzumab with U3-1287 has an additional effect on cell survival[173]. MM121 blocks HER3 activation upon HRG stimulation and single use of MM121 seems effective in some cell lines, however, HER2-overexpressing BT474 cells are resistant to MM121, probably because BT474 cells do not express measurable HRG[170]. Although preclinical results are promising, the clinical efficacy of these antibodies seems limited[175,176]. The reasons for this could include the selection of target patients and limited availability of biomarker (s).

MET also draws much attention as a drug target since MET is also a key regulator of the AKT/PI3K and MAPK pathways[93]. There are several approaches to inhibit MET activity through blocking HGF binding to MET, MET antibodies, and MET tyrosine kinase inhibitors[93,177]. A MET monoclonal antibody that blocks

HGF binding to MET, onartuzumab, is one of the most promising antibodies which is now in phase III trial for MET-positive lung cancer patients in combination with erlotinib (EGFR tyrosine kinase inhibitor)[178]. Since MET is known to be overexpressed and interact with HER3 in gefitinib resistant cells, the combination therapy of MET targeted drug and EGFR inhibitor has been suggested[118]. No additional benefit of onartuzumab was found in the phase II trial that compares erlotinib alone to erlotinib and onartuzumab for non-small cell lung cancer patients[179]. However, patients with positive MET expression gain survival benefit from onartuzumab treatment compared to those whose tumours are MET-negative, suggesting that MET expression can be a biomarker for this treatment[179,180]. There are also several MET monoclonal antibodies in preclinical use including AF276 which promotes internalisation of MET[177,181].

MET tyrosine kinase inhibitors are at a more advanced stage of clinical development than monoclonal antibodies. MET tyrosine kinase inhibitors are designed to compete in the ATP binding site[181]. Tivantinib, however binds to inactive, non-phosphorylated MET and keeps MET in silent mode[182]. Tivantinib is a highly selective MET kinase inhibitor, which is now under investigation in

several phase III trials and is the most advanced in drug development among all the MET inhibitors. In a randomised phase II trial, the efficacy of tivantinib and erlotinib was assessed in non-small cell lung cancer patients. Tivantinib and erlotinib combination therapy improved progression-free survival significantly (16.1 months *vs.* 9.7 months). MET gene amplification detected by FISH was assessed as a biomarker for tivantinib treatment, but no benefit for patients with MET amplified tumour was identified[183]. However, tivantinib as a second-line treatment for hepatocellular carcinoma was found to be effective in MET-overexpressing tumours[184]. These results indicate that MET overexpression may be associated with a favourable response to these MET targeting agents.

1.12 Aims of the project

This study is based on the hypothesis that HER3 plays a role in the response to anti-HER2 treatment, especially focusing on trastuzumab. There are 2 main projects and subtopics regarding this project in this thesis.

1. Assessing the clinical impact of HER3 subcellular localisation on response to trastuzumab treatment

- To investigate nuclear HER3 expression in HER2-positive breast cancer cell lines with regard to trastuzumab response
- To clarify the mechanism of nuclear HER3 translocation
- To assess the clinical impact of nuclear HER3 in HER2-positive breast cancer patients

2. Understanding the relationship of HER3 phosphorylation and MET receptor on response to trastuzumab treatment in HER2-positive breast cancer
    - To assess HER3 phosphorylation upon trastuzumab treatment
    - To assess MET expression in HER2-positive cell lines and its relation with trastuzumab response
    - To understand whether MET and HER3 interact in breast cancer cells
    - To identify the clinical significance of MET expression in breast cancer patients

CHAPTER 2. MATERIALS AND METHODS

2.1 Cell lines

The SKBr3 and BT474 cell lines were obtained from Cancer Research UK (Lincolns' Inn Fields laboratory). The MDA-MB-361 and MDA-MB-453 cell lines were purchased from ATCC. The HCC1954, HCC1569, and UACC732 cell lines were provided by Prof. John Crown's group (St. Vincent's University Hospital, Dublin). The NCI-H2170, MKN-7, and Calu-3 cell lines were obtained from Dr. Fumiaki Koizumi (National Cancer Centre Hospital, Tokyo), and the SKOv3 cell line was provided by Dr. Ahmed Ahmed (University of Oxford). The SKBr3, MDA-MB-361, UACC732, and Calu-3 cell lines were kept in Dulbecco's Modified Eagle Medium (DMEM) supplemented with 10% heat-inactivated fetal bovine serum (FBS) and penicillin-streptomycin. The BT474, NCI-H2170, MDA-MB-453, HCC1954, HCC1569, and MKN-7 cell lines were maintained in RPMI supplemented with 10% heat-inactivated FBS and penicillin-streptomycin. SKOv3 cell line was kept in McCoy's Medium supplemented with 10% heat-inactivated FBS and penicillin-streptomycin. Trastuzumab and lapatinib were purchased from the Pharmacy department at the John Radcliffe Hospital, Oxford.

Non-specific human and goat IgG antibodies were purchased from R&D systems. Trastuzumab-resistant cells were generated in the laboratory. The cells were continuously treated with trastuzumab at 40 μg/mL for more than 8 months to generate acquired trastuzumab-resistant cells[32]. Lapatinib was also used to generate acquired lapatinib-resistant SKBr3 cells by dose escalating exposure to lapatinib up to 250 nM for 8 months. The lapatinib resistant cells were provided and generated by another laboratory member, Dr. Fenix Leung. All the cells were kept at 37 ºC in 5% CO_2 and 95% of humidity. The mycoplasma test was regularly performed by multiplex PCR assay (Qiagen).

2.2 Cell viability assay

Optimal cell density for the viability assay was predetermined based on the proliferation rate of individual cell lines. The viability of the cells was determined by resazurin assay (CellTiter-Blue, Promega) to confirm acquired trastuzumab or lapatinib resistance. Briefly, the cells were seeded in 96-well plates and were treated with trastuzumab or lapatinib for 5 days. The fluorescent signal was measured by $560_{Ex}/590_{Em}$ nm and a fitted curve was drawn from 3 independent

experiments in triplicate using GraphPad Prism. The effects of ADAM17 inihibitor (10 μM of INCB4298, Incyte) and gamma-secretase inhibitor (25 μM of γ-secretase inhibitor IX (DAPT), Calbiochem), anti-HER3 monoclonal antibody (SGP1), HER3 knockdown, and MET knockdown were examined by the colony formation assay. Predetermined density of the cells were seeded onto the 6-well plates and were treated with the indicated drug(s) or the vehicle for 14 days. The medium was replaced every 3 days. The colonies were fixed and stained by 0.2 % methylene blue in 50% of ethanol. The images were captured by MultiImage II (Alpha Innotech) and the colonies were counted by image J. The cell counting assay was used to assess the cell growth on treatment with MET monoclonal antibody and MET tyrosine kinase inhibitor. Equal numbers of cells were seeded in 6-well plates and were treated with MET antibody (AF276, R&D systems) or MET tyrosine kinase inhibitor (SU 11274, Sigma-Aldrich) for 5 days. The cells were trypsinised and counted with cell counter (Coulter counter).

2.3 Western blotting

The cells were grown and treated in 6-well plates or 100 mm-dishes. The plate was then placed on ice and washed with ice-cold PBS twice. The cells were

scraped into lysis buffer (No17, R&D systems) after 10 minutes of incubation on ice. For immunoprecipitation, the following lysis buffer was used: 10mM EDTA, 20mM Tris (pH7.5), 150mM NaCl, 10mM $Na_2P_2O_7$, and 100mM NaF with 1% Triton X-100, protease inhibitor cocktail (Roche), and phosphatase inhibitor cocktail 2 and 3 (Sigma-Aldrich). A fractionation kit (NE-PER, Thermo Scientific) was used for nuclear extraction. The samples were centrifuged at 4 ºC and the supernatants were collected. The protein concentration was measured by Bradford assay and equal amounts of protein were loaded and separated on NuPage 4-12% gels at 120V, and were semi-dry-transferred to PVDF (Millipore Corp) membrane at 12V for 2 hours. The membrane was blocked with 5% bovine serum albumin (BSA) in TBS-tween (0.1%), and the primary antibody was applied overnight at 4 ºC. HRP-conjugated secondary antibody (GE Healthcare) was applied at room temperature for 1 hour and was visualized with enhanced chemiluminescence (ECL) system (GE Healthcare). The following antibodies were purchased from Cell Signalling Technology: anti-pHER3 (Y1289, Y1197), anti-AKT, anti-pAKT (S473, T308), anti-MET, anti-pMET (1234/1235), anti-HER2, anti-pHER2 (Y1221/1222), anti-Calnexin, anti-NaK ATPase, anti-Histone H3, anti-GAPDH, and anti-actin antibody. Anti-HER3 (ab34641) and anti-Golgin

antibody were obtained from Abcam. The concentration and incubation time for these antibodies are summarised in Table 2.1. Heregulin (HRG) (R&D systems) at 100 ng/mL and HGF (R&D systems) at 50 ng/mL were used to stimulate HER3 and MET respectively.

Table 2.1. The list of antibodies for western blotting.

antibody	concentration	incubation time	Supplier
HER3 (Rabbit pAb)	1:1000	overnight	Abcam
pHER3 (Y1197) (Rabbit mAb)	1:1000	overnight	Cell Signaling
pHER3 (Y1289) (Rabbit mAb)	1:1000	overnight	Cell Signaling
MET (Rabbit mAb)	1:1000	overnight	Cell Signaling
pMET (Y1234/1235) (Rabbit mAb)	1:1000	overnight	Cell Signaling
HER2 (Rabbit mAb)	1:1000	overnight	Cell Signaling
pHER2 (Y1221/1222) (Rabbit mAb)	1:1000	overnight	Cell Signaling
AKT (Rabbit mAb)	1:1000	overnight	Cell Signaling
pAKT (S473) (Rabbit mAb)	1:1000	overnight	Cell Signaling
pAKT (T308) (Rabbit mAb)	1:1000	overnight	Cell Signaling
Calnenix (Rabbit mAb)	1:1000	overnight	Cell Signaling
NaK ATPase (Rabbit pAb)	1:1000	overnight	Cell Signaling
Histone H3 (Rabbit mAb)	1:1000	overnight	Cell Signaling
GAPDH (Rabbit mAb)	1:1000	overnight	Cell Signaling
β-actin (Rabbit mAb)	1:1000	overnight	Cell Signaling
Golgin 97 (Rabbit pAb)	1:1000	overnight	Abcam
ADAM17 (Rabbit pAb)	1:1000	overnight	Abcam
PEN2 (Rabbit mAb)	1:1000	overnight	Cell Signaling

2.4 siRNA transfection and quantitative real-time PCR (qRT-PCR)

The cells were transfected with two different short interfering RNAs (siRNA) for HER3 (Qiagen) and MET (Qiagen). The cells were plated to be 30-40% confluence prior to transfection before DharmaFECT1 (Thermo Scientific) and the siRNA (final concentration, 20nM) in serum-free OptiMEM was added into the well and incubated overnight. The medium was then replaced with full-serum medium. AllStars non-targeting siRNA (Qiagen) was used as a control. Total RNA was isolated using Total RNeasy Mini Kit (Qiagen) after 48 hours of transfection and cell lysates for western blotting were collected 72 hours after transfection. The purity of RNA extracts was determined by measuring the absorbance ratio 260 nm (A260) to 280 nm (A280) in a Nanodrop spectrometer. The preparation of cDNA was done using Highcapacity cDNA Reverse Transcription Kit (Applied Biosystems) according to the manufacturer's instructions. Briefly, 2 μg of RNA in 20 μl was used for reverse transcription. The following thermal cycle was used: 10 minutes at 25 ℃, 120 minutes at 37 ℃, 5 minutes at 85 ℃, and hold at 4 ℃. cDNA products were stored at -80℃. Following cDNA preparation, the quantitative RT-PCR assays were performed using standard SYBR-Green methodology. Briefly, 20 μg of cDNA was mixed with

qPCR master mix (SensiMix SYBR Hi-ROXX qPCR) and final volume of 50 µl were analysed. The following primers were designed (http://www.lifescience.roche.com) and used for qRT-PCR: HER3 forward; 5'-CTG ATC ACC GGC CTC AAT-3', HER3 reverse; 5'-GGA AGA CAT TGA GCT TCT CTG C-3', MET forward; 5'-TGA AAT TCA TCC AAC CAA ATC TT-3', MET reverse; 5'-AAT AGA AAA CTG ACA ATG TTG AGA GG-3', beta-actin forward; 5'-ATT GGC AAT GAG CGG TTC-3', beta-actin reverse; 5'-GGA TGC CAC AGG ACT CCA T-3'. The qRT-PCR assay was carried out on the Mx3005P QPCR System**.** Thermal cycling was initiated with 5 minutes at 95ºC, followed by 40 cycles of 10 seconds at 95ºC and 1 minute at 60°C. The exponential route of C_T value was converted into a linear form using the $2^{-\Delta\Delta CT}$-relative calculation method. For this purpose, β-actin was used as the house-keeping gene.

2.5 Co-immunoprecipitation

The cells were grown to 80% confluence in 150mm-dishes and were collected as described above. The protein amount was measured before applying non-specific IgG antibody. The non-specific protein was immunoprecipitated by

incubation with 5 μg of non-specific IgG antibody for 1 hour at 4 ºC followed by 1 hour incubation with 50 μl of anti-mouse antibody coated beads at 4 ºC (TureBlot® , Rockland Pharmacy). The mouse IgG-beads complex was removed by centrifugation (3000 rpm, 10 minutes, 4℃) before applying the primary antibody. The lysate was incubated with primary antibodies (5 μg of antibody for 1000 μg of protein) against HER3 (RTJ2, Abcam), MET (B2, SantaCruz), or non-specific mouse IgG (Abcam) for 1 hour at 4 ºC, and the protein-antibody complex was captured with anti-mouse antibody coated beads overnight at 4 ºC (50 μl of beads for 5 μg of antibody). The beads were washed with lysis buffer [10mM EDTA, 20mM Tris (pH7.5), 150mM NaCl, 10mM $Na_2P_2O_7$, and 100mM NaF with 1% Triton X-100, protease inhibitor cocktail (Roche), and phosphatase inhibitor cocktail 2 and 3 (Sigma-Aldrich)] more than twice after the removal of the supernatant and boiled for 10 min at 95 ºC with 2 ×LDS buffer. Samples were centrifuged (3000 rpm, 10 minutes, 4 ºC) and supernatants were applied to SDS-PAGE for western blotting.

2.6 Confocal microscopy

Approximately 20,000 cells were seeded onto coverslips in 24-well plates. Coverslips were washed with PBS twice and were fixed with 4% paraformaldehyde (PFA) for 10 minutes. The cells were permeabilised with 0.5% Triton-X for 10 minutes. Samples were blocked with 10% BSA and 0.5% FBS overnight at 4 ºC. Primary antibodies for HER3 (ab34641, abcam and sc292557, SantaCruz) were then applied in 5% BSA for overnight at 4 ºC. The cells were rinsed with PBS over 1 hour at room temperature with gentle shaking and secondary antibody conjugated to Alexa 488 (Invitrogen) in 5% BSA was applied for 1 hour at room temperature in the dark. The cells were rinsed with PBS over 1 hour at room temperature with gentle shaking and mounted with DAPI (4',6-diamidino-2-phenylindole) Fluoromount-G (Southern Biotech). Mid-slice images to detect nuclear proteins were captured by Zeiss LSM510 confocal microscope.

2.7 Immunohistochemistry (IHC)

Cell pellets and xenograft samples used in this project were provided by Dr. Neil O'Brien at the UCLA except for the SKBr3 and trastuzumab-resistant SKBr3 cell line pellets. All cell pellets samples prepared for IHC were parental cell lines except for trastuzumab-resistant SKBr3 cells. For the SKBr3 and the trastuzumab resistant SKBr3 cell lines, cells were grown in 15cm-dish up to 80% confluence and cells were collected by trypsinisation. Cells were fixed with 4% PFA at 4 ºC overnight and the fixed cell pellets were resuspended in 400 µl of agarose mixture (2% agarose and 4% formaldehyde in PBS) at 60 ºC. The cells were immediately centrifuged at 13500 RPM for 1 minute. The gelled pellets were set in a cassette for paraffin processing. The cassettes were processed at the Oxford Centre for Histopathology to be embedded in paraffin blocks. Samples were sectioned at 4 µm using a microtome (Leica) to be set on the slides (VWR).

Xenograft samples were generated in 6-week-old CD-1 athymic nude mice. Xenograft samples were developed subcutaneously. All the samples used in this project were duplicated xenograft for each cell line[185]. Briefly, tumours were measured 3 times a week by a caliper after becoming visible. Trastuzumab at 10mg/kg in PBS was given intraperitoneally twice a week for a period of 7 weeks.

Tumours were then excised, formalin fixed, and paraffin-embedded[185]. Responders were defined as no tumour growth or observed tumour decrease in size after trastuzumab treatment. Non-responders were all others. For the cell pellet samples, responders were defined by three dimensional proliferation assay as previously described[186]. Briefly, cells were seeded on agarose gel with or without 15 μg/mL of trastuzumab and allowed to form colonies for 3 weeks. The sensitive cell lines were defined as the cells with a ≥20% decrease in colony number[186].

The human tissue samples used in this study were provided by the Breast Cancer Campaign, the FinHER trial, and a locally conducted prospective study in Cremona, Italy. The use of TMA slides from the FinHER trial was approved by the Helsinki University Central Hospital Ethics Committee (331/E6/07, 17 Oct 2007). The human tissue samples from a locally conducted prospective trial in Cremona were obtained with appropriate local ethical approval (Protocol CE-21392/2012). The TMA samples from the Breast Cancer Campaign were transferred in an agreement between the laboratory and the organisation. The samples from the Breast Cancer Campaign and the FinHER trial were Formalin-

Fixed Paraffin-Embedded (FFPE) tissues mounted as a tissue microarray, and all cores were duplicated. These samples were surgically resected tumours as a definitive surgery for early breast cancer patients. No neoadjuvant therapy had been administered to these patients. The samples from Breast Cancer Campaign included HER2-positive and HER2-negative samples, however, clinical data were available only for HER2-positive patient samples. The FinHER trial samples were all HER2-positive samples. Samples from a locally conducted prospective trial in Cremona were biopsy samples and surgically removed samples for the patients with HER2-positive early breast cancer and received trastuzumab and chemotherapy as a neoadjuvant therapy.

The same procedure was used for all the samples used for IHC. Sections of 4 μm were mounted on glass slides. The slides were heated at 65℃ and were immersed into Histoclear (National Diagnosis) followed by rehydration in ethanol. H_2O_2 (3%) in methanol was used for peroxidase blocking for 30 minutes. The antigen retrieval was performed by the target retrieval solution (DAKO S2375) at 97℃ for 40 minutes for MET staining. The antigen retrieval for HER3 staining was performed using the target retrieval solution (DAKO S2031) at 121℃ for 15

minutes. Following blocking in 10% horse serum in PBS for 10 minutes, the following antibodies were applied: the primary HER3 antibody (ab34641, abcam) at a dilution of 1:1000 at 4℃ overnight, or the primary MET antibody (CVD13, Invitrogen) at a dilution of 1:100 at room temperature for 1 hour in antibody diluent (s2022, DAKO). The primary antibody was visualised by EnVision systems (DAKO k4063) followed by counterstaining of haematoxylin. All HER3 and MET staining was evaluated by Dr. Ioannis Roxanis (a NHS consultant pathologist) and myself by immunoreactive scoring system (IRS)[187] (Table 2.2). Only the invasive component was evaluated and clinical data were blinded at the time of evaluation. The cut-off point was set based on the median IRS score for HER3 cytoplasm expression (IRS = 6) and nuclear expression (IRS = 2). For MET expression, the cut-off value was explored in this study.

Score for staining intensity	Score for distribution of positive cells
0 = negative	0 = < 1%
1 = weak	1 = 1-10%
2 = intermediate	2 = 11-50%
3 = strong	3 = 51-80%
	4 = > 80%

IRS score is calculated intensity x distribution (range: 0-12)

Table 2.2. Immunoreactive scoring system (IRS).

2.8 Statistical analysis

Statistical analysis was performed using the statistical software, GraphPad Prism version 5.04 and SPSS (version 19). For western blot analysis, intensities of target proteins were semi-quantified by Image J from three different experiments and were normalised to the loading control unless specified. One-way ANOVA test with Bonferroni correction was used to test the means between three or more groups. For the technically and biologically repeated experiments (qRT-PCR and colony formation assay), two-way ANOVA with Bonferroni correction was performed. To compare 2x2 tables, chi-square test was applied unless specified. Tumour response was evaluated by caliper measurement for human tissue samples and for xenograft samples. For survival analyses, survival curves were drawn by Kaplan-Meier method and log rank test was used to detect the statistical significance. The progression-free survival was calculated from the date of surgery or date of randomisation to the date of disease progression or any cause of death. The distant metastasis-free survival was calculated from the

date of surgery to the date of the detection of distant metastasis. Contralateral breast tumour was not regarded as distant metastasis. The overall survival was calculated from the date of randomisation or surgery to the date of any cause of death. The cause specific survival was calculated from the date of surgery to the date of death caused by breast cancer. Cox multivariate analyses were performed to determine independent factors associated with survival. All the statistical significance was set at less than 0.05 by two tailed manner. Statistical analyses for the FinHER trial samples were performed by the FinHER trial data centre.

CHAPTER 3.

ASSESSING HER3 SUBCELLULAR LOCALISATION IN RELATION TO TRASTUZUMAB RESPONSE AND RESISTANCE

3.1 Introduction

HER3 is the preferential dimerisation partner for HER2 and is important for cell survival in HER2-positive breast cancer[56,168]. As discussed in chapter 1, HER3 has a nuclear variant, $HER3_{80kD}$, which is known to interact with the promoter region of cyclin D1 in the nucleus, which increases the proliferation rate[132]. However, the exact mechanism of HER3 nuclear localisation is still unclear. It was previously shown that trastuzumab induces HER4 cleavage and nuclear translocation in HER2-positive breast cancer cells[134]. In cells treated with trastuzumab, it is not clear what factors determine HER3 localisation. Furthermore, the clinical impact of nuclear HER3 has been unclear. Therefore, this chapter aimed to assess HER3 subcellular localisation and its mechanisms.

3.2 Results

3.2.1 The generation of trastuzumab resistant HER2-positive cell lines

To assess the clinical impact of HER3 subcellular localisation in relation to trastuzumab treatment, a panel of HER2 highly expressing cell lines were first tested for their trastuzumab sensitivity. The SKBr3 and BT474 cells are two representative HER2-positive cell lines and were sensitive to trastuzumab treatment (IC50; 0.17 μg/mL and 0.06 μg/mL, respectively) (Figure 3.1). The IC50 values of all other cell lines was not obtainable since their cell viability did not decrease below 50%. However, the viability of NCI-H2170, MDA-MB-453, and MDA-MB361 cell lines was found to be decreased by approximately 30% (Figure 3.1). It should be noted that the NCI-H2170 and Calu3 cells are lung cancer cell lines, the SKOv3 cells are ovarian cancer, and MKN-7 is a gastric cancer cell line.

Figure 3.1

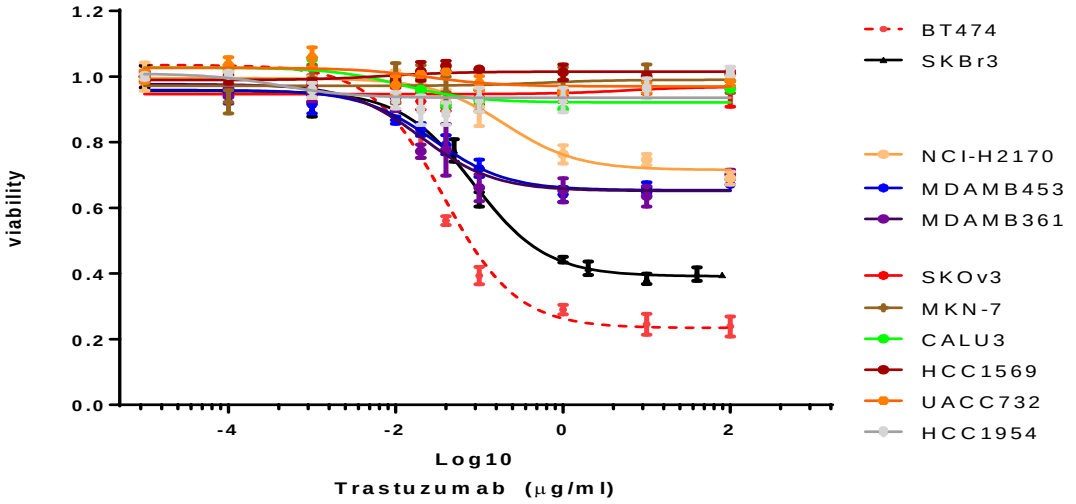

Figure 3.1 Trastuzumab sensitivity in a panel of HER2-positive cell lines. Predetermined number of cells were seeded in 96-well plates and the cells were allowed to attach to the plate before starting trastuzumab treatment at different doses for 5 days. The cell viability was determined by resazurin assay. Each point represents a mean of 3 independent experiments in triplicate and fit curve was drawn. The IC50 was calculated for the BT474 and SKBr3 cells based on the fit curve.

The SKBr3, BT474, MDA-MB-453, MDA-MB-361, and NCI-H2170 cells were continuously treated with trastuzumab at 40 µg/mL until the cells became resistant to trastuzumab (Figure 3.2).

Figure 3.2

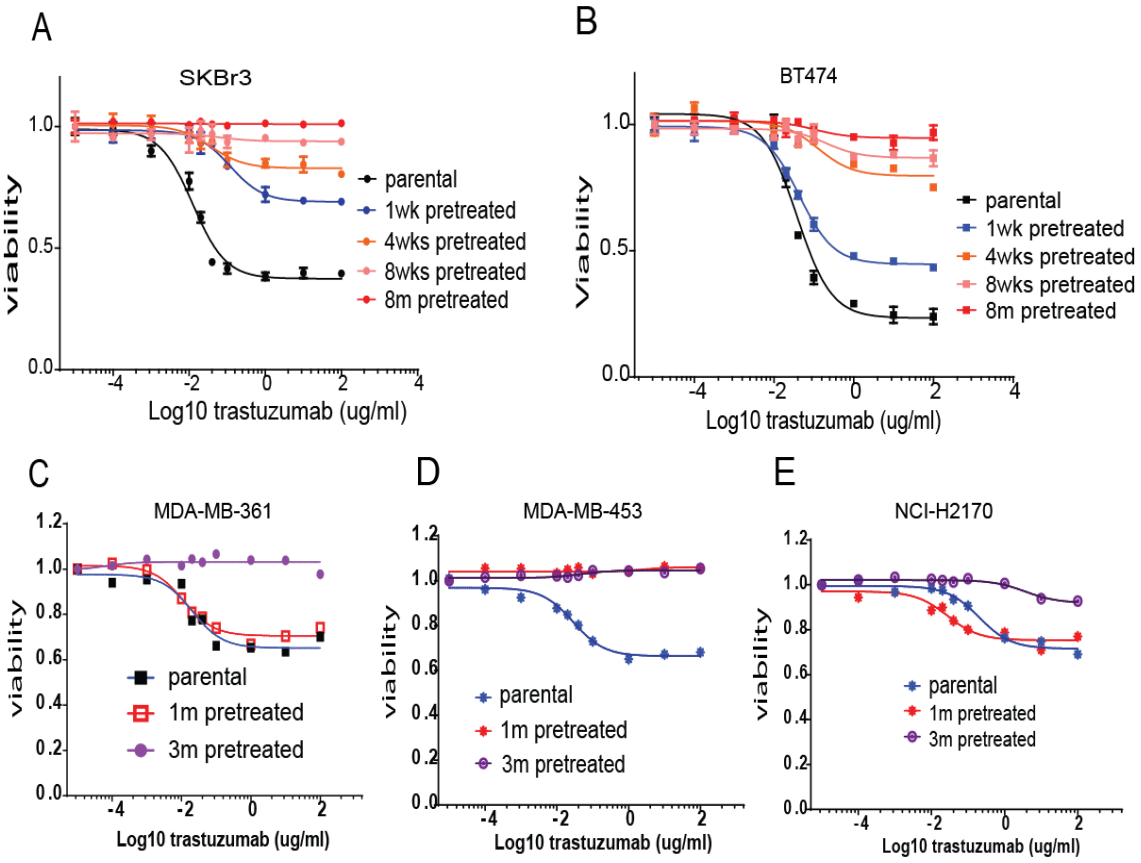

Figure 3.2. Generation of acquired trastuzumab resistant cells by long-term trastuzumab treatment. The SKBr3 (A) and BT474 cells (B) were pre-treated with trastuzumab for indicated durations before starting the viability assay. Predetermined number of cells were seeded in 96 well plates without trastuzumab at different concentrations. The cells were allowed to attach for 8 hours before starting trastuzumab treatment. The Resazurin assay was applied as shown in Figure 3.1. Similarly, the MDA-MD-361 (C), MDA-MB-453 (D), NCI-H2170 (E) cells were continuously treated with trastuzumab for indicated durations, and sensitivity to trastuzumab was assessed.

3.2.2 HER3 fragment at 100kD is a specific immunoreaction.

HER3 has been reported to have several different fragments below 180kD, which is the size of full length of HER3[129]. To identify the specific immunoreactivity of several HER3 bands in western blot, the cell lysates were immunoprecipitated with HER3 antibody (RTJ2, C-terminus) and immunoblotted with another HER3 antibody (ab34641, C-terminus). There were several products below 180kD detected by this HER3 antibody, but only $HER3_{180kd}$ and $HER3_{100kD}$ were immunoprecipitated and detected in both the parental and acquired resistant SKBr3 and BT474 cells (Figure 3.3A, B). The non-specific mouse IgG was used as a negative control and $HER3_{100kD}$ was found to be undetectable by this IgG.

Figure 3.3

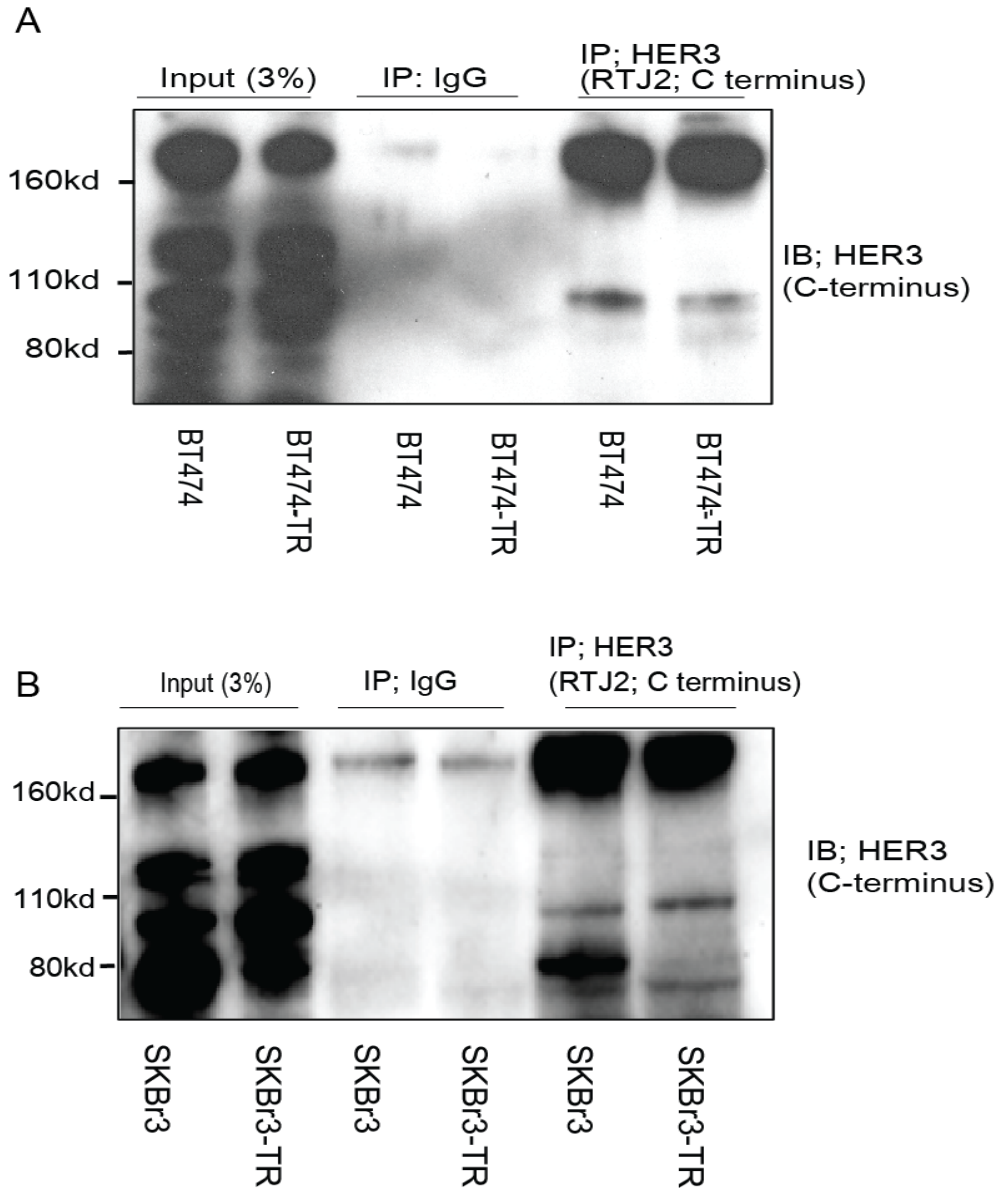

Figure 3.3 The detection of immunoprecipitated $HER3_{100kD}$ and $HER3_{180kD}$ by two different HER3 antibodies raised against C-terminus. A, Equal amount of proteins from the BT474 and acquired trastuzumab-resistant BT474 cells (BT474-TR) were subject to immunoprecipitation (IP) with HER3 antibody (RTJ2) or non-specific mouse IgG followed by immunoblotting (IB) analyses of HER3 (C-terminus, ab34641). For input, 3% of total amount of proteins used for immunoprecipitation were loaded. B, Similarly, equal amount of proteins from the SKBr3 and acquired-trastuzumab resistant SKBr3 cells (SKBr3-TR) were subject to IP followed by IB with HER3 antibody.

Since $HER3_{180kD}$ and $HER3_{100kD}$ were the only 2 bands immunoprecipitated and detected in these cell lines, it was hypothesised that $HER3_{100kD}$ could be a specific immunoreactive form of HER3. To confirm this result, HER3 was knocked down in these cell lines and immunospecificity was assessed. Two siRNAs against HER3 were optimised and HER3 mRNA level was quantified by qRT-PCR (Figure 3.4A). Following the optimisation of HER3 knockdown, the specificity of the antibody was assessed by western blot. Immunoblotting of the cell lysates from HER3 knockdown showed a significant decrease of the HER3 protein expression at both 180kD and 100kD in the BT474 (Figure 3.4B) and SKBr3 cells (Figure 3.4C). HER3 localisation was visualised by confocal microscopy and was found to be in the cytoplasm and the nucleus. Interestingly, membrane HER3 staining was not very obvious as compared to the previous reports. [66,79,80,125,129]. HER3 knockdown decreased HER3 expression in the cytoplasm and the nucleus (Figure 3.5). These results indicate that $HER3_{100kD}$ is a specific immunoreactive product of the HER3 gene, and HER3 can be localised to the nucleus as well as the cytoplasm.

Figure 3.4

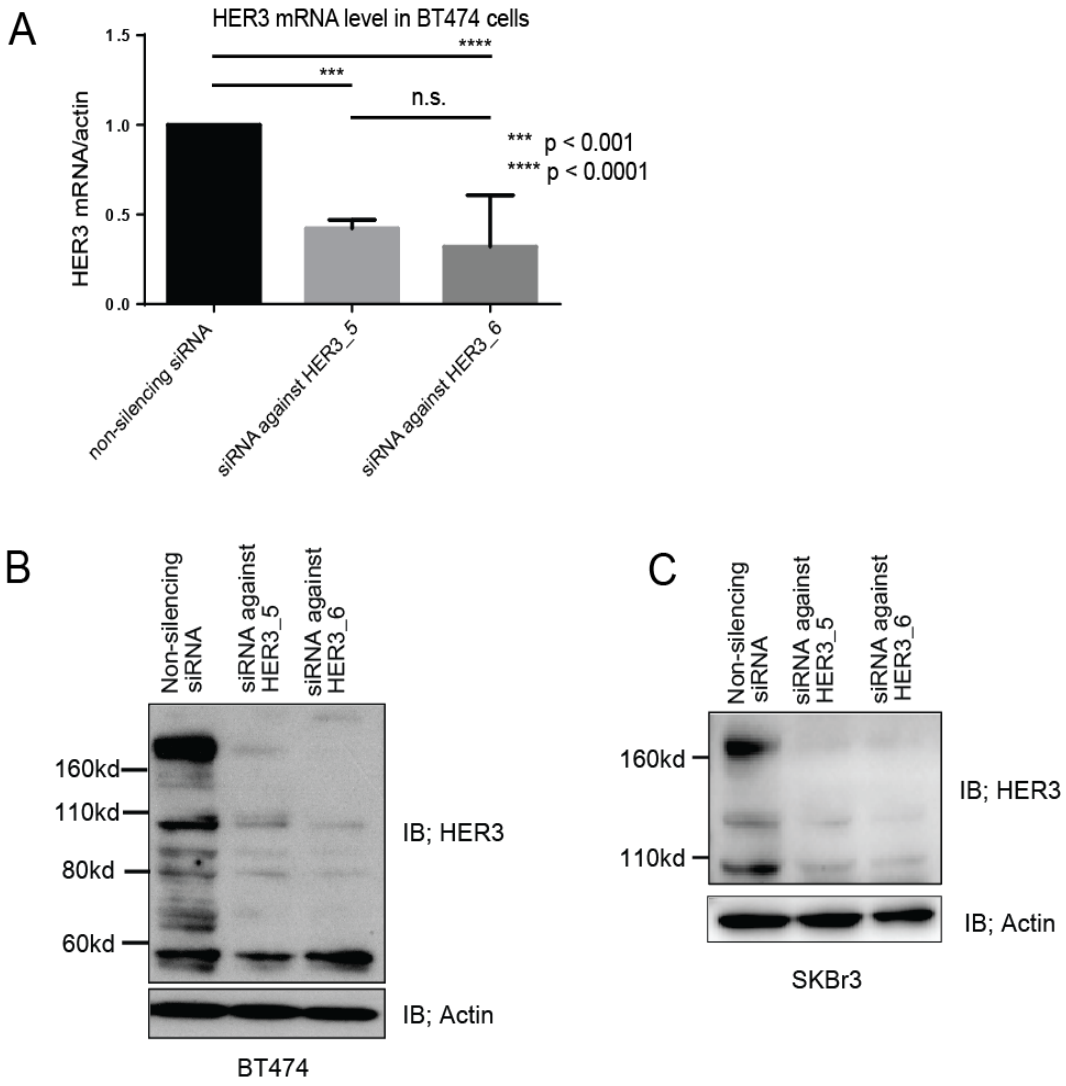

Figure 3.4 $HER3_{100kD}$ as a specific immunoreactive form of HER3. A, The BT474 cells were transfected with 2 different siRNAs against HER3 (HER3_5 and HER3_6) or non-silencing siRNA for 48 hours. RNA was extracted and quantified by real-time PCR (HER3 normalised to actin). HER3 mRNA level was compared to the control (non-silencing siRNA). Two-way ANOVA and Bonferroni correction was used to detect the statistical significance of 3 independent experiments in triplicate. Bars show means with SEM. Similarly, the BT474 (B) and SKBr3 cells (C) were transfected with 2 different siRNAs against HER3 or non-silencing siRNA. Equal amount of proteins from these cells were subject to immunoblotting with HER3 and actin.

Figure 3.5

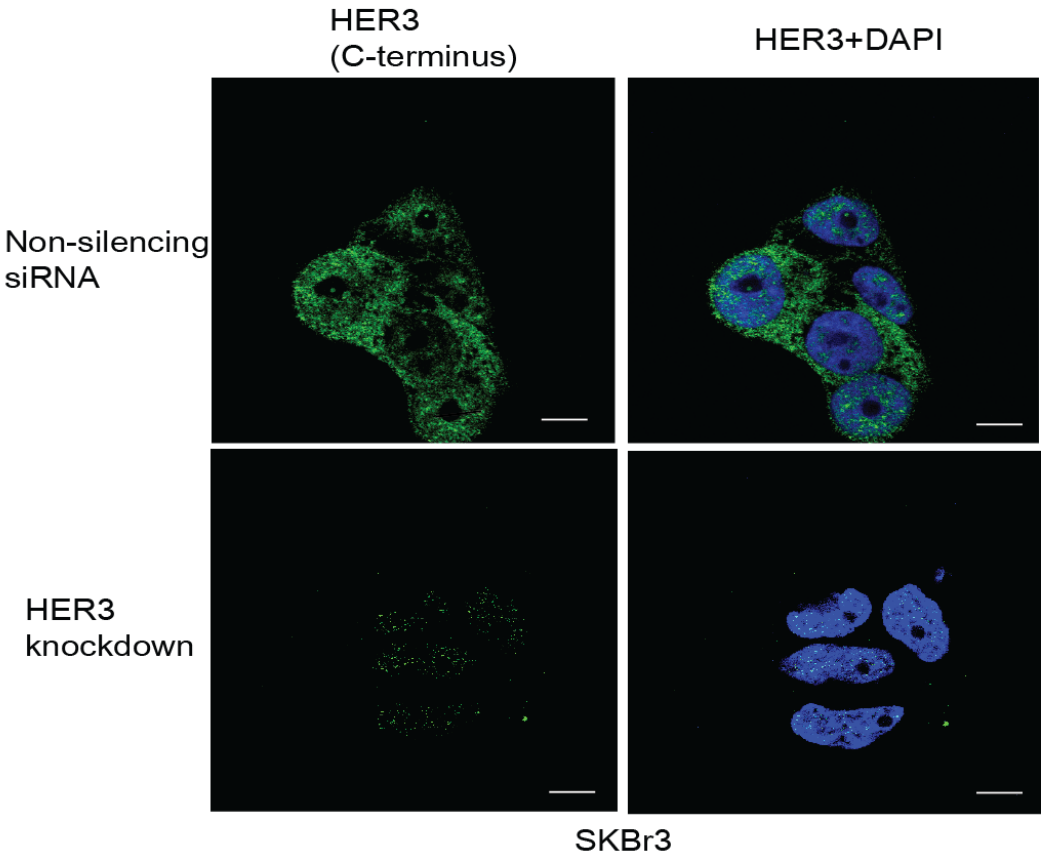

Figure 3.5 HER3 in cytoplasm and nucleus. Predetermined number of cells were seeded onto the cover slip in 24-well plate and transfected with non-silencing siRNA or siRNA against HER3 (HER3_5) for 72 hours. Cells were fixed and permeabilised followed by blocking. Primary HER3 antibody and secondary antibody conjugated with Alexa488 (green signal) were applied. Nuclei were stained with DAPI (blue). Cells were visualised with confocal microscopy (Scale bar = 10 μm).

3.2.3 An increase in nuclear HER3$_{100kD}$ in acquired trastuzumab-resistant SKBr3 cells

To detect HER3 subcellular localisation, two different HER3 antibodies were used: antibodies raised against HER3 N-terminus and C-terminus. HER3 was detected in the nucleus by both antibodies in parental SKBr3 cells (Figure 3.6A). However, the detection of HER3 N-terminus in the nucleus was decreased in acquired trastuzumab-resistant SKBr3 (SKBr3-TR) cells, while the C-terminus of HER3 in the nucleus was increased (Figure 3.6A). In the BT474 cells, HER3 detected by N-terminus and C-terminus antibody was similar in both parental and acquired trastuzumab-resistant cells (Figure 3.6A). The HER3 localisation of the parental MDA-MB-361 and MDA-MB-453 cells were also compared with their acquired resistant cells but the observation seen in the SKBr3 cells was not found (Figure 3.6B). These results indicate that HER3 may be cleaved, and only HER3 from the C-terminus part translocated to the nucleus, and thus the detection of N-terminus HER3 was reduced in the nucleus when the SKBr3 cells became resistant to trastuzumab.

Figure 3.6

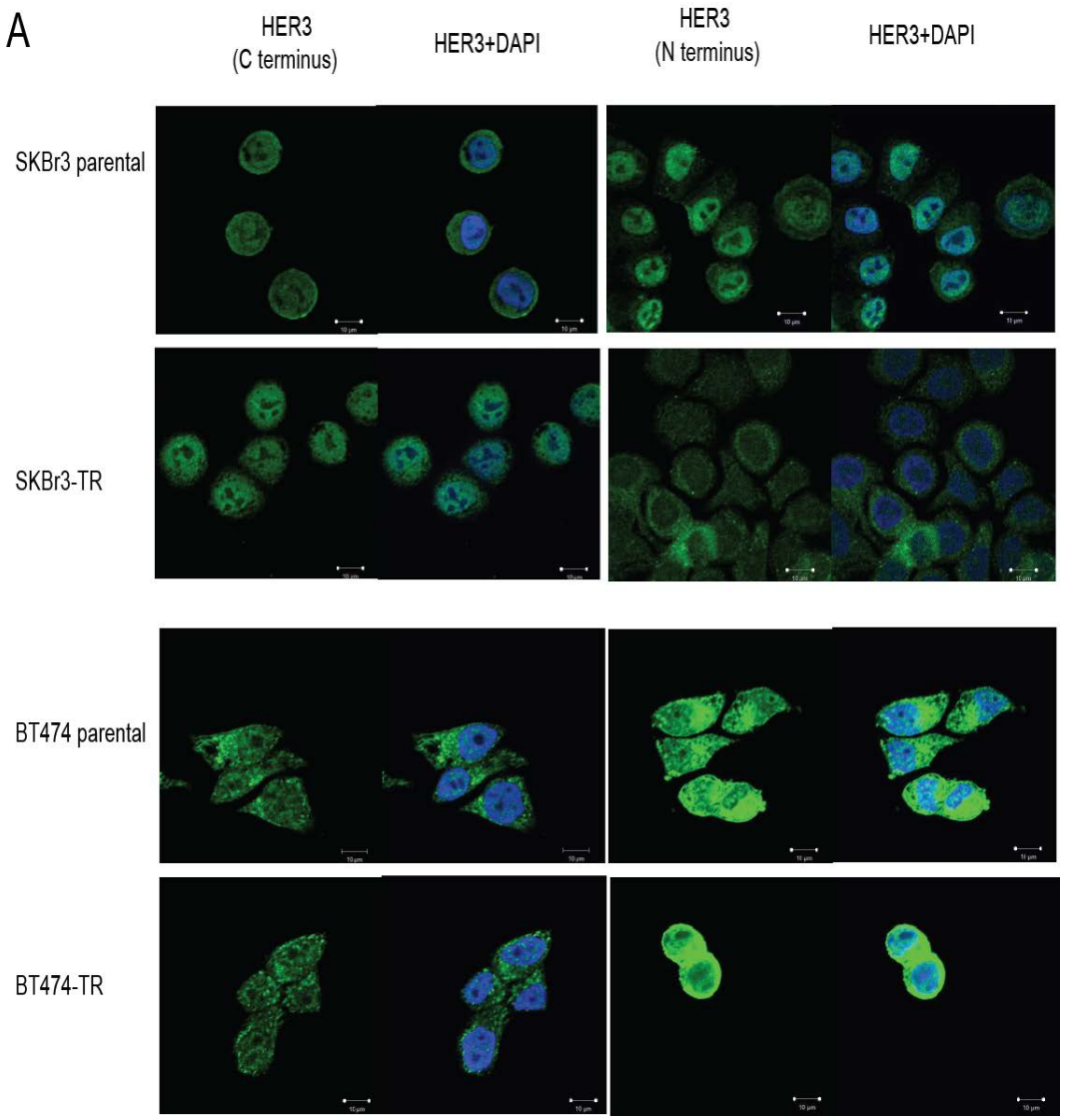
A
HER3
(C terminus)
HER3+DAPI
HER3
(N terminus)
HER3+DAPI
SKBr3 parental
SKBr3-TR
BT474 parental
BT474-TR

Figure 3.6

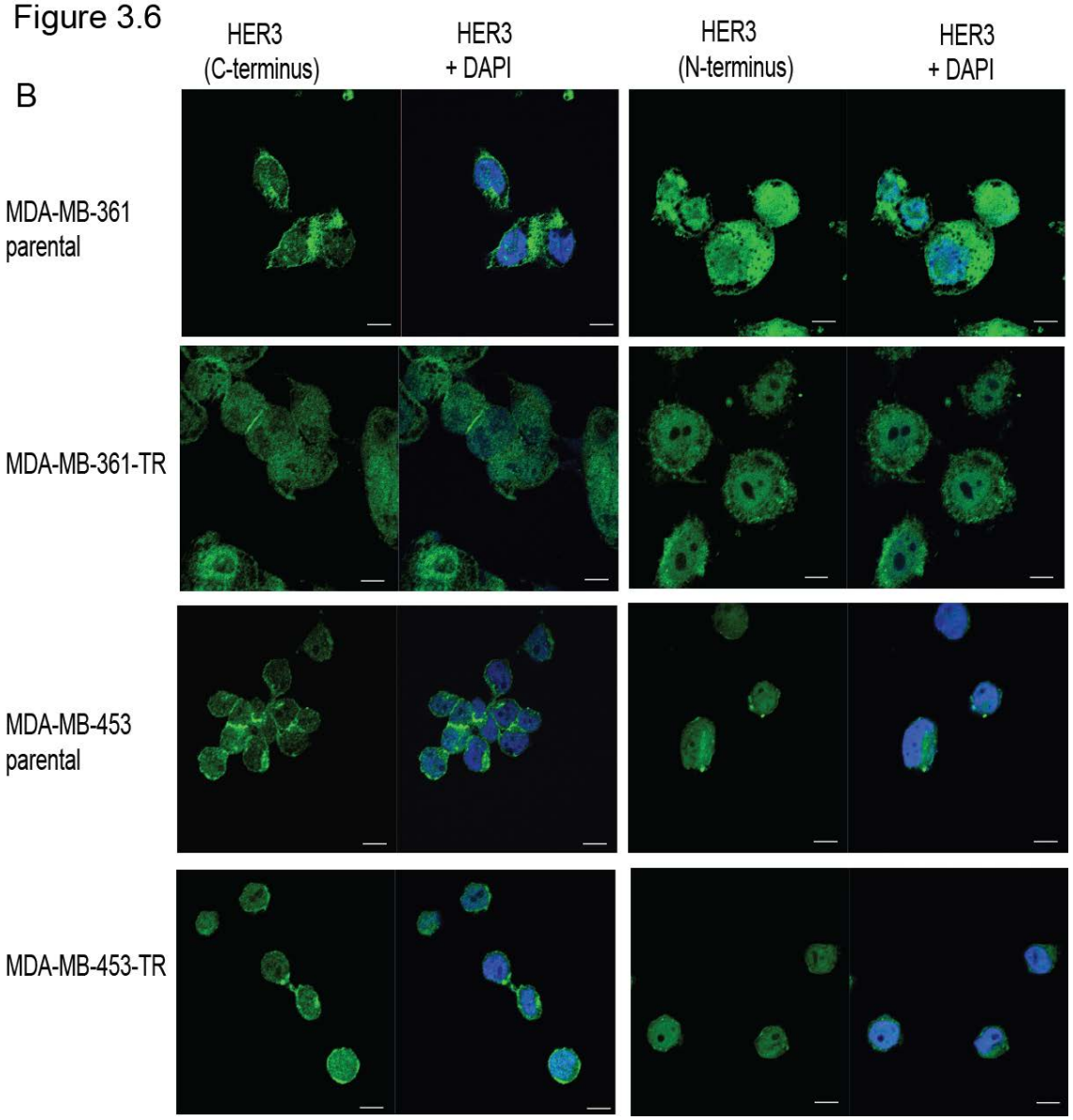

Figure 3.6 An increase of nuclear HER3 from C-terminus in the acquired-trastuzumab resistant SKBr3 (SKBr3-TR) cells. A, The SKBr3, SKBr3-TR, BT474, acquired-trastuzumab resistant BT474 (BT474-TR) cells were seeded onto the cover slip in 24-well plate. The cells were fixed and permeabilised followed by immunostaining with HER3 antibodies (green) (HER3 antibody raised against its C-terminus and N-terminus). Nuclei were stained with DAPI (blue). Cells were visualised with confocal microscopy. The parental cells were treated with human IgG. B, Similarly, MDA-MD-361, acquired-trastuzumab resistant MDA-MD-361 (MDA-MB-361-TR), MDA-MD-453, and acquired-trastuzumab resistant MDA-MD-453 (MDA-MD-453-TR) were stained with HER3 antibodies raised against C-terminus and N-terminus of HER3. Scale bar = 10 μm

To address the decrease of N-terminus HER3 and the increase of C-terminus HER3 in the SKBr3-TR cells, nuclear extraction experiments were performed. Nuclear extracts of SKBr3-TR cells showed an increase of $HER3_{100kD}$ and a decrease of $HER3_{180kD}$ compared with parental cells (Figure 3.7A, B, C). This result indicates that HER3 was cleaved and $HER3_{100kD}$ was more likely to be detected in the nucleus. As a result, the full-length $HER3_{180kD}$ was detected less in the nucleus in the SKBr3-TR cells. The possibility of contamination of the nuclear extracts with other subcellular components seems unlikely since plasma membrane marker (Na-K ATPase), Golgi marker (golgin), and the endoplasmic reticulum marker (calnexin) were at very low levels (Figure 3.7A). Interestingly, the SKBr3 cells treated with trastuzumab for 2 months did not show an increase of $HER3_{100kD}$ in the nucleus although they were resistant to trastuzumab at this point (Figure 3.7A). This result suggests that only long-term trastuzumab treatment induced enriched nuclear HER3, possibly due to the selection of pre-existing cells since 30-40% of the BT474 and SKBr3 cells were able to survive trastuzumab treatment even at a high concentration (40 μg/mL) (Figure 3.1). Taken together, C-terminus $HER3_{100kD}$ in the nucleus was increased in the SKBr3-TR cells.

Figure 3.7

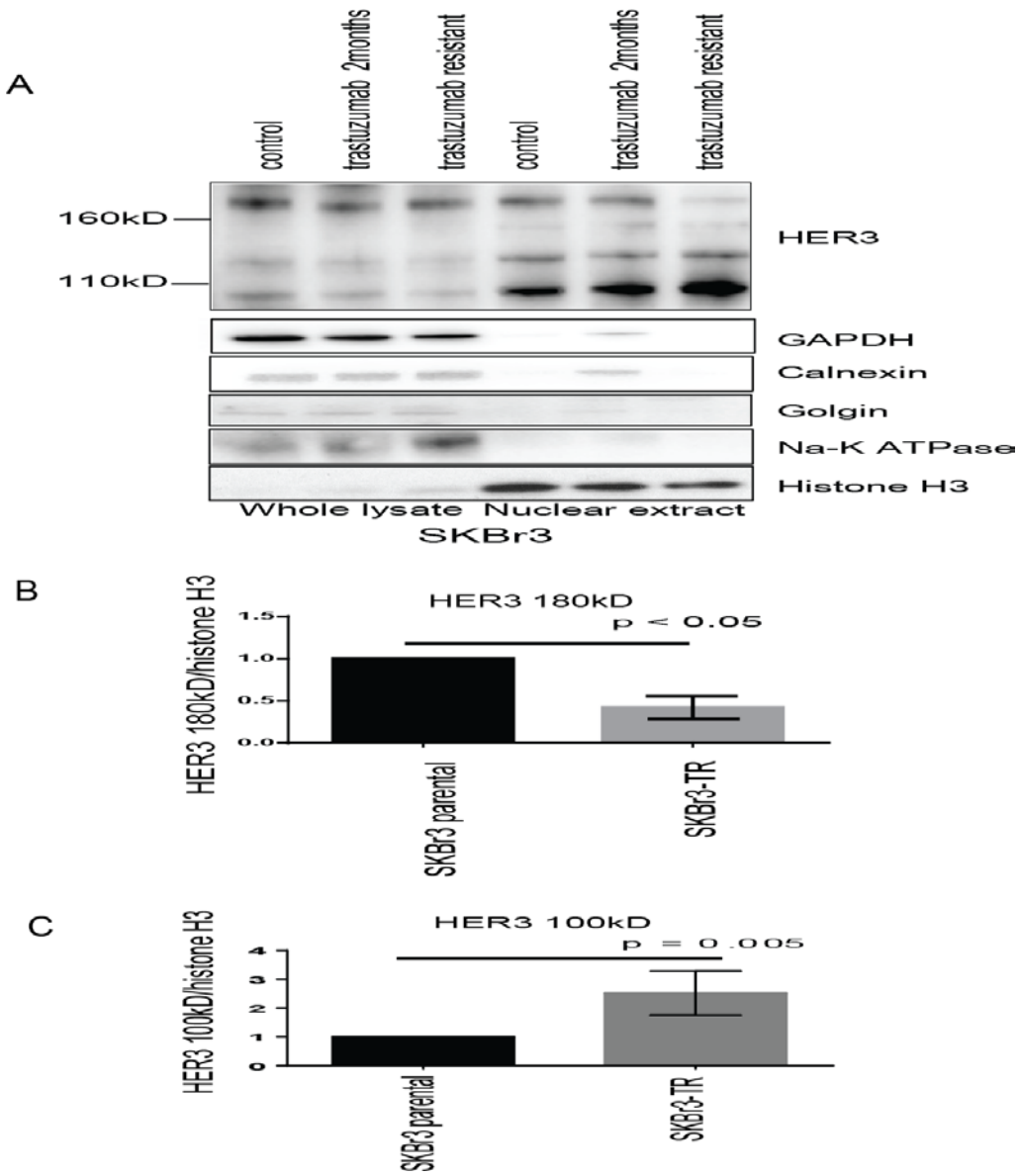

Figure 3.7 An increase of nuclear HER3$_{100kD}$ from C-terminus in the acquired-trastuzumab resistant SKBr3 (SKBr3-TR) cells. A, Equal amount of proteins from whole cell lysates (left 3 lanes) or nuclear extractions (right 3 lanes) of SKBr3 parental, pre-treated with trastuzumab for 2 months, or acquired trastuzumab-resistant SKBr3 cells were subject to immunoblotting with HER3, GAPDH, Calnexin, Golgin, Na-K ATPase, and Histone H3. The control cells were treated with human IgG. Statistical analysis was performed by using semi-quantification of HER3 at 180kD (B) and HER3 at 100kD (C) for SKBr3 parental and SKBr3-TR cells from 3 different experiments. Bars indicate means ± SEM. Paired *t*-test was used to detect the statistical significance from 4 repeated experiments.

3.2.4 Translocation of HER3$_{100kD}$ to the nucleus in lapatinib treatment and short-term trastuzumab treatment

To assess nuclear HER3 localisation on treatment with lapatinib (dual tyrosine kinase inhibitor for EGFR and HER2), acquired lapatinib resistant SKBr3 (SKBr3-LR) cells were generated in our laboratory (generated by Dr. Fenix Leung) by gradual increase in lapatinib concentration over 8 months up to 250nM (Figure 3.8A). The lapatinib IC50 of SKBr3-LR cells was approximately 1000 times higher than that of parental SKBr3 cells (77.0 μM *vs.* 95.9 nM). The SKBr3-LR cells were cross-resistant to trastuzumab (Figure 3.8C), while SKBr3-TR cells have a similar sensitivity to lapatinib compared to the parental SKBr3 cells (Figure 3.8B). These results indicate that SKBr3-TR cells were sensitive to lapatinib but SKBr3-LR cells were not sensitive to trastuzumab.

Figure 3.8

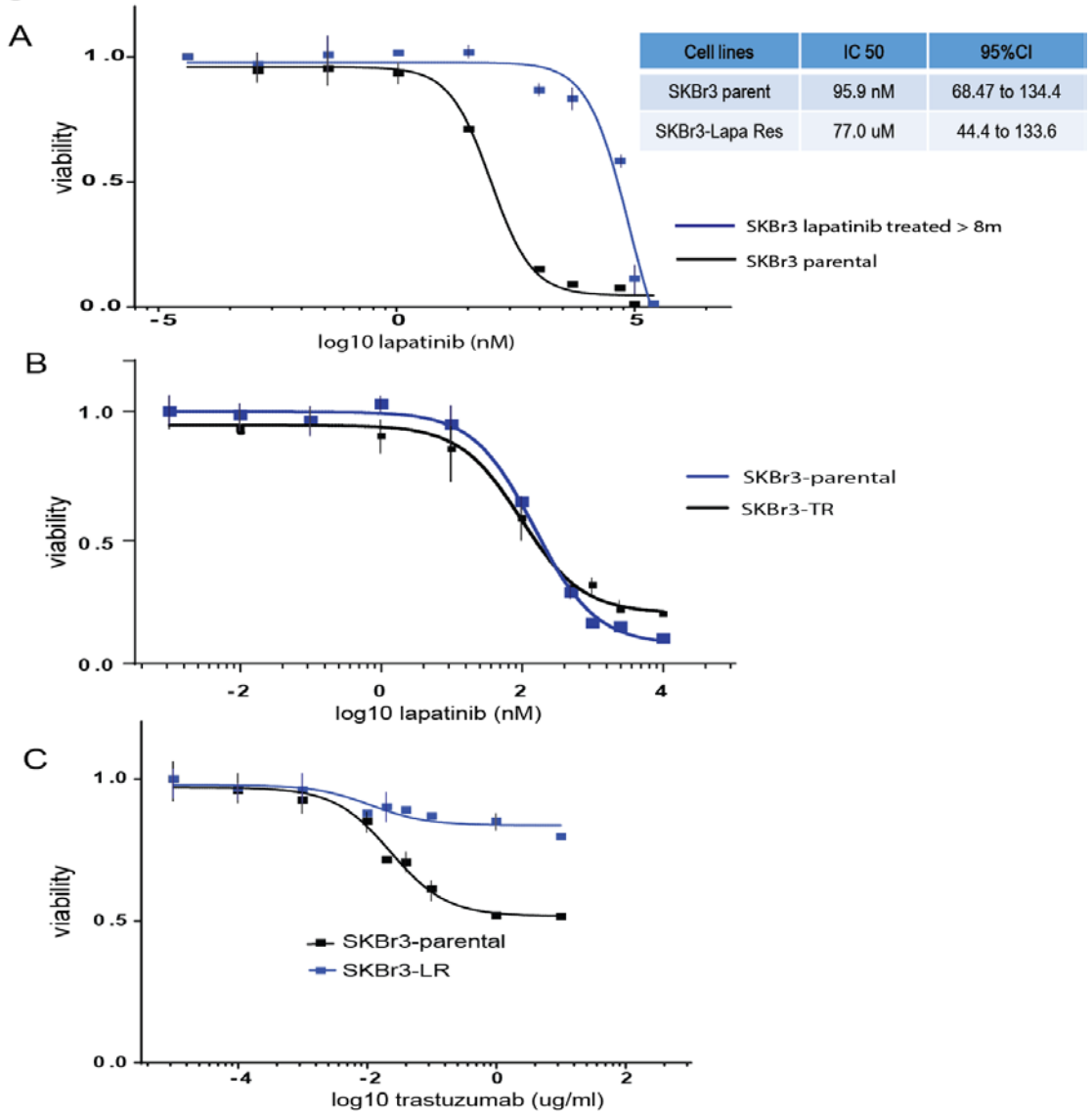

Figure 3.8 Response of lapatinib-resistant SKBr3 cells to lapatinib or trastuzumab. Acquired lapatinib-resistant SKBr3 (SKBr-LR) cells were raised by continuous exposure to lapatinib for more than 8 months. A, Predetermined number of cells were seeded in 96-well plate, and cells were allowed to attach for 24 hours before starting lapatinib treatment at different concentrations. Resazurin assay was applied to detect the cell viability after 5 days of treatment. Fit curve was drawn from 3 independent experiments in triplicate. . B, Similarly, parental and trastuzumab-resistant SKBr3 (SKBr3-TR) cells were seeded in 96-well plate. Cells were treated with lapatinib at different doses for 5 days and resazurin assay was applied. C, Similarly, the cells were seeded in 96-well plate and the cells were treated with trastuzumab at different doses for 5 days. Resazurin assay was applied. Bars indicate SEM.

It was hypothesised that lapatinib resistance may induce nuclear HER3 translocation as seen in trastuzumab resistance. However, the detection of C-terminus of HER3 ($HER3_{100kD}$) and a loss of N-terminus of HER3 in the SKBr3-TR cells was only observed in trastuzumab resistance since the SKBr3-LR cells did not show nuclear enrichment of the C-terminus of HER3, nor a loss of nuclear N-terminus of HER3 (Figure 3.9A). To confirm this result, nuclear extraction of HER3 was assessed by immunoblotting and it was shown that the level of $HER3_{100kD}$ in the nucleus was similar to that of SKBr3-LR cells (Figure 3.9B). This result indicates that lapatinib did not influence nuclear HER3 localisation, and enriched nuclear $HER3_{100kD}$ was observed only in trastuzumab resistant SKBr3 cells.

Figure 3.9

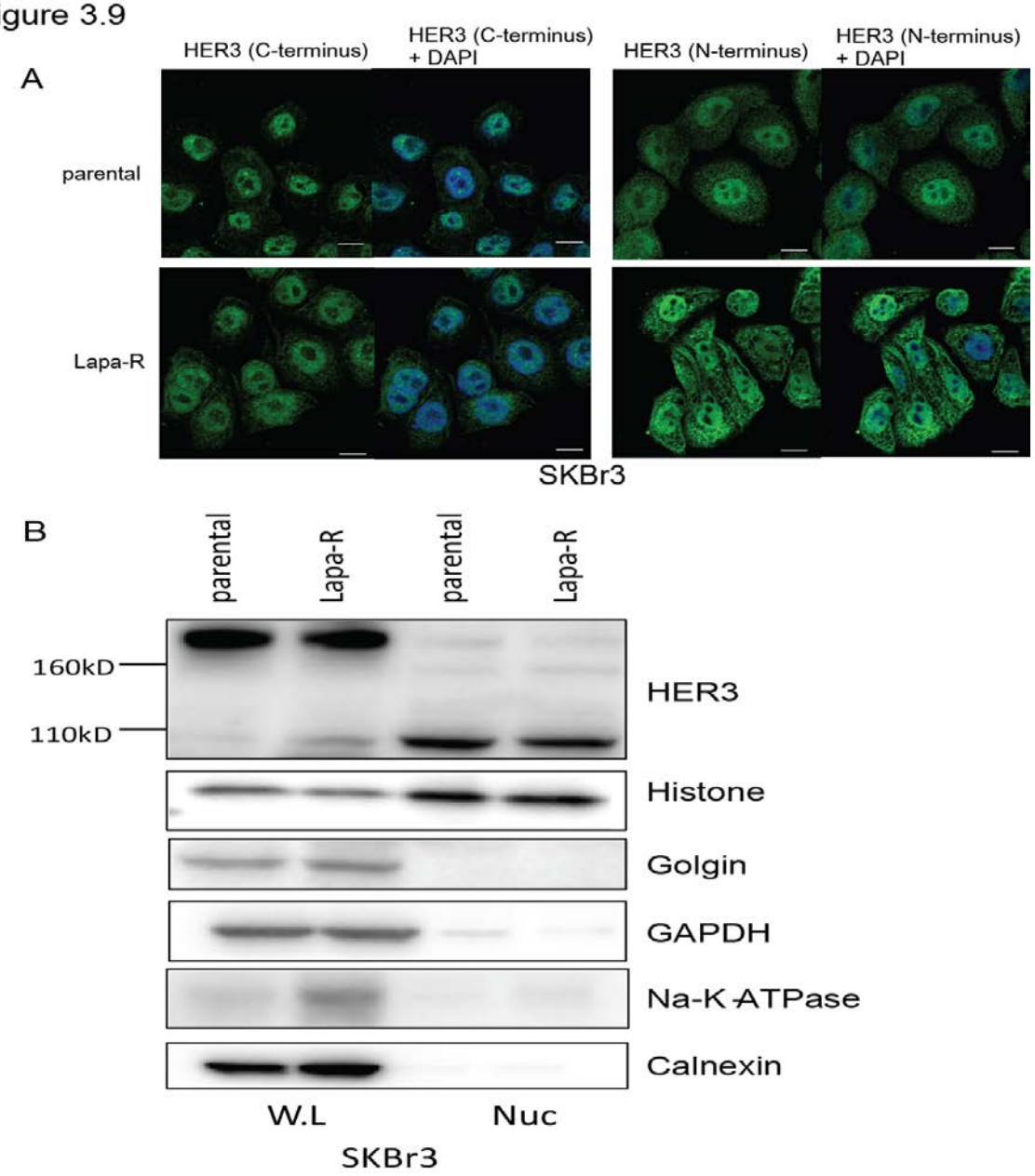

Figure 3.9 C-terminus HER3$_{100kD}$ in lapatinib resistant SKBr3 cells. A, The SKBr3 and acquired lapatinib-resistant cells (Lapa-R) were seeded onto the coverslip in 24-well plates. The cells were fixed and were subject to immunostaining for confocal microscopy. Nuclei were stained with DAPI (blue). The parental cells were treated with vehicle (Dimethyl sulfoxide, 0.1%). B, Equal amount of proteins from whole cell lysates (WL) (left 2 lanes) or nuclear extractions (Nuc) (right 2 lanes) of SKBr3 parental and acquired lapatinib-resistant SKBr3 (Lapa-R) cells were subject to immunoblotting with HER3, GAPDH, Calnexin, Golgin, Na-K ATPase, and Histone H3. Scale bar = 10 μm.

To examine whether nuclear HER3 localisation is induced by short-term trastuzumab treatment, the SKBr3 cells and BT474 cells were treated with trastuzumab for 1 hour, 4 hours, and 24 hours. Altered nuclear HER3 localisation as seen in the SKBr3-TR cells was not observed at these time points. HER3 membrane localisation detected by N-terminus HER3 antibody was enriched in both SKBr3 and BT474 cells. Taken together, trastuzumab induced HER3 nuclear localisation was only observed after long-term trastuzumab treatment probably due to the selection of resistant cells by trastuzumab, and an increase in nuclear $HER3_{100kD}$ localisation appeared to be associated only with the phenomenon of trastuzumab resistance in the SKBr3 cells.

Figure 4.3

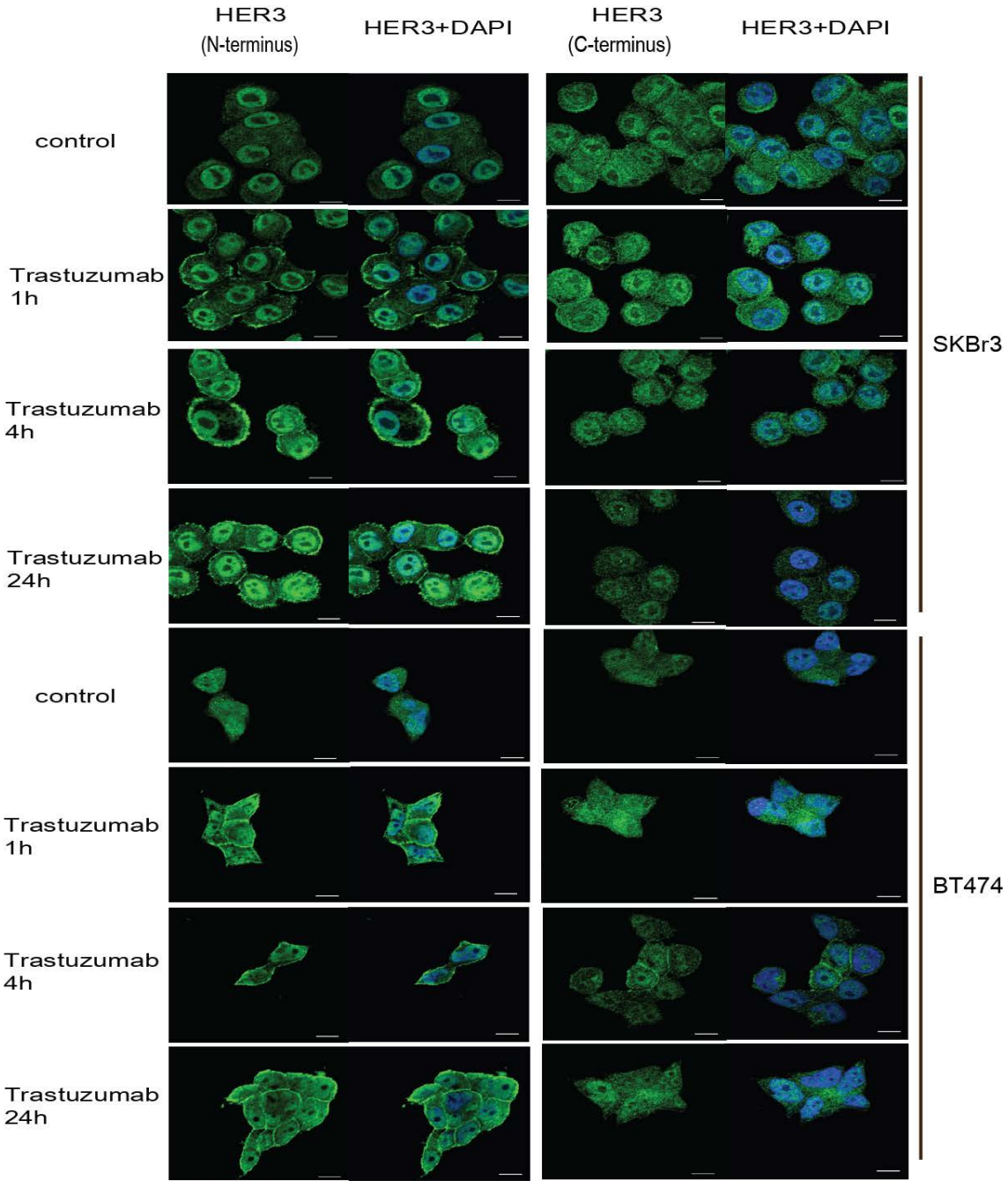

Figure 3.10 Nuclear HER3 localisation on short-term trastuzumab treatment. The SKBr3 and BT474 cells were seeded onto the coverslip in 24-well plate and treated with trastuzumab at indicated durations or human IgG for 24 hours. The cells were fixed and were subject to immunostaining with anti-HER3 antibodies (green) (raised against C-terminus and N-terminus). Nuclei were stained with DAPI (blue). Scale bar = 10 μm

3.2.5 Nuclear HER3$_{100kD}$ was reduced by ADAM17 and γ-secretase inhibitor.

HER4 has been previously shown to undergo a two-step proteolytic cleavage mediated by ADAM17 and γ-secretase[118]. It was therefore hypothesised that the enriched nuclear HER3 at 100kD which was derived from C-terminus in the SKBr3-TR cells may be produced by proteolytic cleavage as seen in HER4. The expression of cleaved ADAM17 was found to be upregulated in the SKBr3-TR cells (Figure 3.11A). On the contrary, PEN2 expression, a component of γ-secretase complex, was decreased in the BT474-TR cells while it was maintained in the SKBr3-TR cells (Figure 3.11A). An ADAM17 inhibitor and a γ-secretase inhibitor significantly reduced HER3$_{100kD}$ in the nucleus and both inhibitors increased HER3$_{180kD}$ in the nucleus in the SKBr3-TR cells (Figure 3.11B, 3.12A, B). These results indicate that the production of HER3$_{100kD}$ was mediated by ADAM17 and γ-secretase in the SKBr3-TR cells since cleaved ADAM17 and PEN2 expression was maintained in these cells. Nuclear HER3 translocation was not observed in the BT474-TR cells, possibly due at least in part to the lower expression of PEN2. Taken together, the results suggest that both ADAM17 and γ-secretase activity should be increased to induce HER3$_{100kD}$ in the nucleus.

Figure 3.11

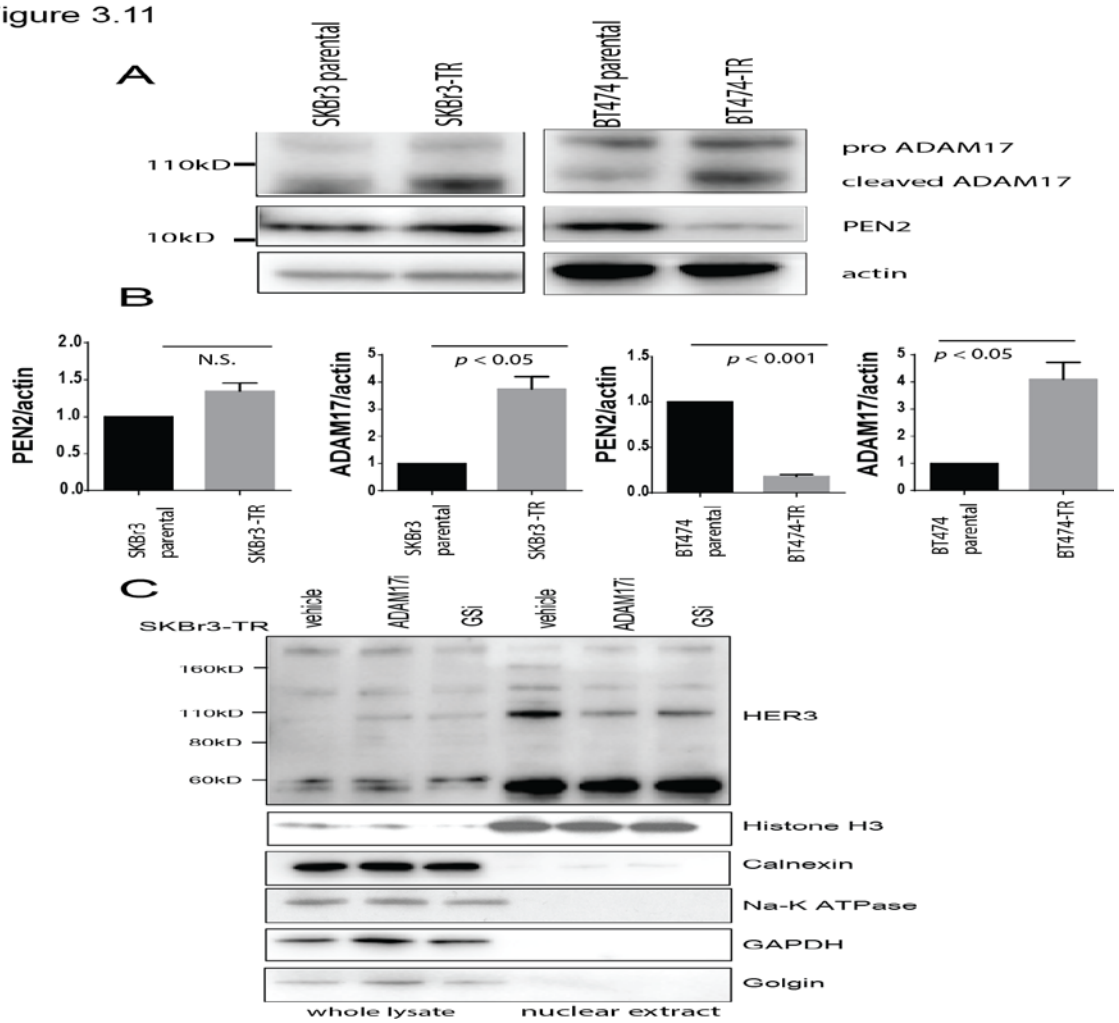

Figure 3.11 A reduction of nuclear HER3$_{100kD}$ by the ADAM17 (A Disintegrin And Metalloproteinase 17) inhibitor (ADAM17i) and the γ-secretase inhibitor (GSi) in the acquired trastuzumab-resistant SKBr3 (SKBr3-TR) cells. A, Equal amount of proteins from SKBr3 parental and SKBr3-TR cells or BT474 parental and trastuzumab resistant BT474 (BT474-TR) cells were subject to immunoblotting with ADAM17, presenilin enhancer 2 (PEN2), and actin. B, Statistical analysis was performed by using semi-quantification of PEN2 and ADAM17 expression for SKBr3 parental, SKBr3-TR, BT474, and BT474-TR cells from 3 different experiments. Bars indicate means ± SEM. Paired *t*-test was used to detect the statistical significance. C, Equal amount of proteins from whole cell lysates (left 3 lanes) or nuclear extractions (right 3 lanes) of the SKBr3-TR cells treated with solvent (0.1% Dimethyl sulfoxide, DMSO) for 24 hours, ADAM17i (10 μM of INCB4298 for 24 hours), or GSi (25μM of DAPT for 4 hours) in serum starved condition were subject to immunoblotting with HER3, GAPDH, Calnexin, Golgin, Na-K ATPase, and Histone H3.

Figure 3.12

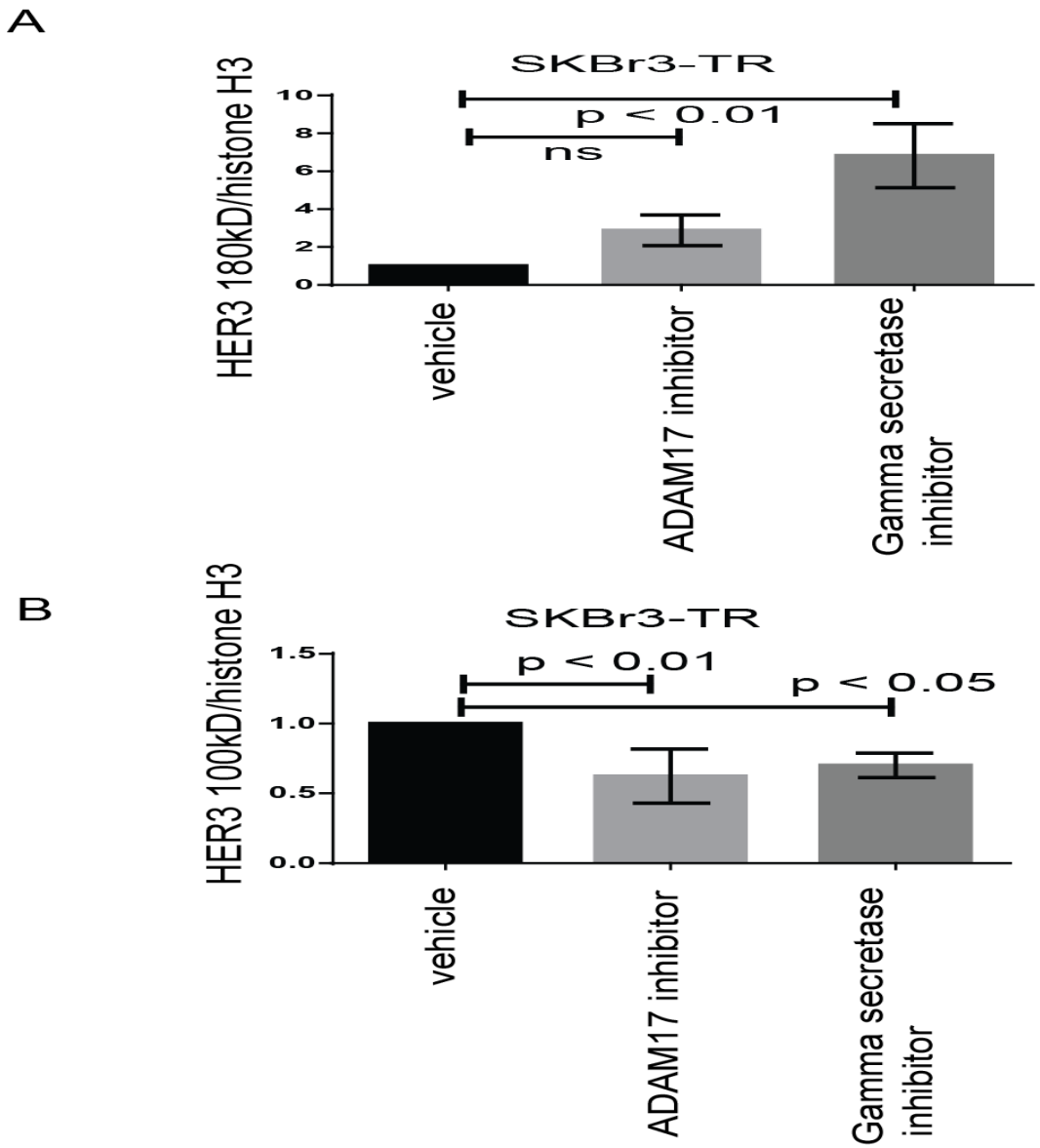

Figure 3.12 Semi-quantification of nuclear HER3 at 180kD and 100kD for SKBr3-TR cells treated with vehicle (DMSO), ADAM17, or gamma-secretase inhibitor. HER3 expression at 180kD and 100kD from 3 independent experiments were semi-quantified and were normalised to Histone H3. DMSO was used as a control. One-way ANOVA with Bonferroni correction was used to detect the statistical significance from 3 repeated experiments. Bars show means with SEM.

As shown previously, HER3 in the nucleus detected by the C-terminus antibody was increased in the SKBr3-TR cells (Figure 3.6A). To examine whether ADAM17 inhibitor or γ-secretase inhibitor could reduce nuclear HER3 as visualised by immunofluorescence, SKBr3-TR cells were treated with these inhibitors. Confocal microscopy images showed that the SKBr3-TR cells treated with these inhibitors reduced nuclear HER3 detected by the C-terminus HER3 antibody (Figure 3.13). The enriched nuclear HER3 was decreased and this corresponded with a decrease of $HER3_{100kD}$ in the nucleus as seen in western blotting (Figure 3.11B). These results suggest that HER3 detected in the nucleus by the C-terminus antibody was derived from $HER3_{100kD}$, and both ADAM17 and γ-secretase were necessary to mediate $HER3_{100kD}$ cleavage and nuclear translocation.

Figure 3.13

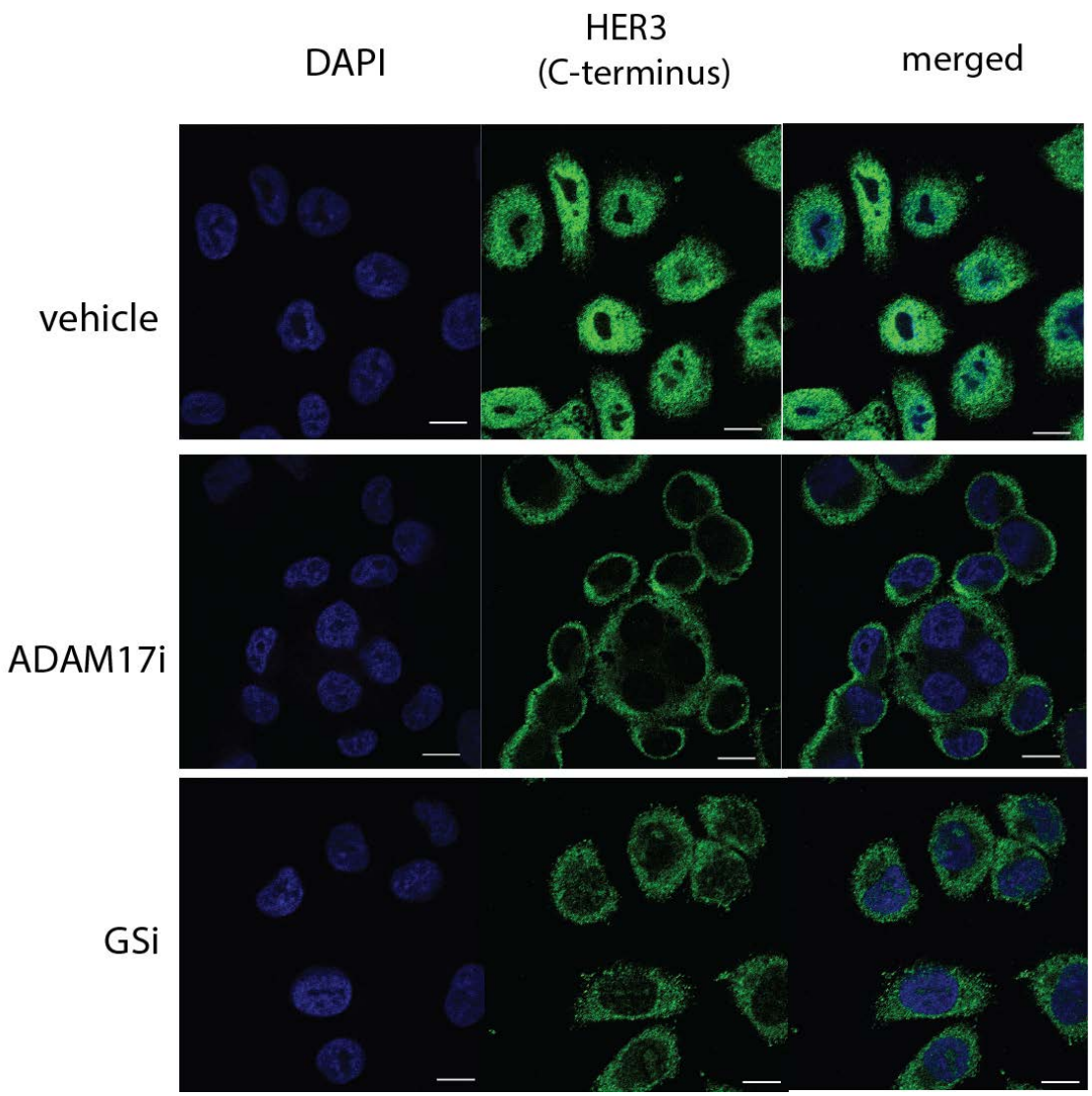

Figure 3.13 Reduction in nuclear HER3 by ADAM17 and γ-secretase inhibitor. The trastuzumab resistant SKBr3 (SKBr3-TR) cells were seeded onto the coverslip and the cells were allowed to attach in full serum media. The media were washed out and replaced with serum starved media. Then the cells were treated with DMSO, ADAM17i, or GSi as shown in figure 3.12. The cells were fixed and immunostained by the HER3 antibody raised against C-terminus (green). The nuclei were stained with DAPI (blue). The images were visualised by confocal microscope. Scale bar = 10 μm

Two-step proteolytic cleavage of HER4 has been reported to begin within 10-15 minutes of HRG binding to HER4[118]. The next experiment tested whether exogenous heregulin stimulation had an effect on HER3 cleavage. Heregulin stimulation for 10 minutes induced $HER3_{180kD}$ translocation into the nucleus (Figure 3.14A, B), while nuclear $HER3_{100kD}$ remained similar on heregulin stimulation (Figure 3.14A). These observations indicate that HER3 could undergo proteolytic cleavage independently of exogenous heregulin stimulation.

Figure 3.14

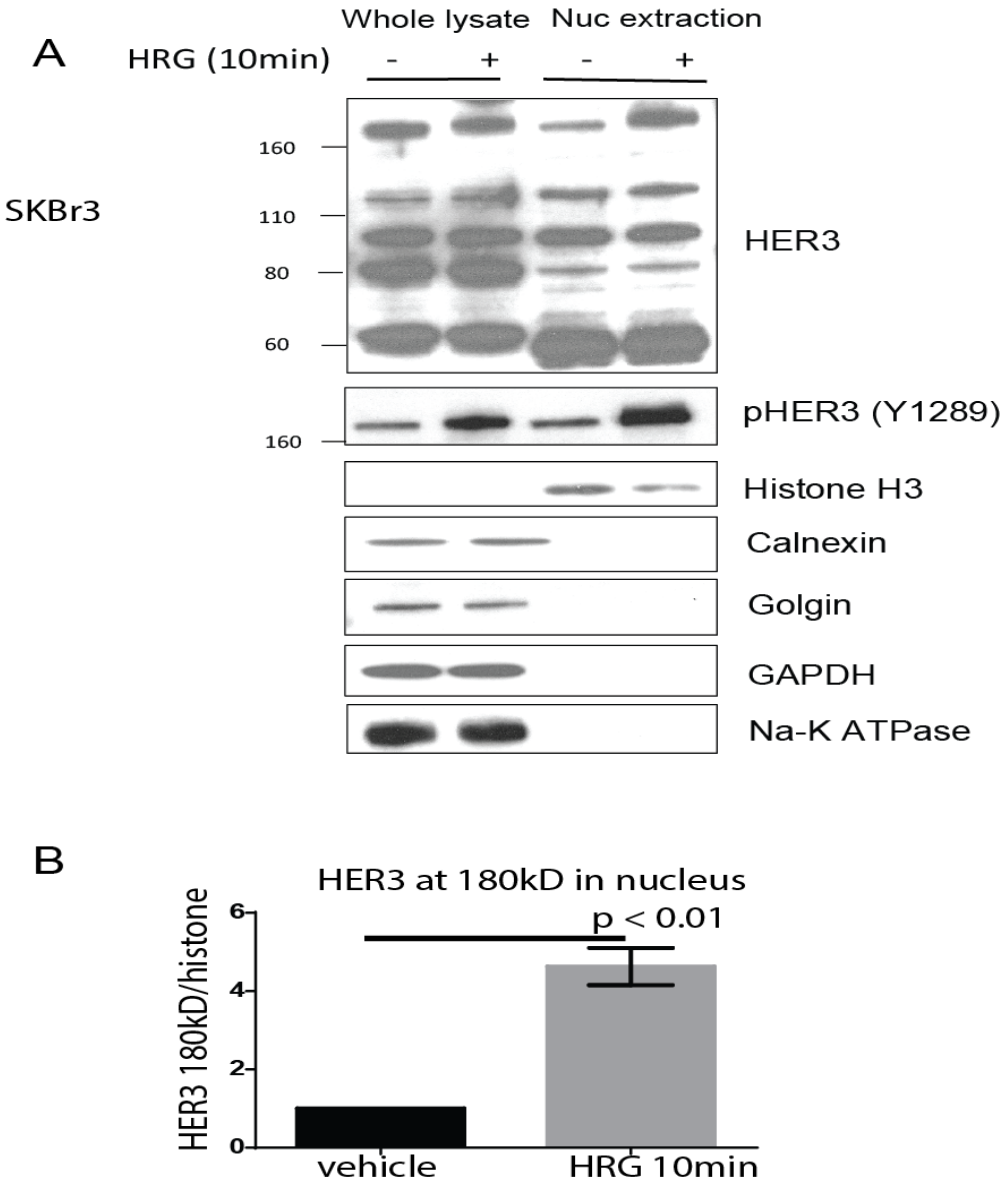

Figure 3.14 An increase of nuclear $HER3_{180kD}$ but not $HER3_{100kD}$ by heregulin (HRG) stimulation. A, The SKBr3 cells were serum-starved overnight and treated with 100 ng/mL of heregulin (HRG) or saline for 10min. Equal amount of proteins from whole cell lysates (left 2 lanes) or nuclear extractions (right 2 lanes) of the SKBr3 cells treated with or without HRG were subject to immunoblotting for HER3, GAPDH, Calnexin, Golgin, Na-K ATPase, and Histone H3. B, Semi-quantification of nuclear HER3 at 180kD relative to histone for the SKBr3 cells treated with HRG or saline. Paired *t*-test was used to test statistical significance from 3 repeated experiments. Bars show means with SEM.

3.2.6 HER3 is important for HER2-positive breast cancer cell survival and modification of HER3 subcellular localisation affects trastuzumab response in the resistant cells.

It is suggested that HER3 is important for cell survival in HER2-positive cell lines[55,56]. Therefore, HER3 knockdown was assessed in the SKBr3-TR cells. HER3 knockdown significantly reduced the number of colonies in the SKBr3-TR cells and BT474-TR cells with or without trastuzumab treatment ($p < 0.001$) (Figure 3.15A, 3.16A), suggesting that HER3 is crucial for proliferation for these HER2-overexpressing cells. However, continuous trastuzumab did not add to effects of HER3 knockdown in SKBr3-TR cells (Figure 3.15A). Since HER3 knockdown reduced colony formation by more than 80% (Figure 3.15A), there was a possibility that any effect of trastuzumab on response to HER3 knockdown was not observed in the SKBr3-TR and BT474-TR cells due to the loss of huge numbers of cells.

Anti-HER3 monoclonal antibody SGP1 blocks HRG binding and has an effect on dose-dependent growth inhibition with trastuzumab in HER2-positive cell lines[14]. SGP1 did not inhibit colony formation without trastuzumab in the SKBr3-TR cells, but inhibition of colony formation was observed when the cells were co-treated with trastuzumab ($p < 0.01$) (Figure 3.15B). Similar observation

was found in the BT474-TR cells (Figure 3.16B). SGP1 did not alter the subcellular localisation of HER3 (Figure 3.15C), hence effects of trastuzumab inhibition with SGP1 could be due to different causes, including its effect on NRG1 binding in these cells. These results indicate that HER3 is important for cell survival in the SKBr3-TR cells and blocking HER3 by the monoclonal antibody with trastuzumab affects cell viability in the SKBr3-TR and BT474-TR cells.

Figure 3.15

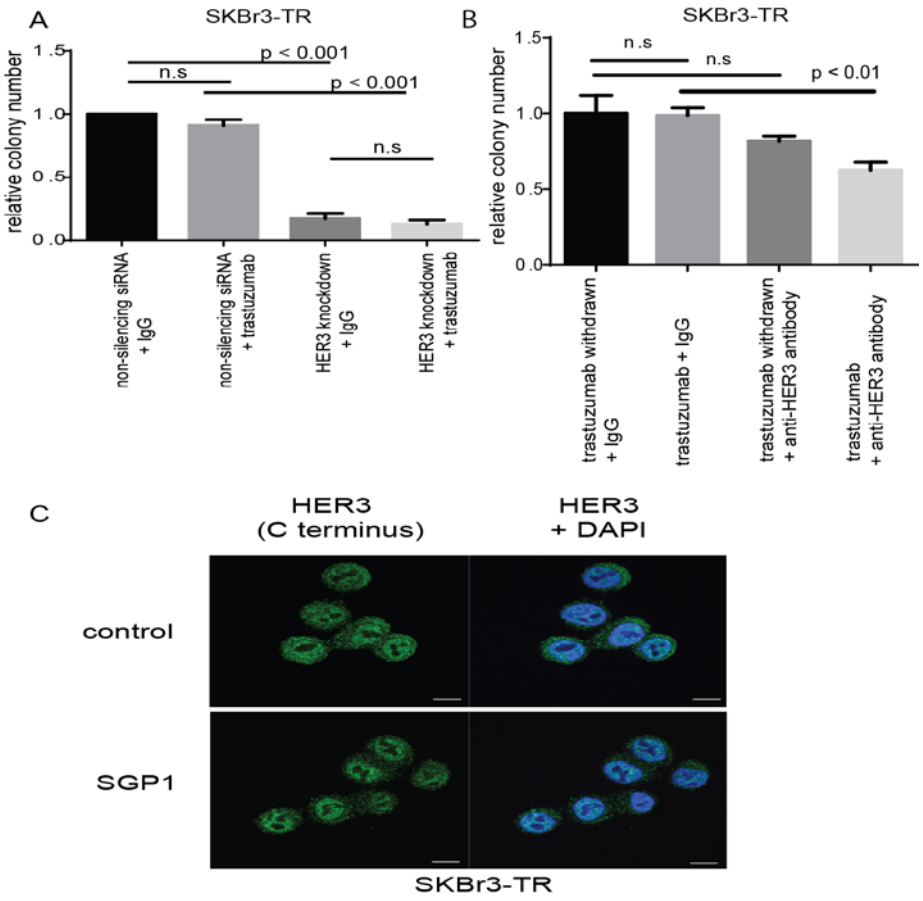

Figure 3.15 Effect of HER3 knockdown and anti-HER3 monoclonal antibody for survival of acquired trastuzumab-resistant SKBr3 (SKBr3-TR) cells. A, The SKBr3-TR cells were transfected with non-silencing siRNA or siRNA against HER3. After 48 hours of transfection, predetermined number of cells were seeded in 6-well plate and treated with trastuzumab or human IgG (40 μg/mL) for 14 days. The relative colony number to IgG treated SKBr3-TR cells with non-silencing siRNA was calculated. Two-way ANOVA with Bonferroni correction was used to detect the statistical significance of 3 independent experiments in triplicate. B, Similarly, predetermined number of cells were seeded in 6-well plate. The SKBr3-TR cells were treated with an anti-HER3 antibody (SGP1) or mouse IgG at 1 μg/mL with trastuzumab or human IgG (40 μg/mL) for 14 days. The relative colony number was normalised to trastuzumab withdrawn + IgG treated cells. Two-way ANOVA with Bonferroni correction was used. Bars show means with SEM. C, The SKBr3-TR cells were treated with SGP1 or mouse IgG together with trastuzumab (40 μg/mL) for 24 hours. The cells were immunostained with HER3 antibody (green) (raised against C-terminus) and nuclei were stained with DAPI (blue) to be visualised with confocal microscope. Scale bar = 10 μm

Figure 3.16

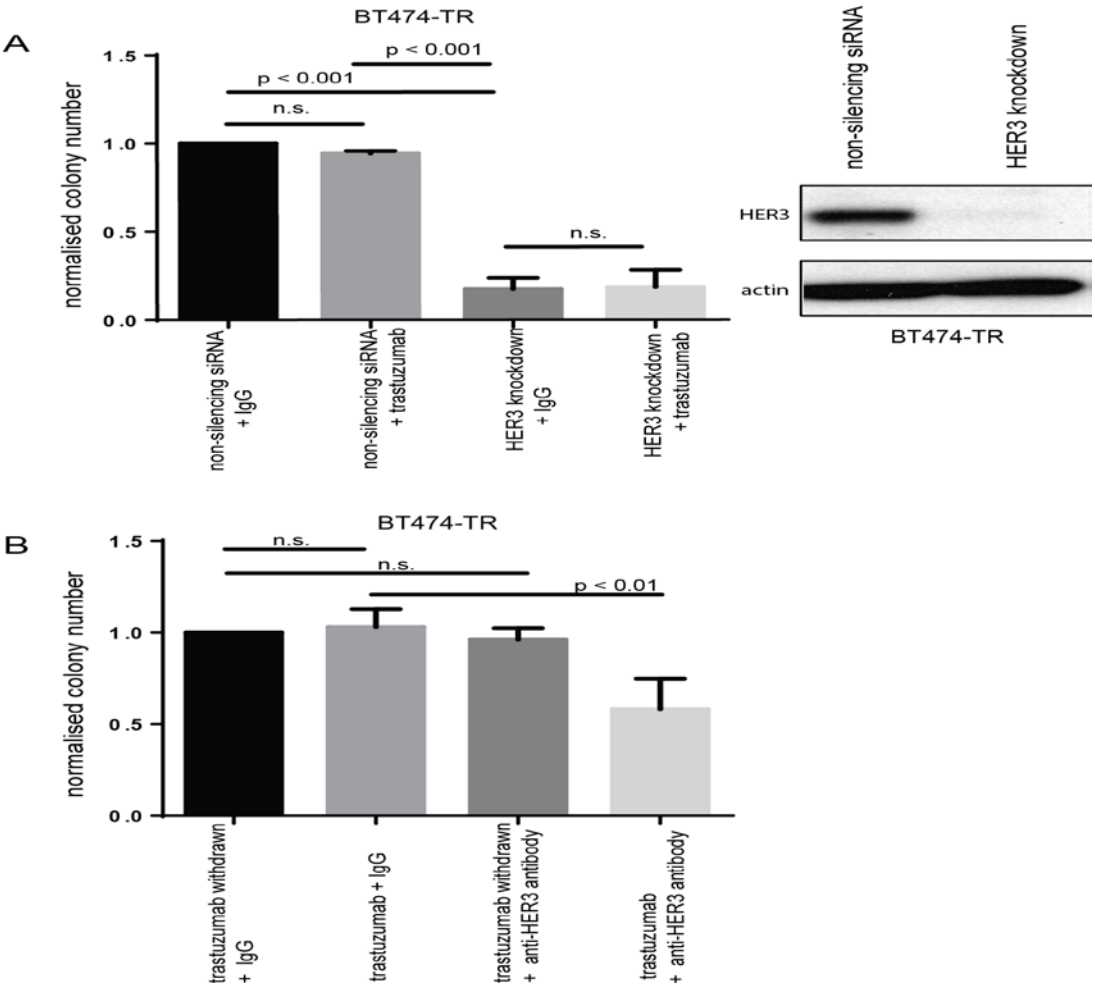

Figure 3.16 Effect of HER3 monoclonal antibody on sensitivity to trastuzumab in the acquired trastuzumab resistant BT474 (BT474-TR) cells. A, Predetermined number of BT474 cells were seeded in 6-well plate and were left for 1 day without trastuzumab. Cells were transfected with non-silencing siRNA or siRNA against HER3. After 48h, predetermined number of the cells were seeded in 6-well plate and were treated with IgG or trastuzumab (40 µg/mL) for 14 days. Colonies were counted and normalised to control (non-silencing siRNA + IgG). Each experiment had 3 replicates and was repeated 3 times. Bars show means with SEM. Two-way ANOVA with Bonferroni correction was used to detect the statistical significance. B, Predetermined number of cells were seeded in 6 well plate and treated with IgG (control), anti-HER3 monoclonal antibody (1 µg/mL), with or without trastuzumab (40 µg/mL) for 14 days. Colonies were counted and normalised to control. Each experiment had 3 replicates and was repeated 3 times. Two-way ANOVA with Bonferroni correction was used to detect the statistical significance. Bars show means with SEM.

An ADAM17 inhibitor (INCB4298, 10μM) and a γ-secretase inhibitor (DAPT, 25μM) were shown to decrease nuclear HER3 (Figure 3.11B, 3.13) and, thus these inhibitors were assessed to determine if they could recover the sensitivity to trastuzumab in the resistant cells. INCB4298 at this concentration reduced colony with or without continuous trastuzumab treatment ($p < 0.0001$, and $p < 0.001$, respectively) (Figure 3.17). When trastuzumab was withdrawn, the γ-secretase inhibitor did not inhibit colony formation, while the inhibitor with continuous trastuzumab treatment significantly decreased colony in the SKBr3-TR cells ($p < 0.01$) (Figure 3.17). However, the reduction in colony formation was only 30% with γ-secretase inhibitor with trastuzumab treatment, compared with trastuzumab alone.

Figure 3.17

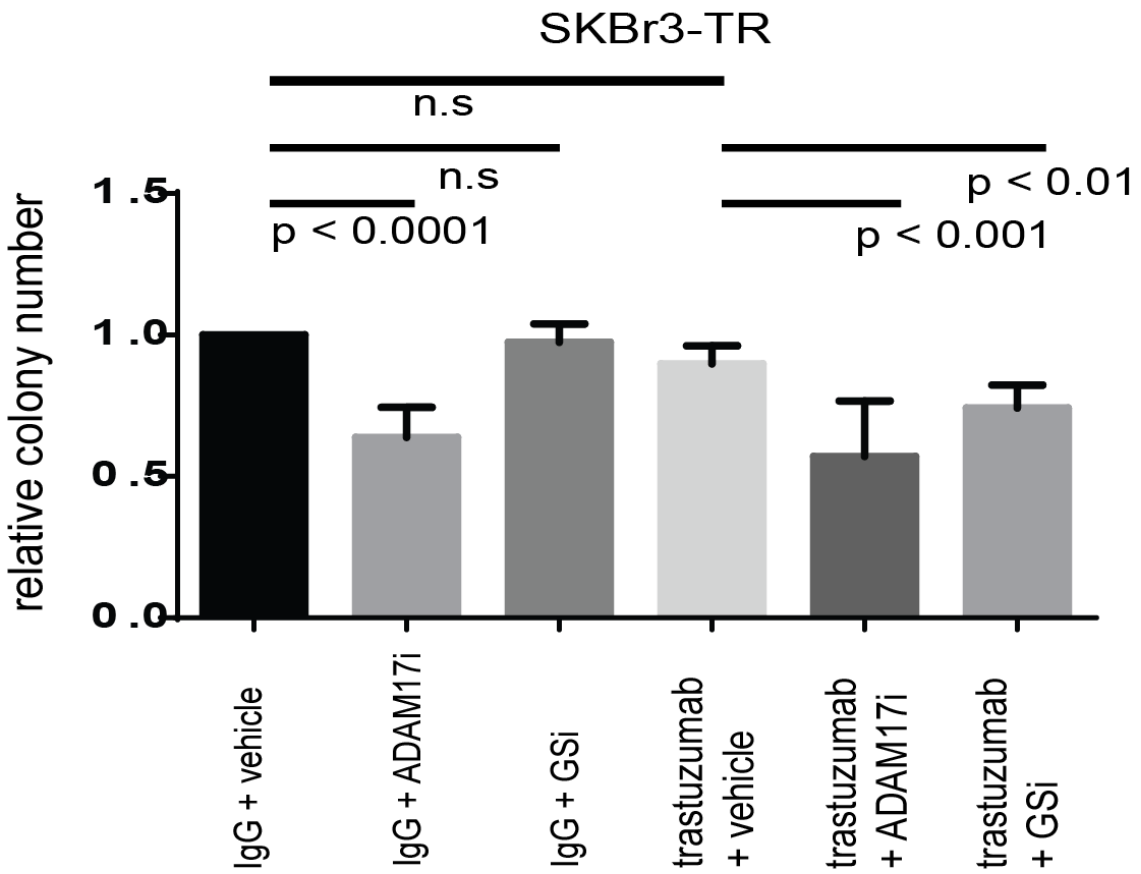

Figure 3.17 Effect of γ-secretase inhibitor (GSi) and ADAM17 inhibitor (ADAM17i) with trastuzumab in the trastuzumab resistant SKBr3 (SKBr3-TR) cells. Predetermined number of cells were seeded in 6-well plate. Trastuzumab was withdrawn 24 hours before starting treatment. The SKBr3-TR cells were treated with vehicle (dimethyl sulfoxide, DMSO), ADAM17 inhibitor (INCB4298, 10 μM), or γ-secretase inhibitor (DAPT, 25 μM) with human IgG or trastuzumab (40 μg/mL) for 14 days. The relative colony number was normalised to DMSO and human IgG treated cells (vehicle only). Two-way ANOVA with Bonferroni correction was used to test statistical significance of 3 independent experiments in triplicate. Bars show means with SEM.

3.3 Discussion

3.3.1 Trastuzumab induces $HER3_{100kD}$ and allows HER3 to translocate into the nucleus.

This is the first study that has studied HER3 subcellular localisation in relation to trastuzumab treatment and resistance. The first observation was that HER3 detected by an antibody raised against its N-terminus was detected less intensely in the nucleus when SKBr3 cells became resistant to trastuzumab. This observation was not seen in the BT474 cells or other breast cancer cells that acquired resistance to trastuzumab. Since several resistant mechanisms have been identified[24-26,28-30,32], these cells may use different routes to acquire resistance to trastuzumab. This study was initiated based on the hypothesis that trastuzumab may affect HER3 due to the close relationship between HER2 and HER3, and thus the focus was on HER3. However, unbiased screening methods including whole genome DNA sequencing or protein array may be able to identify alternative routes for trastuzumab resistance if time and cost had permitted. Short-term trastuzumab treatment (up to 24 hours) did not induce HER3 nuclear localisation. Furthermore, the lapatinib-resistant SKBr3 cells did not show the pattern of HER3 subcellular localisation as seen in trastuzumab resistance. These observations suggest that HER3 nuclear localisation may be observed

only in selected trastuzumab resistant cells since only SKBr3 cells were found to have nuclear HER3 translocation in the initial panel of cell lines examined.

A few published reports have suggested that HER3 has several fragments as shown in western blot, and $HER3_{100kD}$ band is detectable in some figures from these publications (Figure 1B, Adilakshmi et al., Figure 2B, Andrique et al.), although there have been no investigations of the mechanism and the origin of $HER3_{100kD}$[129,132]. Both $HER3_{100kD}$ and $HER3_{180kD}$ could be immunoprecipitated and detected using 2 different antibodies. Furthermore, knockdown of HER3 led to a decrease of $HER3_{100kD}$ in 2 different cell lines. These data support the specificity of the antibody for $HER3_{100kD}$, and if time had permitted, it would have been useful to perform the HER3 knockdown experiment with nuclear extraction to test antibody specificity. It was hypothesised that $HER3_{100kD}$ could be a result of HER3 proteolytic cleavage by proteases and may be induced by trastuzumab treatment. Previously, other investigators had tested whether HER3 undergoes proteolytic cleavage by proteases in H358 human lung cancer cells by using ADAM17 inhibitor (TAPI2) but the cleavage was not identified[132]. Similarly, several protease inhibitors were tested in Schwann cells for HER3 cleavage but

failed to identify cleaved products[129]. It is possible that HER3 cleavage may occur only in particular cell lines or at certain circumstances since it is not frequently observed. In this project, 2 inhibitors against γ-secretase and ADAM17 were used and they decreased the detection of nuclear $HER3_{100kD}$ in the SKBr3-TR cells.

3.3.2 Nuclear HER3 is reduced by ADAM17 and γ-secretase inhibitor

It has been reported from our laboratory that ADAM17 is upregulated by short-term trastuzumab treatment to maintain phosphorylation of HER receptors by increasing ligand availability[32]. Here, ADAM17 and PEN2, a surrogate marker of γ-secretase activity[166,167], remained increased after long-term trastuzumab treatment in the SKBr3 cells. It is possible that ADAM17 and PEN2 could induce $HER3_{100kD}$ and enable HER3 translocation into the nucleus during trastuzumab treatment, and the surviving cells were enriched with nuclear HER3 during trastuzumab resistance. The upregulation of ADAM17 was also observed in the BT474-TR cells but PEN2 level was decreased. Since ADAM17 sheds the ectodomain and the γ-secretase complex activity can be higher when the length of extracellular domain is shorter[152,161], both ADAM17 and γ-secretase should be

upregulated to induce truncated $HER3_{100kD}$ as seen in the SKBr3-TR cells. Therefore, the lack of PEN2 upregulation may have contributed to a lack of increase in nuclear HER3 in BT474-TR cells. This could be tested by inducing PEN2 expression in the BT474-TR cells and it would be interesting to see if PEN2 activation could induce nuclear HER3 in the BT474-TR cells. HER4 undergoes proteolytic cleavage upon HRG stimulation[118]. The reason why HRG induces HER4 cleavage is unclear. One possible explanation is that HRG may promote HER4 and ADAM17 co-localisation[152]. However, instead of promoting $HER3_{100kD}$ nuclear translocation upon HRG stimulation, HRG induced full-length $HER3_{180kD}$ in the nucleus, probably as a result of the internalisation of whole receptor since ligand stimulation is known to activate internalisation of membrane receptors[55,152,188].

3.3.3 Limitations of the study

There are several limitations of this study. It would be better to have had more cell line models with HER3 nuclear localisation in addition to SKBr3 cell line to investigate the mechanisms of HER3 cleavage. HER3 cleavage site could also

be identified by using mass spectrometry. It would be interesting if mutated HER3 cleavage site could inhibit nuclear $HER3_{100kD}$ in the SKBr3-TR cells. Afterwards, it would be a further test of the phenotype conferred by HER3 cleavage if $HER3_{100kD}$ could be introduced into the sensitive cell lines to see whether it confers resistance in the trastuzumab sensitive cells. Furthermore, the target(s) of $HER3_{100kD}$ in the nucleus is unclear although HER3 has been reported to interact with cyclin D1 in the nucleus[132]. As a future direction, ChIP-sequence could be suggested for this purpose, using the antibody to the carboxyl-terminus of HER3. Treatment of SKBr3-TR cells with ADAM17 inhibitor or γ-secretase inhibitor was not sufficient to recover trastuzumab sensitivity since only 20-30 % of growth inhibition was observed (Figure 3.17). In addition, it would be interesting to investigate a specific compound that inhibits nuclear localisation of HER3 or assessing cell cycle inhibitor to inhibit the upregulation of cyclin D1 due to HER3 interaction in the nucleus.

CHAPTER 4.

ASSESSING THE PREDICTIVE AND PROGNOSTIC VALUES OF NUCLEAR HER3 IN RELATION TO TRASTUZUMAB TREATMENT AND CLINICAL OUTCOMES

4.1 Introduction

In chapter 3, nuclear HER3 was observed in the trastuzumab resistant SKBr3 cells and was shown to be induced by ADAM17 and γ-secretase. These results indicate that nuclear HER3 could be a biomarker for trastuzumab resistance in HER2-positive breast cancer. It has been identified that nuclear HER3 can be detected by both N-terminus and C-terminus anti-HER3 antibody on human tissue samples[74,140], However, it is unclear whether nuclear HER3 could be a biomarker. As discussed, HER3 is often co-expressed with HER2, and HER3 is important for HER2-positive breast cancer[35]. In this chapter, nuclear HER3 was assessed by IHC in cell pellets as well as tumour samples from xenograft models and HER2-positive breast cancer patients. The prognostic and predictive values

of HER3 expression in relation to trastuzumab treatment and patients' outcome were further assessed in different cohorts of patients.

4.2 Results

4.2.1 Nuclear HER3 is associated with trastuzumab resistance in HER2-positive breast cancer cell lines

To examine if the existence of HER3 in the nucleus is related to innate trastuzumab resistance, a method was developed for HER3 immunohistochemical staining, and was applied to a panel of HER2-positive breast cancer cells. The formalin-fixed cell pellets of these HER2-positive cell lines (n = 18) were provided from the collaborators at UCLA with the exception of SKBr3 and SKBr3-TR cells which were prepared in Oxford as described in Materials and Methods. Initial titration of the carboxyl-terminal anti-HER3 antibody (ab34641) was performed using the SKBr3 cell line transfected with non-silencing siRNA or siRNA against HER3 (Figure 4.1A). As observed in the confocal microscopy images, HER3 was found mainly in the cytoplasm in the SKBr3 and BT474 cell lines (Figure 4.1B). HER3 in the nucleus was observed in the SKBr3-TR cells (Figure 4.1B), corresponding to the distribution seen by

immunofluorescence (Figure 3.6A). HER3 nuclear staining was assessed as per protocol described in the Methods section. Trastuzumab sensitivity was determined according to the previous publication from the collaborator[186]. Of the 18 HER2-positive breast cancer cell lines, 2 cell lines (UACC732 and SKBr3-TR cells) possessed nuclear HER3 among trastuzumab resistant cells (n = 12), while none of trastuzumab sensitive cells was found to have nuclear HER3 (n = 6) (chi-square test, p = 0.29) (Table 4.1).

Figure 3.18

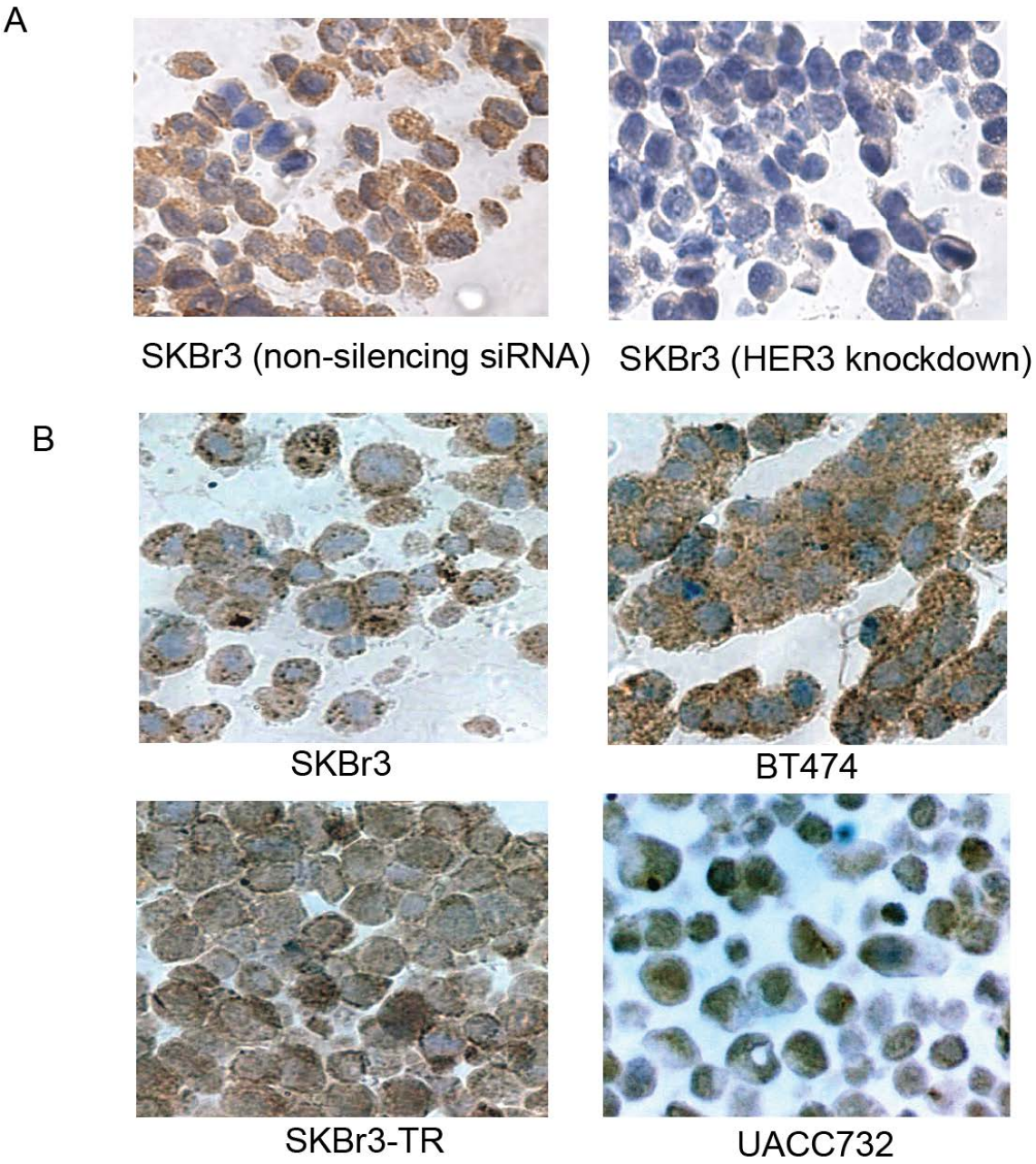

Figure 4.1 Representative pictures of HER3 immunohistochemistry (IHC). A, The SKBr3 cells transfected with non-silencing siRNA and siRNA against HER3 were subject to immunohistochemistry (IHC) with HER3 antibody raised against its C-terminus. B, Representative pictures of HER3 immunohistochemistry for the SKBr3, BT474, acquired trastuzumab-resistant SKBr3 (SKBr3-TR) cells, and UACC732 cells (x40).

Table 4.1 Nuclear HER3 in a panel of HER2-positive breast cancer cell lines.

Cell line	Nuclear HER3	Trastuzumab sensitivity
SKBr3-TR	+	R
UACC732	+	R
MDA-MB-361	-	R
SUM190	-	R
SUM225	-	R
HCC1954	-	R
HCC1419	-	R
JIMT1	-	R
HCC202	-	R
HCC1569	-	R
MDA-MB-453	-	R
UACC893	-	R
UACC 812	-	S
ZR75-30	-	S
SKBr3	-	S
EFMA192A	-	S
HCC2218	-	S
BT474	-	S

Note: All the samples were non-trastuzumab treated samples except for acquired trastuzumab resistant SKBr3 cells (SKBr3-TR). These samples were fixed in formalin and were subject to immunohistochemistry. Chi-square test was used to assess nuclear HER3 in the trastuzumab sensitive and resistant cells.

4.2.2 Nuclear HER3 was associated with trastuzumab resistance in xenograft studies.

To investigate whether nuclear HER3 is associated with trastuzumab resistance in xenograft samples, 11 cell lines were inoculated into athymic mice and were treated with trastuzumab for 7 weeks and tumours were taken for IHC (These experiments were done by Dr. Neil O'Brien, ULCA). There were 2 xenografts from each cell line (sample A and B). The samples were provided from the collaborators at UCLA. Representative images are shown in Figure 4.2. As seen in cell pellets, HER3 was mainly observed in the cytoplasm. Nuclear HER3 was found in 2 of 6 trastuzumab resistant tumour samples, while none was found in 16 sensitive tumour samples (chi-square test, p = 0.015) (Table 4.2). Some tumours were resistant *in vitro* but showed response to trastuzumab in animal models (for example, BT474-TR), presumably due to ADCC activity. The HCC1569 cells were innately trastuzumab-resistant, but did not have detectable nuclear HER3 by IHC in the cell pellet sample. However, nuclear HER3 was clearly identified in the xenograft samples. A possible explanation for this is that nuclear HER3 in the HCC1569 cells could be due to trastuzumab-induced nuclear localisation. Since the antibody used for HER3 staining detects C-terminus of

HER3 but it is not specific to $HER3_{100kD}$, these results imply that nuclear HER3, either cleaved or non-cleaved, could be related to trastuzumab resistance.

Figure 4.2

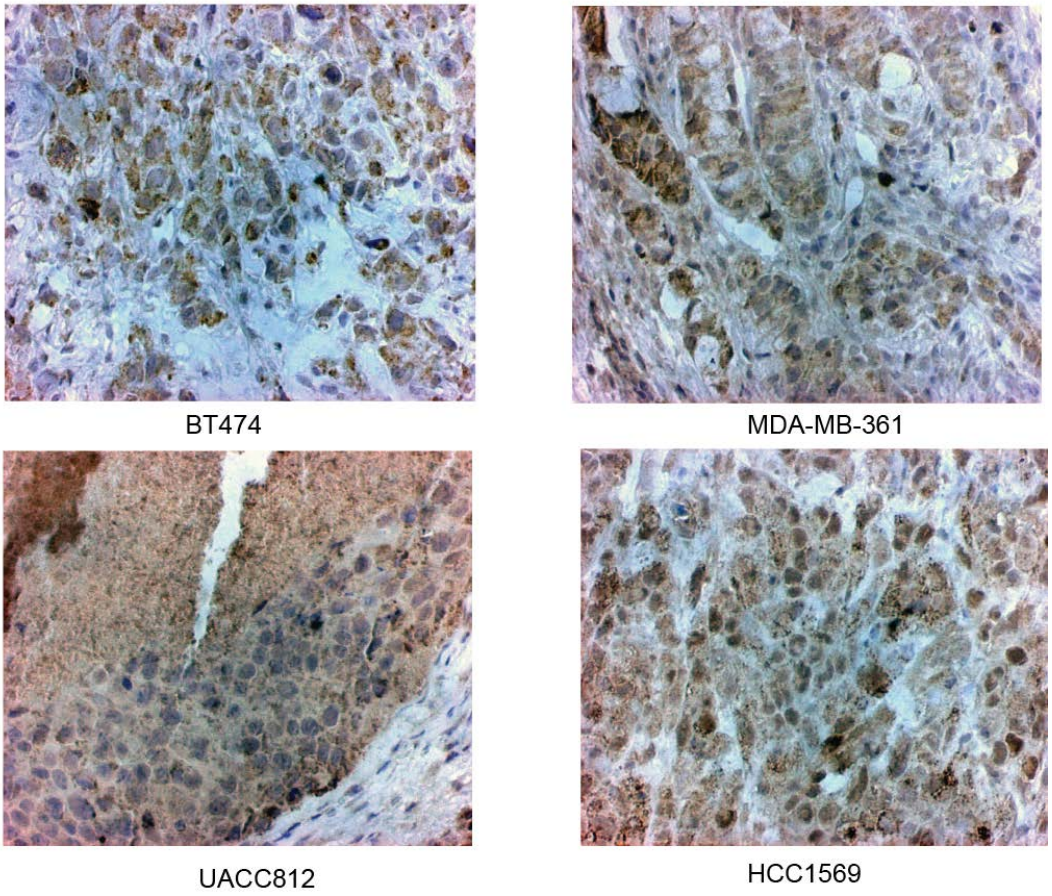

Figure 4.2 Nuclear HER3 in trastuzumab-resistant tumours in mice. Mice harbouring xenografts generated from human breast cancer cells were treated with trastuzumab at 10mg/kg intraperitoneally twice a week for 7 weeks. Responders were defined as no tumour growth or observed tumour decrease in size after trastuzumab treatment. Non-responders were all others. Representative pictures of HER3 staining in breast tumours (BT474, MDA-MB-361, UACC812, HCC1569) are shown (x40).

Table 4.2 Nuclear HER3 in HER2-positive tumours in mice and trastuzumab sensitivity.

Xenograft	Nuclear HER3	Trastuzumab sensitivity
HCC1569 A	+	R
HCC1569 B	+	R
SUM190-TR A	−	R
SUM190-TR B	−	R
JIMT1 A	−	R
JIMT1 B	−	R
BT474-TR A	−	S
BT474-TR B	−	S
BT474 A	−	S
BT474 B	−	S
HCC1954 A	−	S
HCC1954 B	−	S
MDA-MB-361A	−	S
MDA-MB-361B	−	S
EFM192A A	−	S
EFM192A B	−	S
SUM190 A	−	S
SUM190 B	−	S
SUM225 A	−	S
SUM225 B	−	S
UACC812 A	−	S
UACC812 B	−	S

Note: TR means trastuzumab resistance. The cells were inoculated in athymic mice and treated with trastuzumab intraperitoneally for 7 weeks. All the samples were duplicated (A, B). Tumour response were defined as stated in the method section. Mice were sacrificed and tumour samples were collected for immunohistochemistry. The chi-square test was used to evaluate nuclear HER3 and trastuzumab sensitivity.

4.2.3 Nuclear HER3 is induced by trastuzumab and docetaxel treatment

To test the hypothesis that the nuclear HER3 in innate and acquired trastuzumab-resistant tumours could be a key factor for trastuzumab response, pairs of human tissue samples (n = 5) of pre- and post-trastuzumab monotherapy (8 mg/kg, q3w) in the neoadjuvant setting provided by Dr. Daniele Generali (Institute Ospitalieri di Cremona, Italy) were assessed. Briefly, patients with HER2-positive invasive breast cancer were eligible for this prospective window of opportunity trastuzumab trial in Italy. Patients underwent tumour size evaluation by caliper measurement and tumour biopsy before and after one dose of trastuzumab monotherapy, followed by 4 cycles of trastuzumab (6 mg/kg, q3w) and docetaxel (100 mg/m^2, q3w). Finally, definitive surgery was performed after measuring tumour response by caliper measurement (Figure 4.3A). Representative pictures of HER3 staining of human breast cancer are shown in Figure 4.3B.

Twelve patient samples were available and 5 of these were pre- and post-trastuzumab samples. Post trastuzumab monotherapy samples were not available for other 7 samples because re-biopsy was declined by these patients. Tumour response and nuclear HER3 at baseline, after 1 cycle of trastuzumab

treatment, and after 4 cycles of docetaxel and trastuzumab treatment were summarised in Table 4.3. Nuclear HER3 (any positivity) was found in 5 patients at baseline and 7 patients at the end of trastuzumab and docetaxel therapy (41.7% vs. 58.3%, chi-square test; $p = 0.41$) (Table 4.3). There was no statistical difference in nuclear HER3 between the baseline and 1 cycle of trastuzumab, but nuclear HER3 was increased after 4 cycles of trastuzumab and docetaxel treatment ($p < 0.05$) (Figure 4.4A, B). Cytoplasmic HER3 was similar between base line and after 1 cycle of trastuzumab treatment or 4 cycles of trastuzumab and docetaxel treatment (Figure 4.4C, D). Nuclear HER3 at baseline was not correlated with tumour response (% of tumour size change) after a single dose of trastuzumab treatment (n = 12) (r = -0.28, $p = 0.38$) (Figure 4.5A), or after 4 cycles of docetaxel and trastuzumab treatment (n = 10) (r = 0.28, $p = 0.44$) (Figure 4.5B).

For the 5 paired samples, an increase of nuclear HER3 was observed in 1 patient, while a decrease of nuclear HER3 was found in 1 patient (Table 4.3). Although nuclear HER3 at baseline was not associated with tumour response (Figure 4.5A, B), more tumours had nuclear HER3 after trastuzumab and docetaxel therapy (Table 4.3, Figure 4.4B). These results indicate that

trastuzumab could induce nuclear HER3 or the tumour cells which possess nuclear HER3 could be enriched after surviving trastuzumab and docetaxel treatment. Although macroscopic residual tumours were removed by surgery in these patients, it is possible that some of microscopic invisible residual cancer cells with nuclear HER3 could survive and contribute to eventual tumour relapse. Therefore, it would be interesting to assess nuclear HER3 in patients with HER2-positive breast cancer who received trastuzumab as an adjuvant treatment.

Figure 4.3

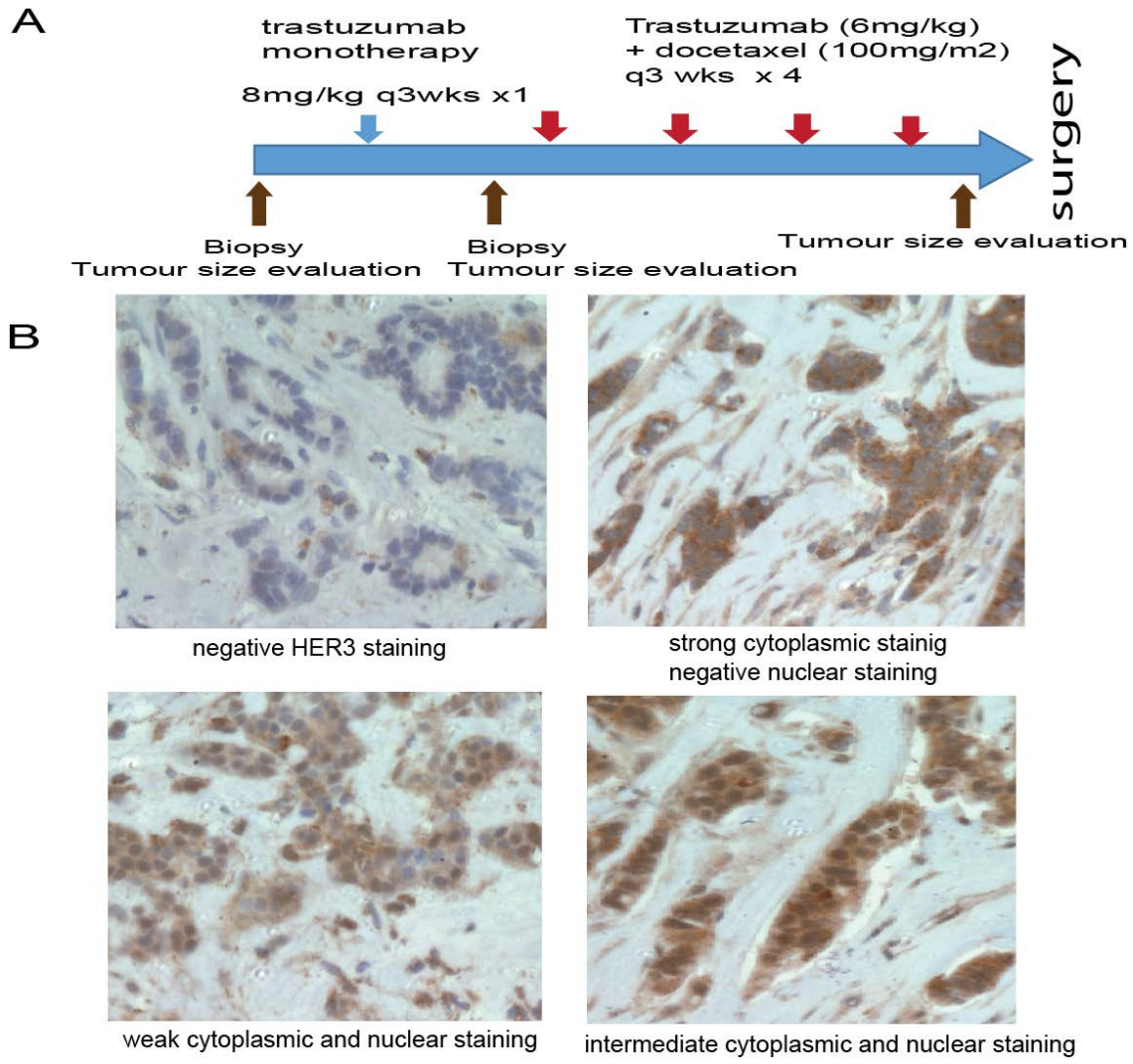

Figure 4.3 A prospective biomarker study of response to trastuzumab in neoadjuvant treatment for HER2-positive, early breast cancer patients. A, Schematic diagram of a prospective biomarker trial to evaluate trastuzumab efficacy in the neoadjuvant setting for HER2-positive breast cancer patients. B, Representative pictures of negative (left upper), weak cytoplasmic and nuclear (left lower), strong cytoplasmic and negative nuclear (right upper), and intermediate cytoplasmic and nuclear staining of HER3.

Figure 4.4

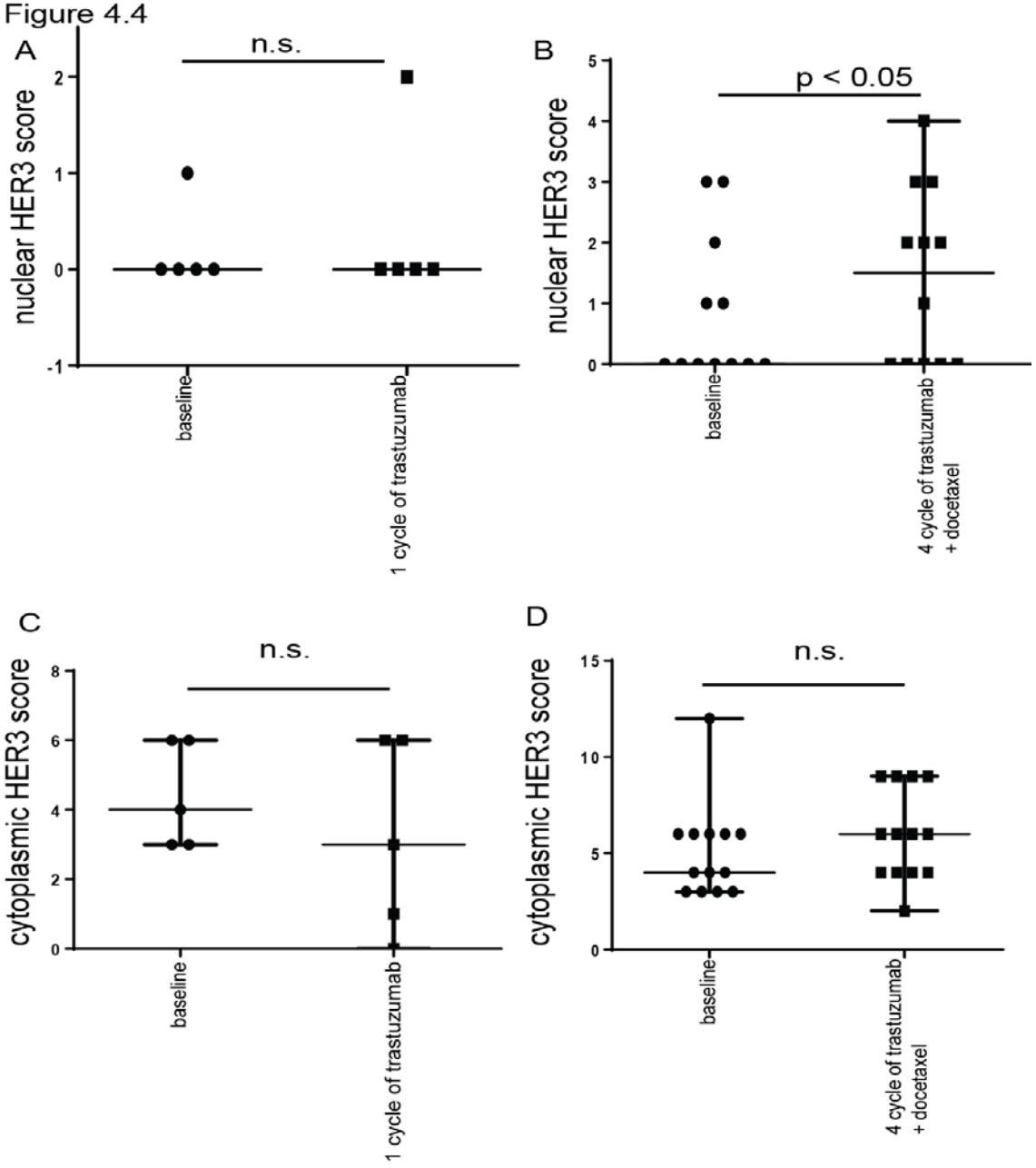

Figure 4.4 Nuclear and cytoplasmic HER3 at baseline, after 1 cycle of trastuzumab treatment, and after 4 cycles of trastuzumab and docetaxel treatment. Nuclear HER3 at baseline and after 1 cycle of trastuzumab treatment (A) (n = 5) or after 4 cycles of trastuzumab and docetaxel treatment (B) (n = 12) were assessed by immunoreactive scoring system (IRS). The median IRS value was compared by Wilcoxon paired test. Similarly, cytoplasmic HER3 was assessed at base line and after 1 cycle of trastuzumab treatment (n = 5) (C) or after 4 cycle of trastuzumab and docetaxel treatment (n = 12) (D). Bars indicate medians with ranges.

Figure 4.5

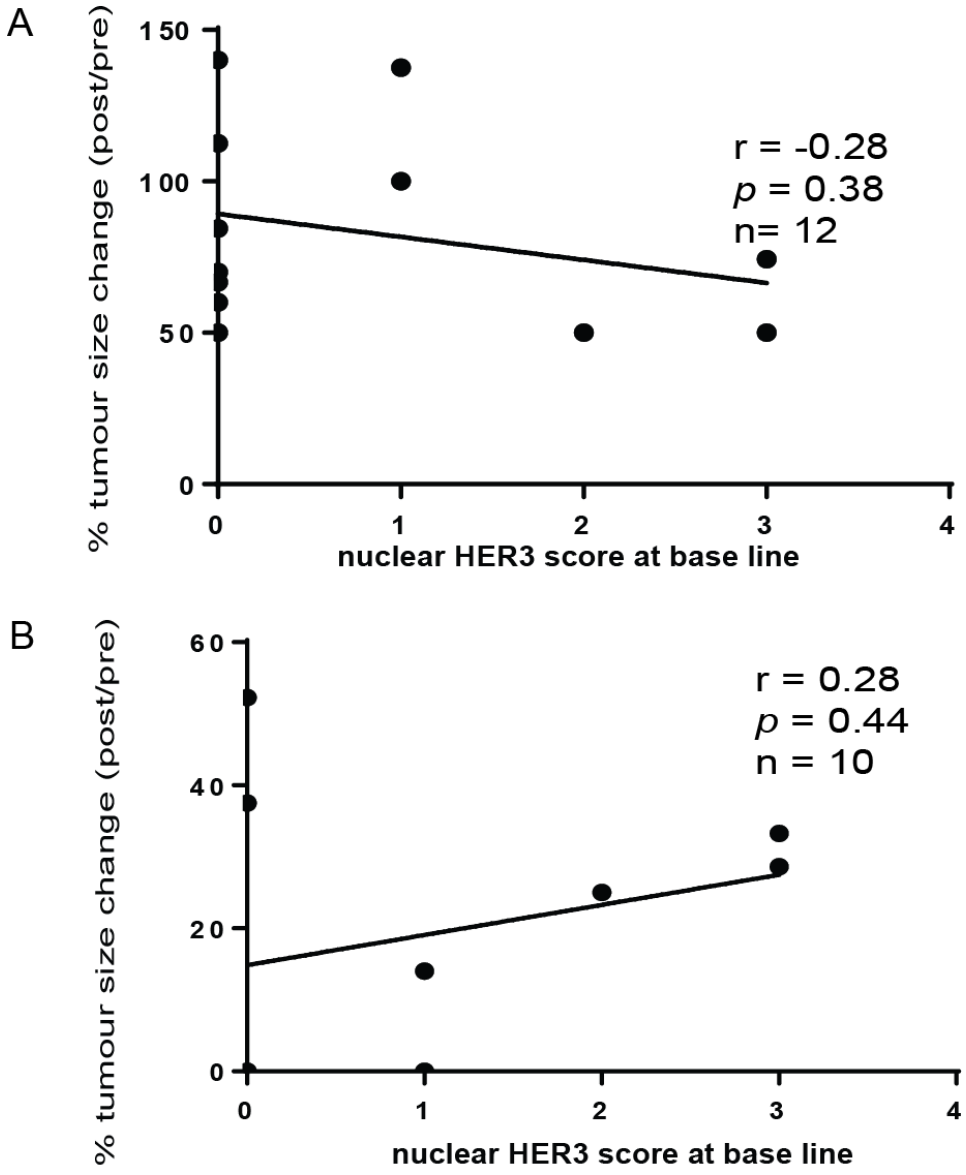

Figure 4.5 Nuclear HER3 at baseline and tumour response after 1 cycle of trastuzumab treatment and after 4 cycle of trastuzumab and docetaxel treatment. A, Nuclear HER3 at base line was plotted against % of tumour size change (tumour size after 1 cycle of trastuzumab/baseline x100) (n = 12). B. Nuclear HER3 at base line was plotted against % of tumour size change (tumour size after 4 cycle of trastuzumab + docetaxel/baseline x100) (n = 10). Nuclear HER3 scoring was based on immunoreactive scoring system and the correlation was calculated by the Pearson correlation test.

Table 4.3 Tumour response and nuclear HER3 score at baseline, and after 1 cycle of trastuzumab monotherapy, and 4 cycles of trastuzumab and docetaxel combination therapy.

	Nuclear HER3 scoring			% of tumour size change	
Case	Baseline	After 1cycle of trastuzumab	After trastuzumab + docetaxel	After 1cycle of trastuzumab	After trastuzumab + docetaxel
1	0	0	0	140	0
2	0	2	0	112.5	37.5
3	0	0	0	50	0
4	1	0	2	100	14
5	0	0	4	66.7	0
6	0	NA	0	84.4	NA
7	3	NA	3	74.3	28.6
8	2	NA	2	50	25
9	0	NA	0	60	NA
10	1	NA	2	137.5	0
11	0	NA	1	70	52.3
12	3	NA	3	50	33.3

Nuclear HER3 was evaluated by immunohistochemistry at baseline (before treatment), after 1 cycle of trastuzumab treatment, and post chemotherapy (4 cycles of trastuzumab + docetaxel). Nuclear HER3 staining was semi-quantified by immunoreactive scoring. Tumour response was evaluated at these time points by caliper measurement, and is expressed as % of tumour size change calculated by tumour size of post-treatment/pre-treatment x 100 (%). NA, not applicable due to non-availability of tumour samples as re-biopsy was declined by patients or response was not available.

4.2.4 Nuclear HER3 is a poor prognostic marker for HER2-positive breast cancer patients.

To examine the hypothesis that nuclear HER3 as assessed by IHC staining (regardless of cleaved or non-cleaved), could be a biomarker of trastuzumab treatment, HER3 immunostaining was performed for 2 other different datasets: The first data set consists of 949 breast cancer samples from the Breast Cancer Campaign including 122 HER2-positive samples (the survival data from HER2-negative patients have not been provided by the Breast Cancer Campaign despite recent request but may become available in the future). The samples were surgically removed early breast tumours which were retrospectively collected at different centres. This cohort did not receive adjuvant trastuzumab treatment. The second data set consists of 173 HER2-positive breast cancer patients from the FinHER trial, which was to assess the efficacy of trastuzumab in the adjuvant setting for HER2-positive breast cancer patients, and to compare docetaxel and vinorelbine for HER2-positive and HER2-negative patients[189]. In all datasets, patients were dichotomized according to the median nuclear HER3 and the median cytoplasmic expression of the FinHER samples (IRS 2 ≤ *vs*. IRS > 2 and IRS 6 ≤ *vs*. IRS > 6, respectively).

Of 935 breast cancer samples, nuclear HER3 (IRS >2) was more frequently observed in the HER2-positive subtype compared to other subtypes (8.2% *vs.* 1.4%, chi-square test; $p < 0.0001$) (Table 4.4). High cytoplasmic HER3 (IRS > 6) was also more frequently observed in the HER2-positive subtype than other subtypes (50.8% *vs.* 30.3%, chi-square test; $p < 0.0001$), confirming that HER3 is frequently co-expressed with HER2 (Table 4.4).

Of the 122 HER2-positive tumours, patients were dichotomized as stated above. Nuclear HER3 was identified in 10 samples (IRS > 2). The median follow-up period of this cohort was 21.0 years, and characteristics of the patients were summarised in Table 4.5. None of the patients received trastuzumab as an adjuvant therapy since these patients received breast surgery from 1987 to 1998, i.e. in the pre-trastuzumab era.

Table 4.4 Number of tumours positive for nuclear HER3 and cytoplasmic HER3 in HER2-positive and HER2-negative breast cancer.

	Nuclear HER3 (n = 935)		Cytoplasmic HER3 (n = 935)	
	Positive	Negative	Positive	Negative
HER2-negative	12	801	246	567
HER2-positive	10	112	62	60

Table 4.5 Characteristics of the patients in the retrospectively collected samples.

Factor	N	Tumour nuclear HER3 expression ≤Median n (%)	>Median n (%)	P (chi squared)
WHO PS				
0	160	101 (63)	59 (37)	
1	13	8 (62)	5 (38)	0.909
Histological type				
Ductal	158	102 (65)	56 (35)	
Other	15	7 (47)	8 (53)	0.170
Histological grade				
1 or 2	53	33 (62)	20 (38)	
3	116	74 (64)	42 (36)	0.848
N.A.	4			
ER				
Negative	95	58 (61)	37 (39)	
Positive	78	51 (65)	27 (35)	0.557
PgR				
Negative	117	74 (63)	43 (37)	
Positive	56	35 (38)	21 (63)	0.924
Tumour size (pT)				
≤20 mm	58	35 (60)	23 (40)	
>20 mm	114	73 (64)	41 (36)	0.636
N.A.	1			
Nodal status (pN)				
pN0	28	22 (79)	6 (21)	
pN+	145	87 (60)	58 (40)	0.062
Age at randomization	Median 50.6 yrs (range25-66)			0.200*
Tumour diameter (mm)	Median 24.5 mm (range 6-100)			0.947*

* Mann-Whitney test

Note: These are the 122 HER2-positive cases from the Breast Cancer Campaign tissue set.

Nuclear HER3 was not associated with progression-free survival (p = 0.26) or overall survival (p = 0.31) in the non-trastuzumab treated, HER2-positive patient cohort (Figure 4.6A, B). The distant metastasis-free survival was also assessed for the nuclear HER3-positive group and nuclear HER3-negative group, but the survival was similar [hazard ratio (HR); 0.50, 95% confidence interval (95% C.I.) 0.16-1.60, Log rank test; p = 0.24]. Due to the low frequency of nuclear HER3-positive patients, this study was underpowered and was not appropriate for further subset analysis. Cytoplasmic HER3 was also assessed but it was not associated with progression-free survival (p = 0.36) or overall survival (p = 0.41) (Figure 4.7A, B). Univariate and multivariate analyses for known prognostic factors were summarised in Table 4.6. Only the lymph node status was associated with poor overall survival [hazard ratio (HR); 2.284, 95% confidence interval (C.I.); 1.401-3.723, p = 0.001] among the known prognostic factors, and it was an independent prognostic factor (HR; 2.56, 95% C.I.; 1.508-4.347, p = 0.001). Neither nuclear HER3 nor cytoplasmic HER3 was associated with survival in multivariate analyses (Table 4.6).

Figure 4.6

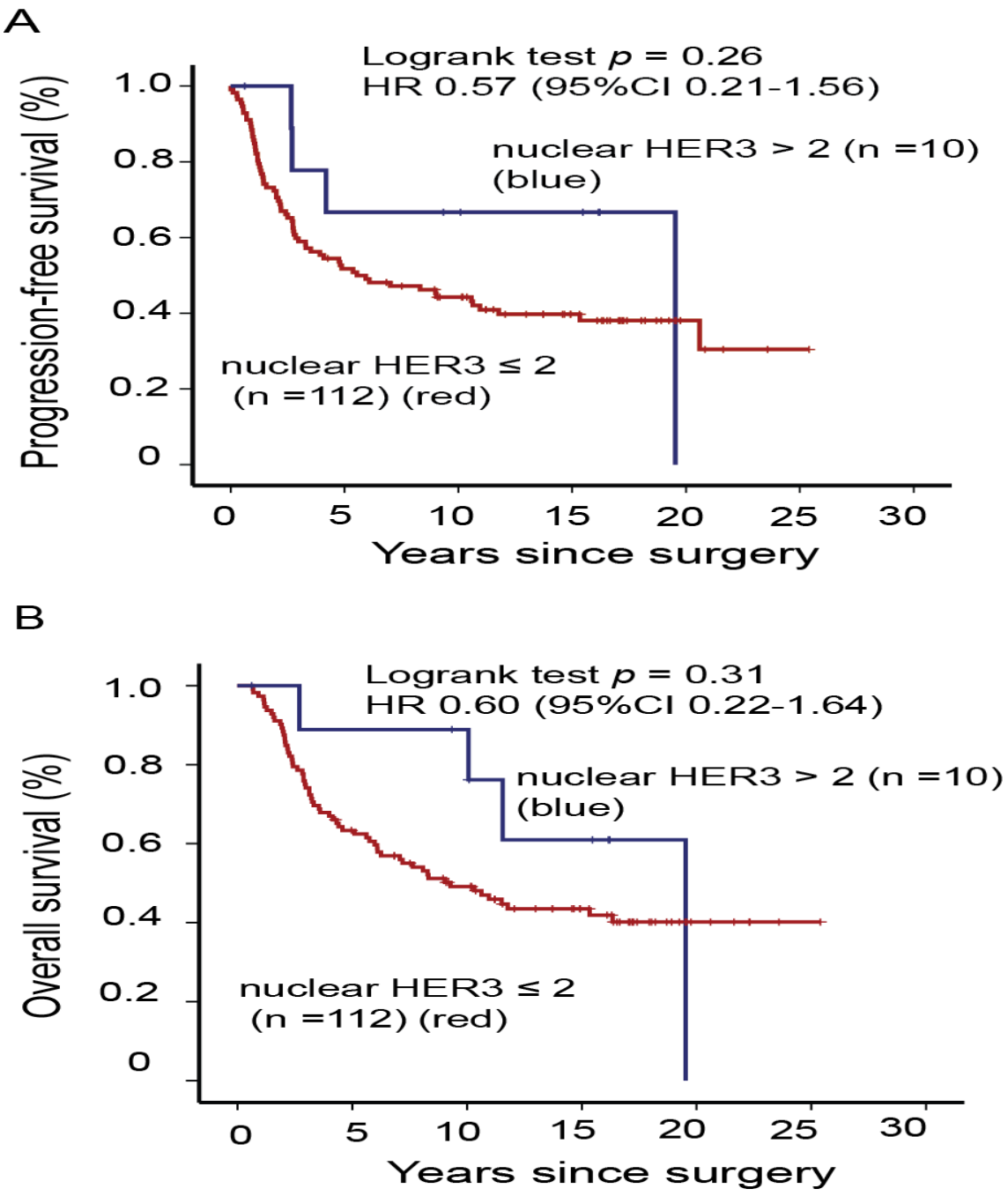

Figure 4.6 Progression-free survival and overall survival according to nuclear HER3 in HER2-positive, trastuzumab non-treated patients. A, Progression-free survival analysis of the 122 HER2-positive breast cancer patients in retrospectively collected samples based on nuclear HER3. HR; hazard ratio, 95% CI; confidence interval. B, Overall survival analysis of the 122 patients based on nuclear HER3.

Figure 4.7

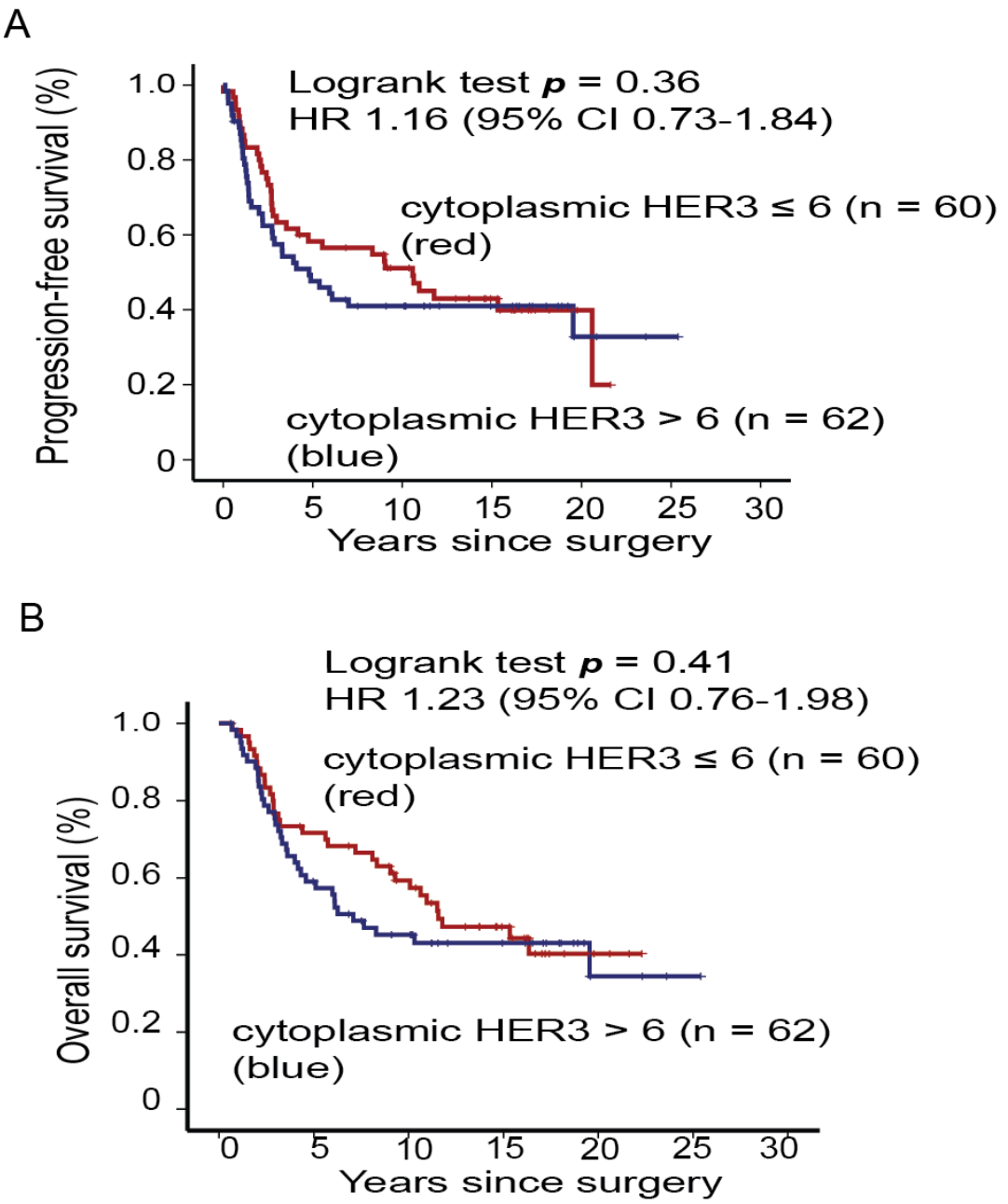

Figure 4.7 Progression-free survival and overall survival according to cytoplasmic HER3 in HER2-positive, trastuzumab non-treated patients. A, Progression-free survival analysis of the 122 HER2-positive breast cancer patients in retrospectively collected samples based on cytoplasmic HER3. HR; hazard ratio, 95% CI; confidence interval. B, Overall survival analysis of the 122 patients based on cytoplasmic HER3.

Table 4.6 Cox univariate and multivariate analyses for progression-free survival including known prognostic factors.

Variables	Univariate analysis			Multivariate analyis		
	HR	95% C.I.	P value	HR	95% C.I.	P value
Estrogen (positive *vs.* negative)	1.143	0.719-1.819	0.571	0.951	0.534-1.691	0.863
Progesteron (positive *vs.* negative)	1.179	0.734-1.894	0.495	1.137	0.624-2.070	0.676
Lymphnode metastases (positive *vs.* negative)	2.284	1.401-3.723	0.001	2.56	1.508-4.347	0.001
Tumour grade (3 *vs.* 1, 2)	0.812	0.436-1.51	0.52	0.717	0.372-1.382	0.32
Cytoplasmic HER3 (high *vs*. low)	1.158	0.729-1.839	0.535	1.284	0.775-2.127	0.332
Nuclear HER3 (high *vs.* low)	0.641	0.257-1.597	0.339	0.62	0.248-1.553	0.308

Estrogen = oestrogen receptor, progesterone = progesterone receptor. This is the 122 HER2-positive tumours from the collection of 935 tumours from the Breast Cancer Campaign.

In the 173 FinHER trial tumour samples from HER2-positive breast cancer patients, nuclear HER3 (IRS > 2) was found in 37% of patients (n = 64). The patients were dichotomised according to nuclear HER3 (IRS > 2 versus IRS $\leq$ 2). The characteristics of the patients were summarised and the known prognostic factors were well balanced in each arm (Table 4.7). The ER and PgR positivity and nodal status were similar in each arm.

Nuclear HER3 was significantly associated with poor progression-free survival (p = 0.047) and overall survival [HR; 3.78, 95%C.I.; 1.67-8.46, p = 0.0006] in the overall cohort (Figure 4.8B). In contrast, cytoplasmic HER3 (> median = 6) was significantly related with better overall survival (HR; 0.30, 95% CI; 0.11-0.81, p = 0.012) (Figure 4.8A). Interestingly, the expression of HER3 in cytoplasm was inversely correlated with nuclear expression (Pearson correlation test, R = -0.437, 95%CI; -0.551 to -0.307, p < 0.0001).

Table 4.7 Characteristics of the patients in the FinHER trial.

Factor	N	Tumour nuclear HER3 expression ≤Median n (%)	>Median n (%)	P (chi squared)
WHO PS				
0	160	101 (63)	59 (37)	
1	13	8 (62)	5 (38)	0.909
Histological type				
Ductal	158	102 (65)	56 (35)	
Other	15	7 (47)	8 (53)	0.170
Histological grade				
1 or 2	53	33 (62)	20 (38)	
3	116	74 (64)	42 (36)	0.848
N.A.	4			
ER				
Negative	95	58 (61)	37 (39)	
Positive	78	51 (65)	27 (35)	0.557
PgR				
Negative	117	74 (63)	43 (37)	
Positive	56	35 (38)	21 (63)	0.924
Tumour size (pT)				
≤20 mm	58	35 (60)	23 (40)	
>20 mm	114	73 (64)	41 (36)	0.636
N.A.	1			
Nodal status (pN)				
pN0	28	22 (79)	6 (21)	
pN+	145	87 (60)	58 (40)	0.062
Age at randomization	Median 50.6 yrs (range25-66)			0.200*
Tumour diameter (mm)	Median 24.5 mm (range 6-100)			0.947*

* Mann-Whitney test

Note: N.A. means not assessed, PS means performance status

Figure 4.8

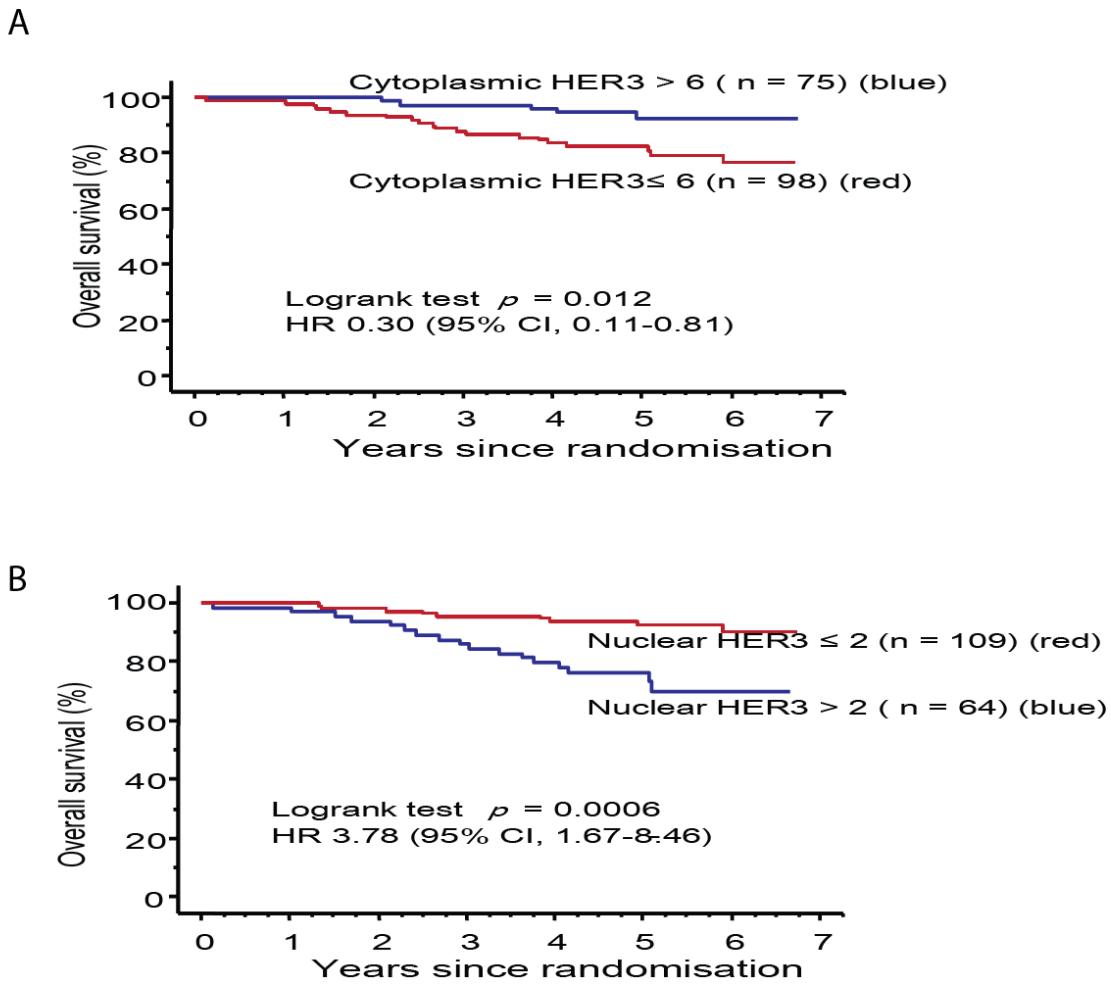

Figure 4.8 Overall survival in HER2-positive breast cancer patients according to cytoplasmic and nuclear HER3. A, Overall survival analysis of 173 HER2-positive breast cancer patients in the prospective FinHER study based on cytoplasmic HER3. HR; hazard ratio, 95% CI; confidence interval. B, Overall survival analysis of the 173 patients based on nuclear HER3.

The primary endpoint of this trial was progression-free survival and 150 events (tumour relapse) were necessary for the final analysis. Death was not required for the analysis of this randomised trial[189]. At the time of writing, 26 events (death) had occurred but the number was not sufficient to perform multivariate analyses including all potential factors. Therefore, only the 3 strongest factors in the univariate analyses were tested for multivariate analyses. Multivariate analyses identified that nuclear HER3 was an independent prognostic factor for HER2-positive patients (HR; 4.37, 95%CI; 1.88-10.2, p = 0.0006) (Table 4.8).

Table 4.8 Cox multivariate analysis for overall survival.

Factor	P	HR (95% CI)
No. of axillary lymph nodes (continuous)	<0.0001	1.141 (1.087-1.198)
Oestrogen receptor expression (negative vs. positive)	0.112	1.967 (0.853-4.533)
Average nuclear expression (> median vs. ≤ median , 2)	0.0006	4.367 (1.880-10.145)

In the subset analyses, nuclear HER3 was correlated with poor overall survival in the patients assigned to both docetaxel and vinorelbine chemotherapy (p = 0.039 and p = 0.001, respectively) (Figure 4.9A, B). Furthermore, nuclear HER3 was associated with poor overall survival for the patients assigned to 9 weeks of trastuzumab treatment as well as the patients without trastuzumab treatment (p = 0.021 and p = 0.016, respectively) (Figure 4.10A, B). These results showed that nuclear HER3 is a poor prognostic factor for HER2-positive breast cancer patients, and trastuzumab may not be able to influence clinical outcomes for these patients with nuclear HER3 (IRS > 2).

Figure 4.9

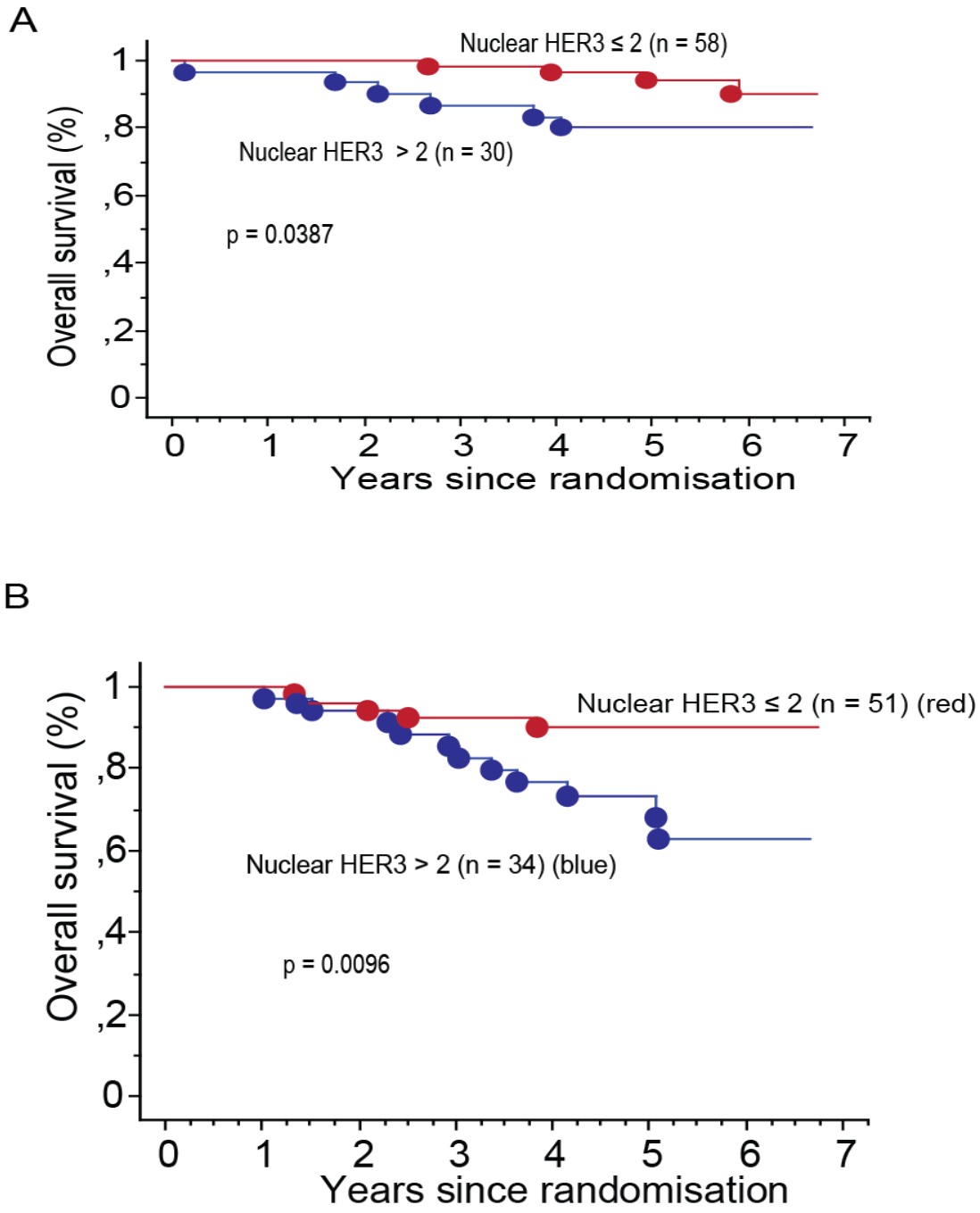

Figure 4.9 Overall survival analysis by nuclear HER3. A, Overall survival analysis of the patients assigned to docetaxel based on nuclear HER3. B, Overall survival analysis of the patients assigned to vinorelbine based on nuclear HER3.

Figure 4.10

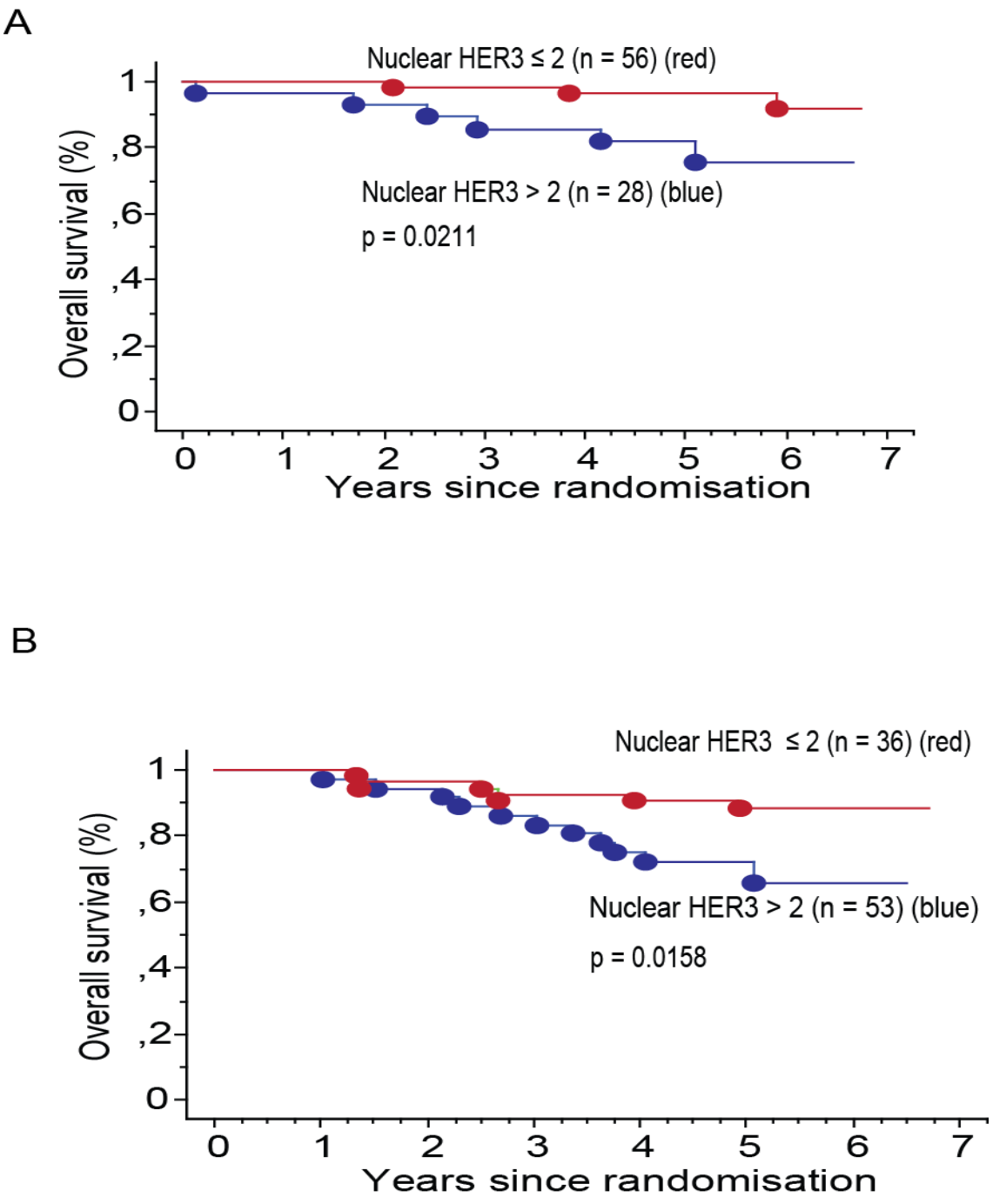

Figure 4.10 Overall survival analysis by nuclear HER3. A, Overall survival analysis of the patients assigned to trastuzumab based on nuclear HER3. B, Overall survival analysis of the patients assigned to non-trastuzumab treatment based on nuclear HER3.

4.3 Discussion

4.3.1 Nuclear HER3 as a biomarker for trastuzumab treatment

To test whether nuclear HER3 could be a biomarker for response to trastuzumab treatment, formalin-fixed cell pellets from a panel of HER2-positive cell lines were obtained from the US collaborator. Nuclear HER3 was seen in only 2 cell lines out of 18 cell lines. Nuclear HER3 was also observed in HCC1569 tumours in mice after trastuzumab treatment although the untreated cells did not show nuclear HER3 localisation *in vitro*. Some trastuzumab-resistant cell lines were sensitive to trastuzumab *in vivo*, but the HCC1569 cells were resistant to trastuzumab both *in vitro* and *in vivo*. Although the frequency of nuclear HER3 observed in the panel of HER2-positive cell line was not high, nuclear HER3 was seen only in the trastuzumab acquired and innately resistant cells.

Currently, there is no specific HER3 antibody available to detect $HER3_{100kD}$. However, detection of HER3 in the nucleus, either in the cleaved or non-cleaved form, was clearly shown in a few trastuzumab resistant cell lines (Figure 4.1, 4.2, Table 4.1, Table 4.2). Previously, an anti-HER3 antibody raised against N-terminus was used in a gastric cancer study and HER3 was found in the nucleus

of the tumours in these patients[74]. However, the clinical significance of nuclear HER3 has not been previously investigated. In the analyses of samples in the prospective neoadjuvant biomarker trial performed here, nuclear HER3 was found at baseline and was increased after docetaxel and trastuzumab treatment (Table 4.3, Figure 4.4B). This study suggests that tumour cells with nuclear HER3 expression may be enriched by trastuzumab and docetaxel treatment, or that nuclear HER3 could be induced by these treatment. Therefore, it is hypothesised that tumours with nuclear HER3 could be associated with resistance to trastuzumab treatment. To test this hypothesis, samples were obtained from the FinHER study. In these samples, nuclear HER3 was associated with poor prognosis in HER2-positive breast cancer patients (Figure 4.8). Since the FinHER trial is a prospective, randomised trial[189], the comparison of nuclear HER3 positivity in trastuzumab treated and untreated patients was possible. The results showed that nuclear HER3 was associated with poor overall survival in HER2-positive breast cancer patients with or without adjuvant trastuzumab treatment. These results suggest that the prognosis of the patients with nuclear HER3 would not be improved by trastuzumab treatment. Given the results in the cell line study, it would be interesting to test whether expression of ADAM17 or PEN2 correlates

with nuclear HER3 in clinical samples, and with prognosis of HER2-positive breast cancer patients. For patients with HER2-positive tumours and nuclear HER3, lapatinib may be indicated as a treatment option. It would therefore be interesting to assess in a clinical trial setting whether HER2-positive breast cancer patients with nuclear HER3 in their tumours would benefit more from lapatinib compared to trastuzumab.

In a previous randomized trial, adjuvant lapatinib did not extend the progression-free survival for HER2-positive breast cancer patients compared to placebo[190]. Although the addition of lapatinib to trastuzumab and chemotherapy doubled the response rate compared to trastuzumab and chemotherapy alone in the neoadjuvant setting[21], the ALLTO trial suggested that the addition of adjuvant lapatinib to trastuzumab did not show additional survival benefit compared with trastuzumab alone[191]. These results indicate that patient enrichment for target treatment is necessary. There is a possibility that lapatinib may be of greater benefit than trastuzumab in those patients whose tumours contain nuclear HER3 although this needs to be tested in a clinical trial setting.

4.3.2 Limitations of the study

In this project, 3 data sets were used to confirm the clinical impact of nuclear HER3 in relation to trastuzumab treatment and patients' outcome. Since it is difficult to obtain tumour samples from patients treated with trastuzumab monotherapy without chemotherapy, especially pairs of pre- and post-trastuzumab treatment samples, the number of patients evaluated for trastuzumab monotherapy is limited in this study. In 122 HER2-positive samples from the Breast Cancer Campaign, nuclear HER3 was not correlated with survival. However, since nuclear HER3 was only positive in 10 samples, the result was underpowered. In this cohort, cytoplasmic HER3 was also assessed but it was not correlated with survival. The FinHER trial included patients who were treated with or without adjuvant trastuzumab, while the Breast Cancer Campaign samples were all from patients who did not receive trastuzumab, and they had been treated with different standard chemotherapies (Cyclophosphamide, methotrexate, 5-fluorouracil vs. anthracycline and cyclophosphamide). It would have been better to have 2 different data sets with similar clinical design in order to obtain a more robust result for nuclear HER3 as a prognostic marker in HER2-positive breast cancer patients. However, tumour samples from a randomised

trial would be better than those which are retrospectively collected since a protocol driven randomized trial would ensure a more homogeneous patient population and the collection of better quality tumour samples.

The frequency of nuclear HER3 was variable among the different datasets although the antibody used for these samples was specific to HER3 and the same protocol and procedures were followed for these samples. Analysis of samples for IHC could be affected by multiple factors: time left in formalin, samples age, time from the sample taken to formalin fixation, and time from making a section to IHC. In the pre- and post-trastuzumab treated paired samples from our Italian collaborator, positive nuclear HER3 staining as defined by IRS >2 was found in 2 of 12 (16.7%) of pre-treatment biopsy samples. In the Breast Cancer Campaign samples, only 10 of 122 samples were found to have positive nuclear HER3 staining (IRS > 2, 8.9%). In the FinHER samples, it was found in 64 of 173 samples (37%). However, the samples from the Breast Cancer Campaign are older and were collected from the pre-trastuzumab era. Many of the breast cancer treatments used during that time have changed. In addition, the characteristics of the patients included in this analysis were variable. The treatment strategy

(adjuvant radiotherapy, chemotherapy and endocrine therapy) was mixed compared to the samples obtained from a well-balanced prospective randomised trial. The inverse correlation of cytoplasmic and nuclear HER3 expression observed in the FinHER samples was not observed in the Breast Cancer Campaign data set, which may be due to the sample size. Therefore, the data obtained from the FinHER trial should be further validated in a large independent data set from a randomized controlled trial so that the prognostic and predictive values of nuclear HER3 in relation to trastuzumab treatment and patients' outcome could be established.

CHAPTER 5.

INVESTIGATING THE ROLE OF MET RECEPTOR IN MAINTAINING HER3 PHOSPHORYLATION AND TRASTUZUMAB RESPONSE AND RESISTANCE

5.1 Introduction

Trastuzumab is known to decrease phosphorylation of HER3[25]. Our group previously reported that phosphorylation of HER3 was increased again after initial deactivation when the cells acquired resistance to trastuzumab by ligand release through ADAM17[32]. MET has been reported to be upregulated by HER family targeted therapy (gefitinib) when the cells acquired resistance and to interact with HER3[114]. Another report suggests that MET is upregulated upon trastuzumab treatment[30]. Therefore, it was hypothesised that MET upregulation and the recovery of HER3 phosphorylation in trastuzumab resistant cells could be related. The aim of this part of my DPhil study was to study the role of MET in maintaining HER3 phosphorylation in response to trastuzumab treatment and to investigate MET expression as a possible biomarker in HER2-positive breast cancer patients.

5.2 Results

5.2.1 Phosphorylation of HER3 and MET expression level in HER2-positive cell lines.

Since HER3 phosphorylation is maintained by transphosphorylation through heterodimerisation with other receptors, especially HER2[35], it was hypothesised that anti-HER2 monoclonal antibody, trastuzumab, could decrease phosphorylation of HER3. Trastuzumab decreased phosphorylation of HER3 on Y1289 and Y1197, and its downstream pathway phosphorylation of AKT on S473 (Figure 5.1A), which was consistent with previous reports[25,32]. Utilizing a panel of HER2-positive cell lines, HER3 and AKT phosphorylation was found to be significantly decreased by trastuzumab in some of the cell lines (SKBr3, BT474, MDA-MD-453, MDA-MB-361, and NCI-H2170 cells) after 4 hour trastuzumab treatment at 40 μg/mL (Figure 5.1B). The percentage change of the phosphorylation of HER3 and AKT corrected for the total protein before and after trastuzumab treatment was plotted in the graph (Figure 5.1C).

Figure 5.1

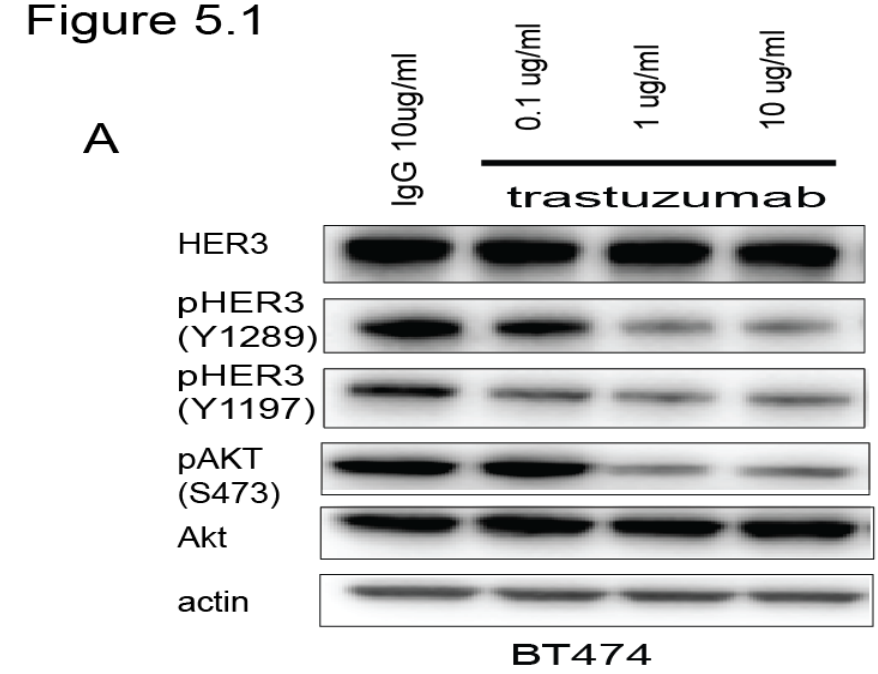
A
IgG 10ug/ml
0.1 ug/ml
1 ug/ml
10 ug/ml
trastuzumab
HER3
pHER3 (Y1289)
pHER3 (Y1197)
pAKT (S473)
Akt
actin
BT474

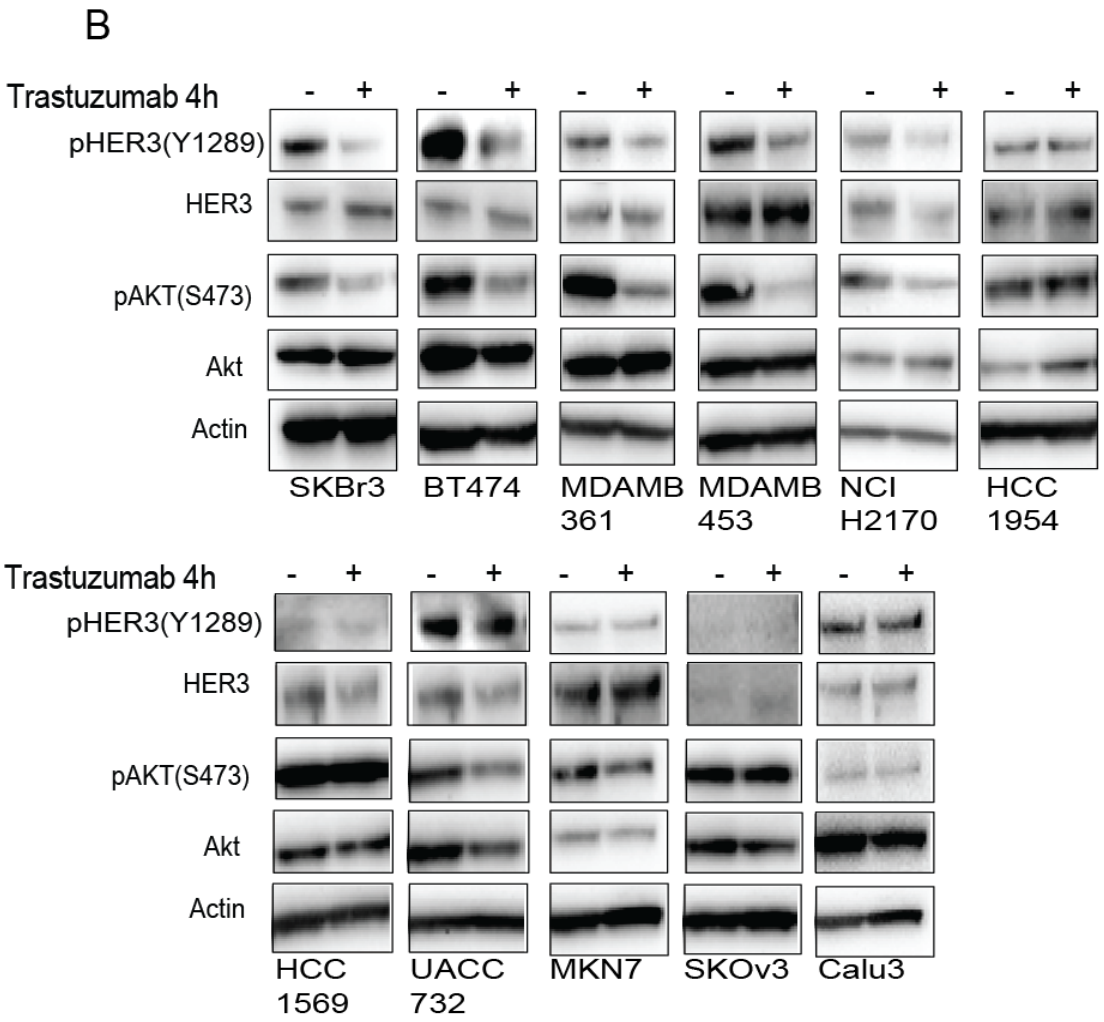
B
Trastuzumab 4h
- + - + - + - + - + - +
pHER3(Y1289)
HER3
pAKT(S473)
Akt
Actin
SKBr3
BT474
MDAMB 361
MDAMB 453
NCI H2170
HCC 1954
Trastuzumab 4h
- + - + - + - + - +
pHER3(Y1289)
HER3
pAKT(S473)
Akt
Actin
HCC 1569
UACC 732
MKN7
SKOv3
Calu3

Figure 5.1

C

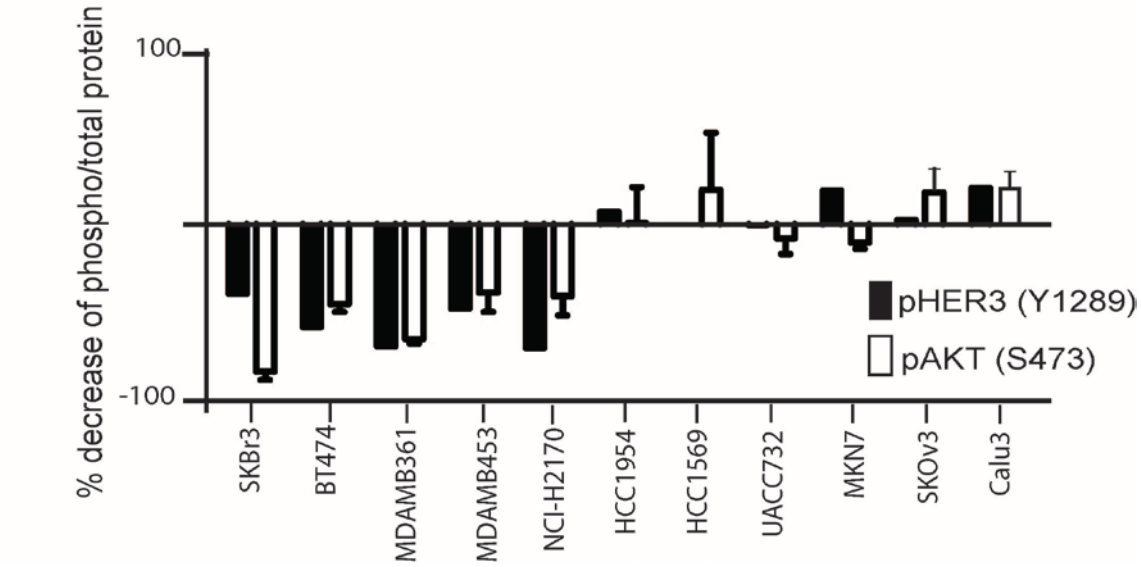

Figure 5.1 Phosphorylation of HER3 and AKT in trastuzumab treatment in HER2-positive cell lines. A, The BT474 cells were treated with human IgG control (10 μg/mL) or trastuzumab at indicated doses for 4 hours. Equal amount of proteins from these lysates were loaded and were subject to immunoblotting with antibodies against HER3, phospho HER3 (pHER3, Y1197, Y1289), AKT, phospho AKT (pAKT S473), and actin. B, HER2-positive cell lines were treated with either human IgG or trastuzumab (40 μg/mL) for 4 hours before the western blot analysis of the indicated proteins. C, Semi-quantification of 3 western blots of pHER3 and pAKT (trastuzumab treatment at 40 μg/mL for 4 hours) relative to their total respective protein levels expresses as % of pre-treatment levels are shown. Bars indicate means with SEM.

To assess the relationship between HER3 phosphorylation level and trastuzumab efficacy, the percentage change in HER3 phosphorylation relative to the total HER3 level after 4 hours of trastuzumab treatment was correlated with the percentage of cell viability after 5 days of trastuzumab treatment at 40 μg/mL (Figure 3.1). Interestingly, phosphorylation of HER3 was maintained regardless of trastuzumab treatment in primary trastuzumab-resistant cells lines. The percentage change in HER3 phosphorylation was positively correlated with trastuzumab sensitivity ($r^2 = 0.63$, $p < 0.01$) (Figure 5.2). These results indicate that the decrease of HER3 phosphorylation after 4 hours of trastuzumab treatment may indicate the response to trastuzumab.

Figure 5.2

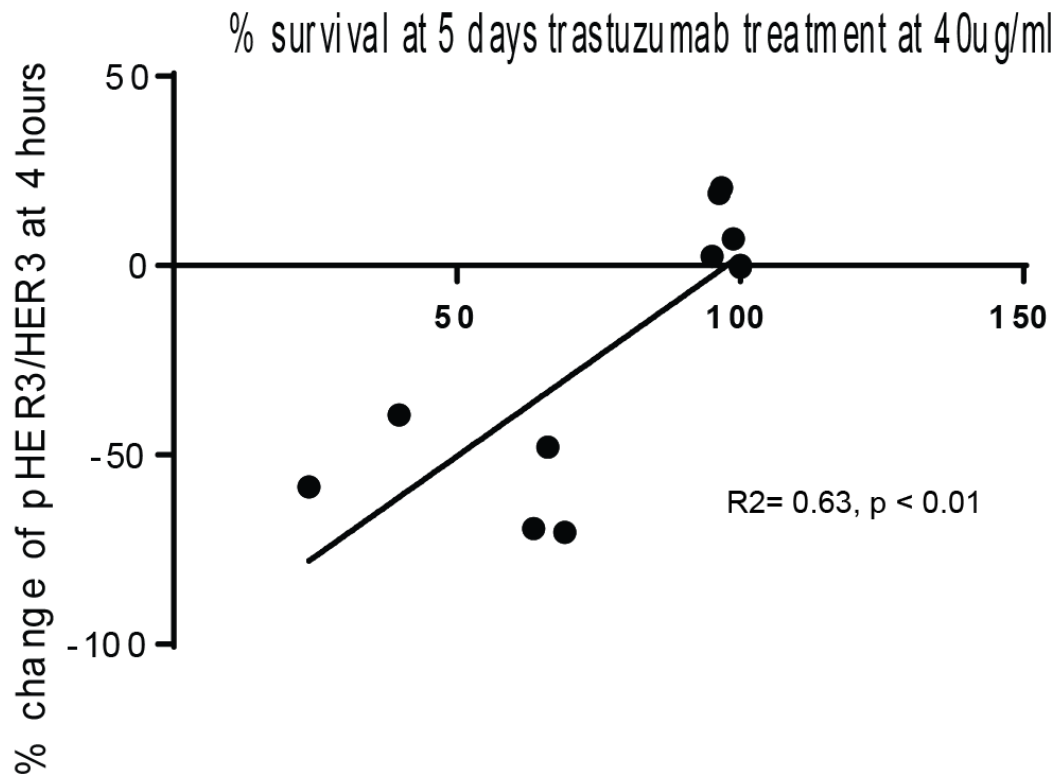

Figure 5.2 The correlation between HER3 phosphorylation and cell viability on trastuzumab treatment. Equal amount of proteins from IgG or trastuzumab treated cell lysates (40 µg/mL, 4h) in HER2-positive cell panel were subjected to immunoblotting and the blots were semi-quantified for pHER3 level relative to total HER3 level. The percentage change of pHER3/HER3 after trastuzumab treatment was plotted on the Y axis, and % cell survival after 5 days of trastuzumab treatment determined by resazurin assay was plotted on the X axis. Correlation was determined by the Pearson's correlation test.

Two representative HER2-positive breast cancer cell lines (BT474 and SKBr3) were examined for the duration of suppression of HER3 phosphorylation upon trastuzumab treatment. In the BT474 cells, HER3 phosphorylation level was decreased immediately with trastuzumab treatment. However, HER3 phosphorylation was found to be recovered after 8 months treatment of trastuzumab when the cells became resistant to trastuzumab (Figure 3.2B) (Figure 5.3A). AKT phosphorylation was increased after 10 minutes of trastuzumab treatment but it was reduced again after 1 hour of trastuzumab treatment. As with HER3 phosphorylation, AKT phosphorylation recovered after 8 months of trastuzumab treatment (Figure 5.3A). MET was found to be increased in 8-month trastuzumab treated BT474 cells although there was also an upregulation of MET expression during acute trastuzumab treatment (10 minutes) (Figure 5.3A, 5.4A). In the BT474-TR cells, MET was processed more than the parental BT474 cells (beta-receptor, 145kD), resulting in an increase of mature MET receptor expression (Figure 5.3A). MET mRNA level was assessed and was found to be increased in the BT474-TR cells (Figure 5.4B). In the SKBr3 cells, MET expression level was similar throughout the treatment durations (Figure 5.3B). HER3 phosphorylation was decreased after 10 minutes of trastuzumab

treatment but the recovery of HER3 phosphorylation as seen in the BT474 cells was not observed (Figure 5.3A, B), suggesting that this cell line may have different trastuzumab resistance mechanism.

Figure 5.3

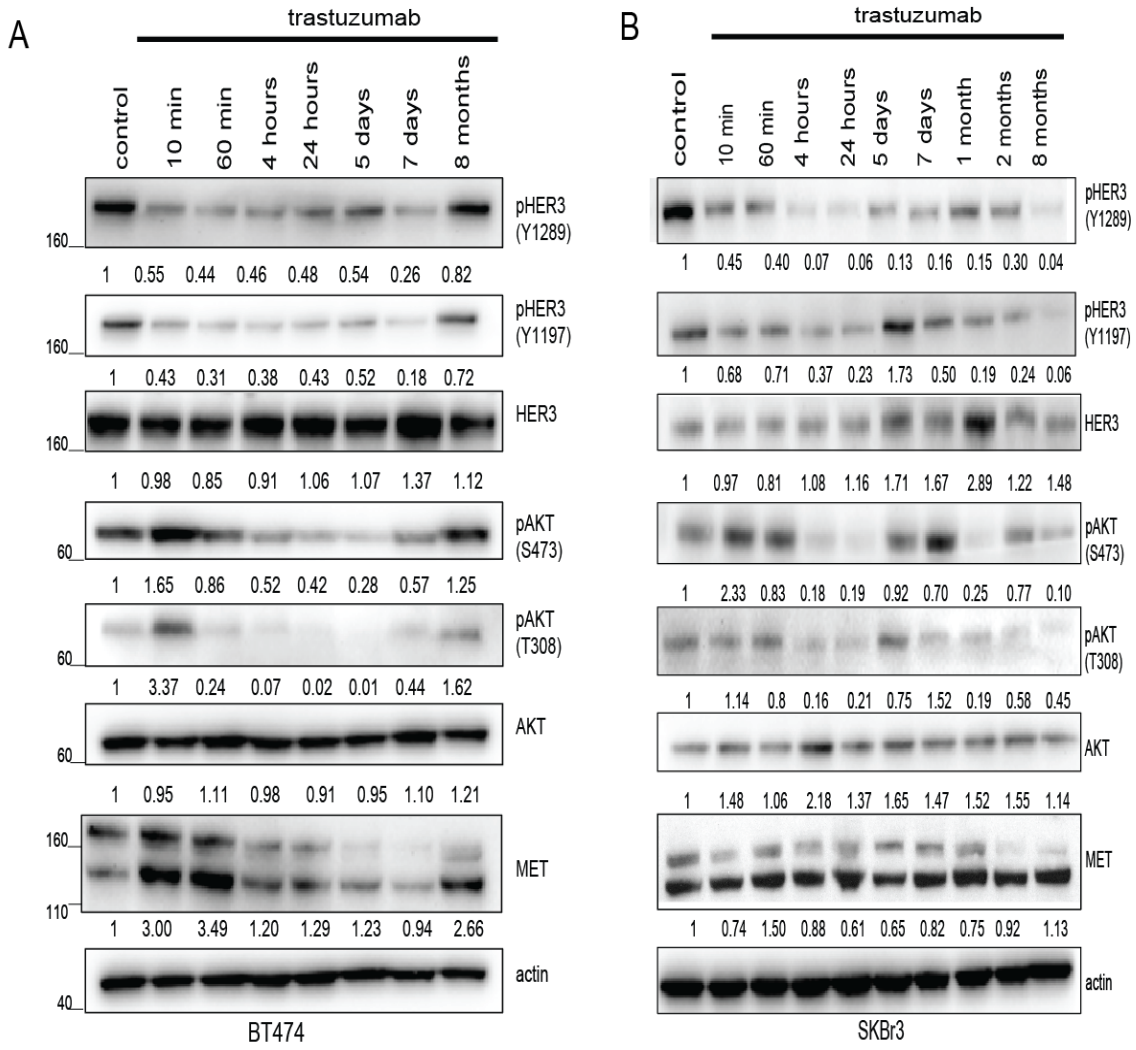

Figure 5.3 HER3 phosphorylation and MET expression on trastuzumab treatment. A, Equal amount of proteins from the SKBr3 and BT474 cells treated with trastuzumab (40 µg/mL) for different durations were subjected to immunoblotting for the indicated proteins and the representative blots of 2 experiments are shown. Total proteins relative to actin and phosphoproteins relative to the relevant total proteins were semi-quantified and normalised to the control. The numbers underneath the blots indicate the total protein expression levels relative to the control. Note that MET has two bands: precursor MET (170kD) and MET beta receptor (145kD).

Figure 5.4

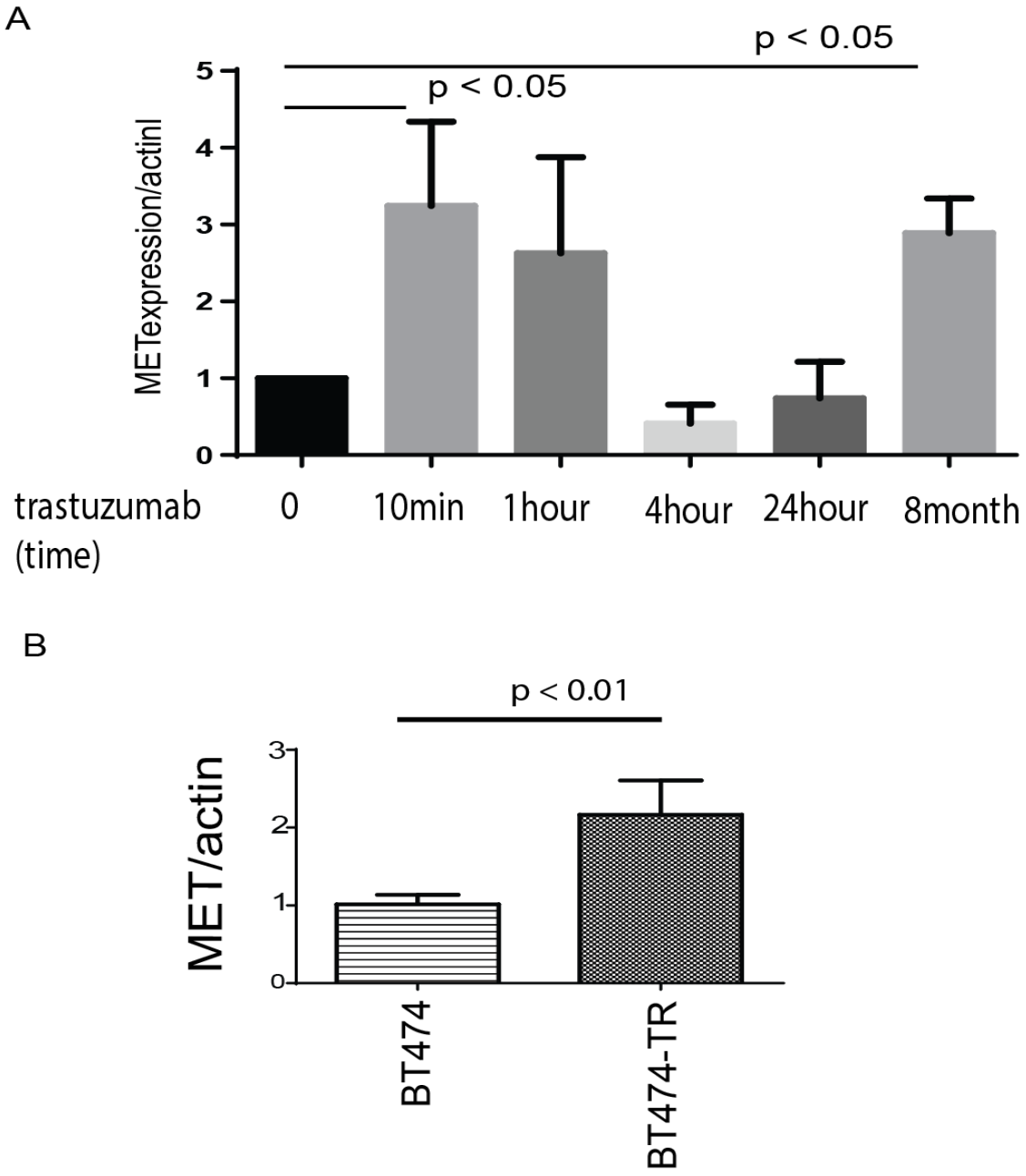

Figure 5.4 MET expression during trastuzumab treatment. A, MET expression relative to the actin level in the BT474 cells was semi-quantified from 3 different western blots. Bars show means with SEM and one-way ANOVA test with Bonferroni correction was applied. B, mRNA level of MET relative to the actin level in the BT474 and acquired trastuzumab resistant BT474 (BT474-TR) cells was compared. Bars show means (n = 3) with SEM and student *t*-test was applied.

To further assess whether increased MET expression contributes to trastuzumab resistance, 3 other HER2-positive cell lines (MDA-MB-361, MDA-MB-453, and NCI H-2170 cells lines) were continuously treated with trastuzumab for more than 3 months until the cells became resistant to trastuzumab (Figure 3.2C, D, E). MET expression was found to be increased in the trastuzumab resistant NCI-H2170 (NCI-H2170-TR) cells, while MET expression in the other cells remained similar (Figure 5.5). As seen in the BT474 cells, HER3 phosphorylation recovered in NCI-H2170-TR cells upon trastuzumab resistance after initial decrease by trastuzumab treatment (Figure 5.5). The level of HER3 phosphorylation was decreased in the MDA-MB-361 and MDA-MB-453 cells even when the cells became resistant to trastuzumab as seen in the SKBr3-TR cells, suggesting these cell lines may have different resistance mechanisms (Figure 5.5). These results indicate that the recovery of HER3 phosphorylation upon trastuzumab resistance could be related to an increased MET expression in some cell lines.

Since MET expression was increased in the BT474-TR cells and NCI-H2170-TR cells, MET is hypothesised to contribute to trastuzumab resistance. Basal MET expression level was assessed in a panel of HER2-positive cell lines

(Figure 5.6A). MET expression was positively correlated with trastuzumab resistance, and this was statistically significant ($r^2 = 0.36$, $p < 0.05$) (Figure 5.6B). These results indicate that MET is associated with, and might contribute to, trastuzumab resistance in HER2-positive cell lines.

Figure 5.5

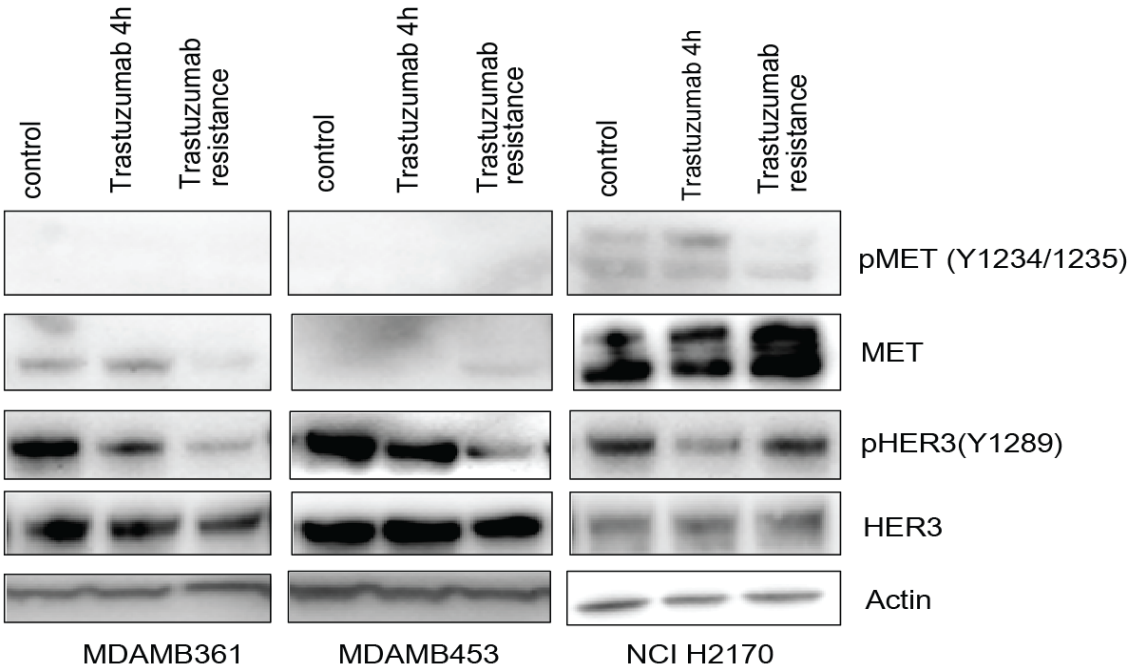

Figure 5.5 MET and phospho-HER3 in acquired trastuzumab resistant cells. Equal amount of cell lysates of MDA-MB-361, MDA-MB-453, NCI-H2170 cells treated with either IgG for 4 hours, trastuzumab for 4 hours, or trastuzumab for more than 3 months (trastuzumab resistance) were subject to immunoblotting with anti-phospho MET (pMET, Y1234/1235), anti- MET, anti-phospho HER3 (pHER3, Y1289), anti-HER3, and anti-actin antibodies.

Figure 5.6

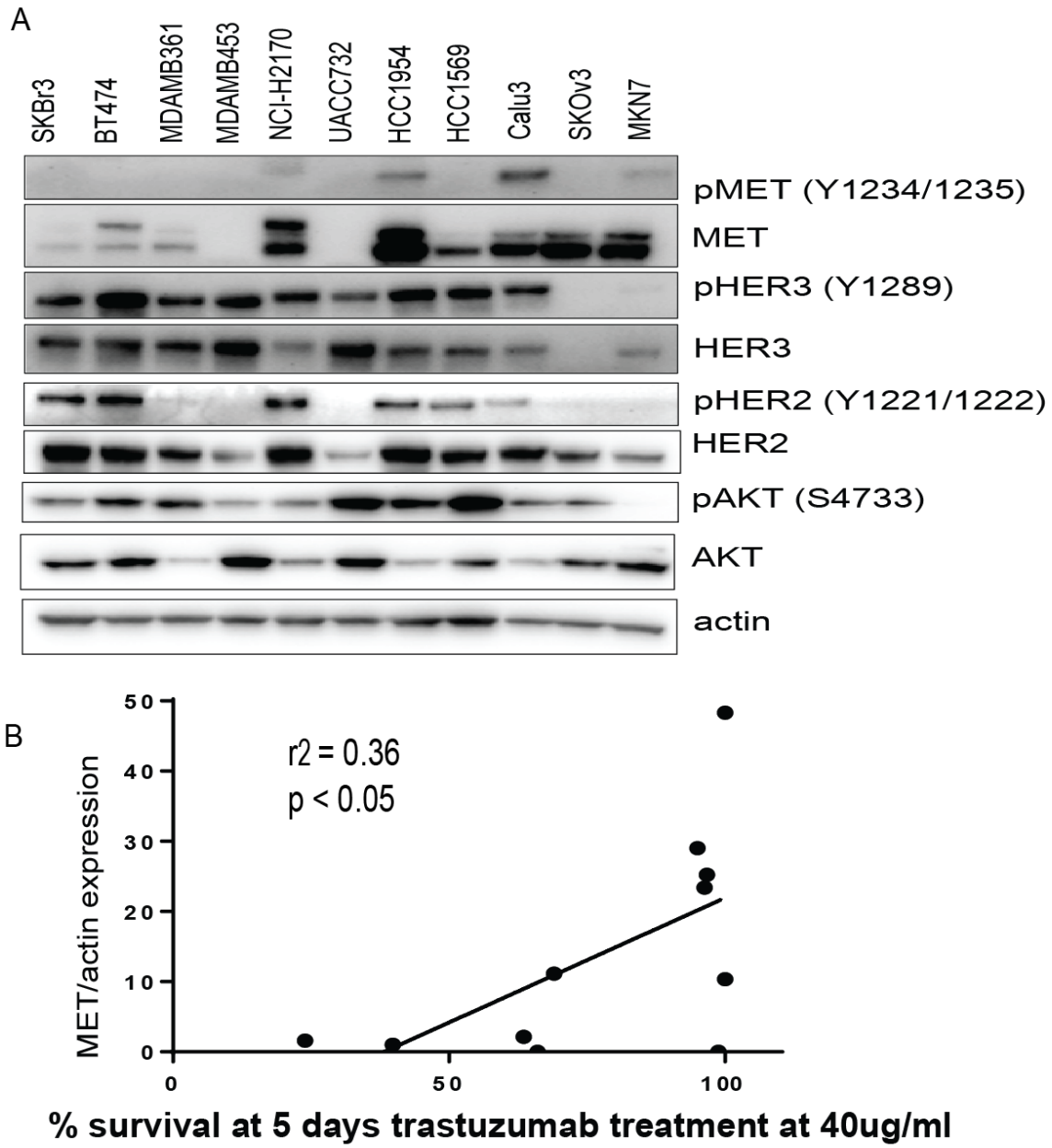

Figure 5.6 The correlation between MET expression and cell viability in trastuzumab treatment. A, Equal amount of cell lysates from a panel of HER2-positive cell lines were subject to immunoblotting with indicated antibodies. B, MET expression relative to the actin level was semi-quantified in a panel of HER2-positive cell lines and plotted on the Y axis. Cell viability at 5 days of trastuzumab treatment (40 μg/mL) of these cell lines was assessed by resazurin assay and plotted on the Y axis, expresses as % of solvent-control. The Pearson's correlation test was applied.

5.2.2 MET contributes to maintain phosphorylation of HER3 in trastuzumab resistant cells.

MET expression was increased in the BT474-TR and NCI-H2170-TR cells when HER3 phosphorylation recovered from trastuzumab treatment (Figure 5.3A, 5.4A, 5.5). Therefore, the interaction of MET and HER3 could contribute to maintain phosphorylation of HER3 in trastuzumab resistance. To test this hypothesis, MET knockdown was first optimised by using 2 different siRNAs against MET and MET mRNA level was measured by qRT-PCR (Figure 5.7A). Then, MET was knocked down in several HER2-positive cells (BT474, BT474-TR, HCC1954, NCI-H2170-TR). MET knockdown decreased the phosphorylation of HER3 without reducing total HER3 expression in all the examined cell lines (Figure 5.7B). This result indicates that MET could contribute to HER3 phosphorylation in these cell lines. To identify whether this is due to the interaction between MET and HER3, immunoprecipitation experiments were carried out. MET and HER3 interaction was increased in the BT474-TR cells compared to parental cells, and so was the interaction of MET and phosphorylated HER3 in the BT474-TR cells (Figure 5.7C). These results suggest that MET and HER3 interaction may contribute to the phosphorylation of HER3 in trastuzumab resistance.

Figure 5.7

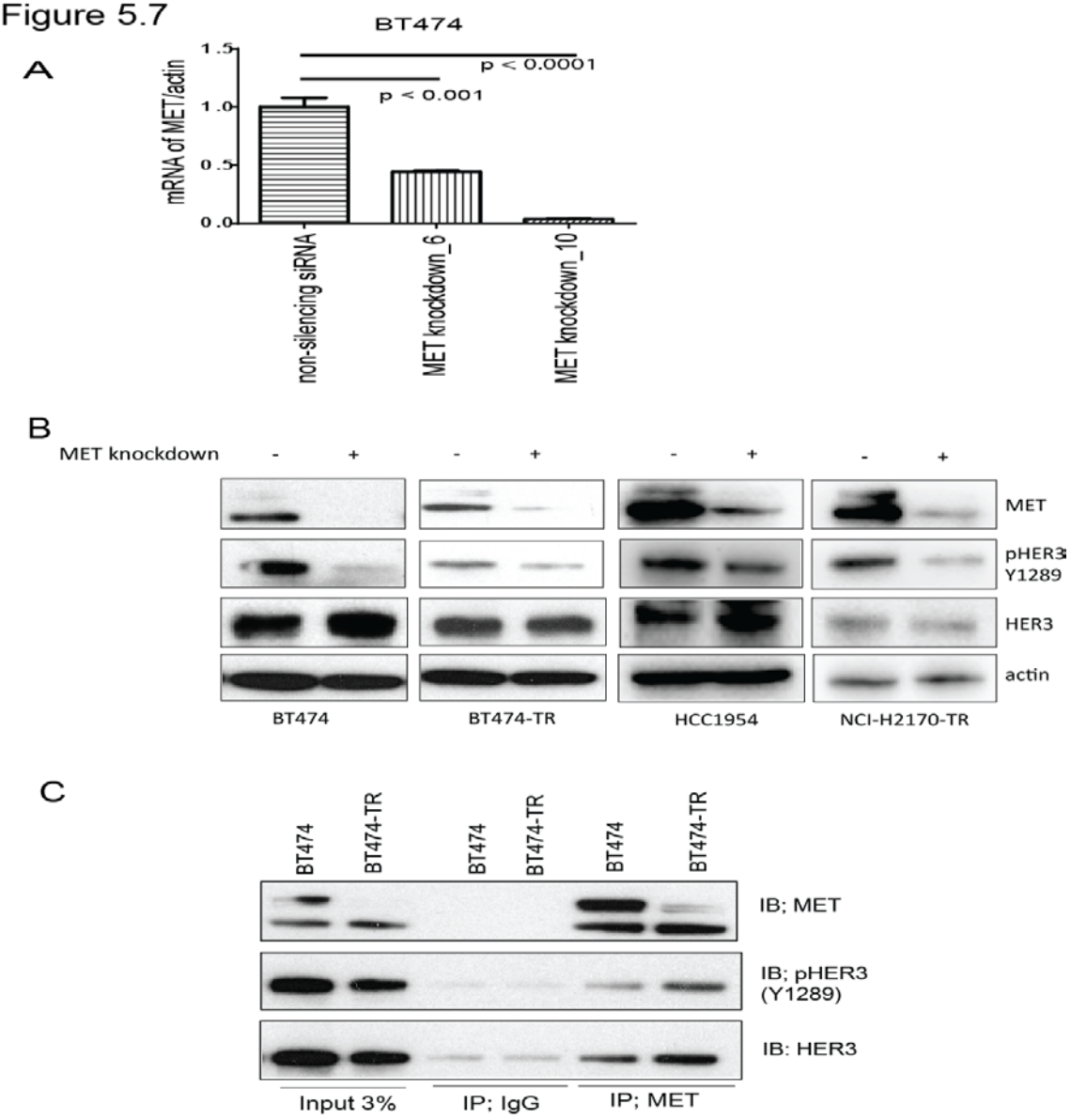

Figure 5.7 The reduction of HER3 phosphorylation by MET knockdown and an increase of MET-HER3 interaction in the acquired trastuzumab resistant BT474 (BT474-TR) cells. A, BT474 cells were transfected with non-silencing siRNA or 2 different siRNAs against MET, and mRNA was measured by real time PCR. Bars show means with SEM. Two-way ANOVA and Bonferroni correction was applied. B, MET was knocked down in a series of HER2-positive cell lines. Equal amount of proteins from cells with non-silencing siRNA transfected cells or siRNA against MET (siMET_10) were subject to immunoblotting for indicated proteins. C, Equal amount of proteins from BT474 and BT474-TR cells were subject to immunoprecipitation (IP) with anti-MET antibody or non-specific mouse IgG followed by immunoblotting (IB) analyses of MET, pHER3, and HER3.

5.2.3 MET is important for HER2-positive, trastuzumab resistant cell lines.

Maintaining HER3 phosphorylation during trastuzumab treatment could contribute to trastuzumab resistance in HER2-positive cell lines. The HCC1954 cells are MET overexpressing and primary trastuzumab resistant breast cancer cells, which have an autocrine HGF loop to maintain spontaneous phosphorylation of MET[192]. Knockdown of MET in the HCC1954 cells led to a decrease of colony formation and sensitised the cells to trastuzumab treatment (Figure 5.8A), which correlated with a decrease of pHER3 as shown in Figure 5.7B. MET knockdown in the BT474-TR cells significantly reduced the number of colonies with or without trastuzumab treatment (Figure 5.8B). These results indicate that MET is important for cell survival in both primary and acquired trastuzumab resistant cell lines.

A monoclonal antibody against MET was assessed to see if it could recover the sensitivity to trastuzumab in the BT474-TR cells. The monoclonal anti-MET antibody (AF276, N-terminus) successfully decreased MET expression but there was no decrease of HER3 phosphorylation in cells treated with a series of increasing concentrations and durations of anti-MET antibody (Figure 5.9A).

Furthermore, the anti-MET monoclonal antibody treatment did not inhibit cell growth with or without trastuzumab treatment (Figure 5.9B). The discrepancy with the results of MET knockdown could be due to the fact that post internalised MET could still have a signalling role[193], and total MET inhibition by knockdown or inhibition of signalling function may be necessary for growth inhibition as well as a reduction of HER3 phosphorylation. Therefore, a MET selective tyrosine kinase inhibitor (SU11274) was also assessed and it was found to be similarly effective in inhibiting growth with or without trastuzumab treatment in the BT474-TR cells (Figure 5.9C). The IC50 of SU11274 for the BT474-TR cells treated with IgG or trastuzumab was 2.31 μM and 3.23 μM, respectively. These results suggest that MET tyrosine kinase inhibition is effective in inhibiting colony formation of the BT474-TR cells, but there is no increased inhibition upon addition of trastuzumab.

Figure 5.8

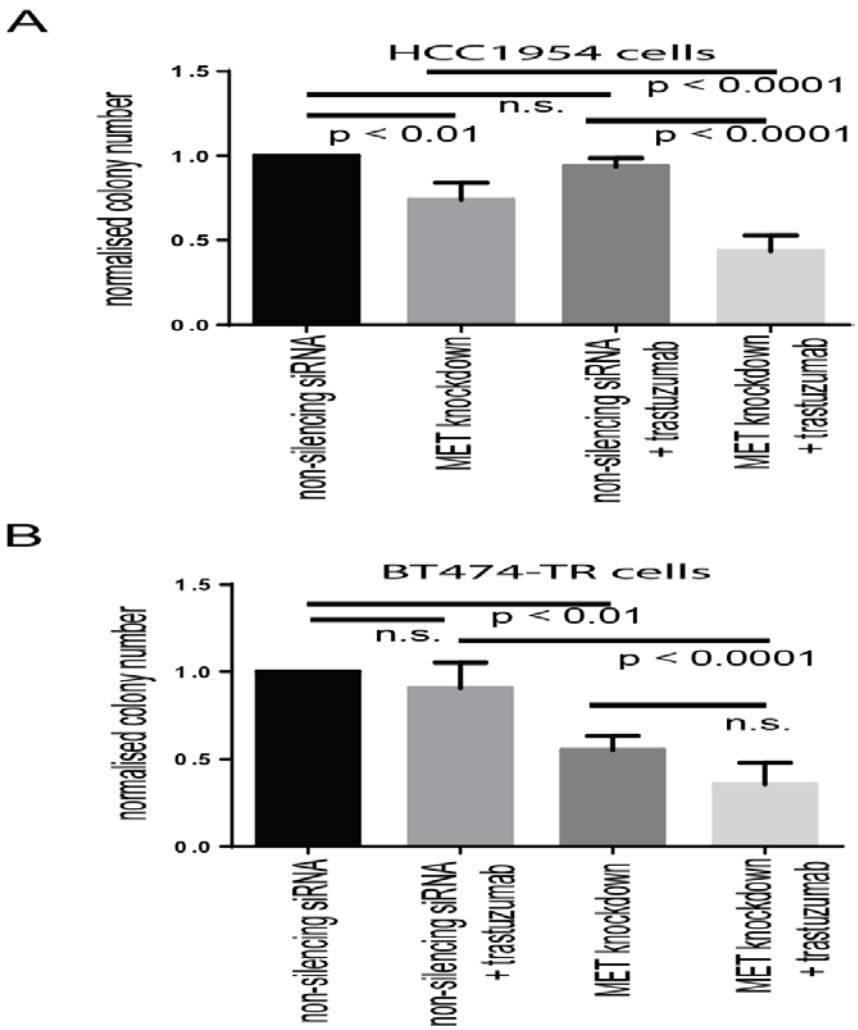

Figure 5.8 The sensitisation of the HCC1954 cells to trastuzumab and the reduction of colony formation in the acquired trastuzumab resistant BT474 (BT474-TR) cells by MET knockdown. A, Equal number of HCC1954 cells transfected with non-silencing siRNA or siRNA against MET were seeded a day after transfection and followed by the treatment of IgG or trastuzumab (40 μg/mL) for 14 days. Colonies were counted and normalised to non-silencing siRNA transfected cells with IgG treatment. Each experiment had 3 replicates and was repeated 3 times. Bars show means with SEM. Two-way ANOVA with Bonferroni correction was used to detect the statistical significance. B, Similarly, equal number of BT474-TR cells with non-silencing siRNA transfection or MET knockdown were seeded a day after transfection and followed by the treatment of IgG or trastuzumab (40 μg/mL) for 14 days. Trastuzumab were depleted a day before transfection. Bars show means with SEM. Two-way ANOVA with Bonferroni correction was used to detect the statistical significance of 3 independent experiments in triplicate.

Figure 5.9

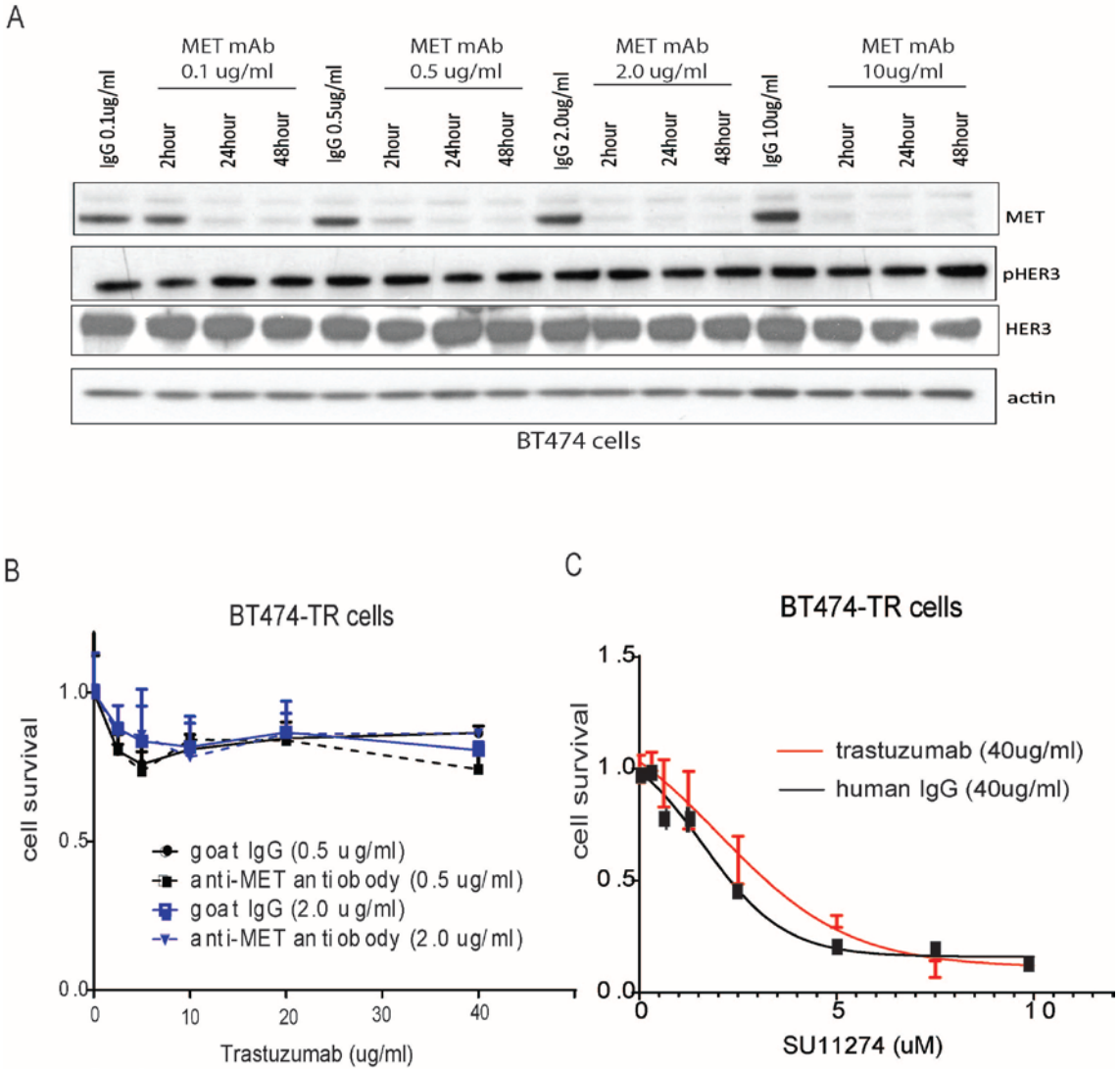

Figure 5.9 Effect of MET monoclonal antibody and MET inhibitor in the cell viability of the acquired-trastuzumab resistant BT474 (BT474-TR) cells. A, a MET monoclonal antibody, AF276 (MET mAB) at indicated doses was applied to the BT474 cells for indicated durations to compare goat IgG (48h) as a control. Equal amount of proteins were subject to immunoblotting for indicated proteins. B, The BT474-TR cells were treated with either goat IgG as a control or anti-MET antibody at 2 different doses for 5 days. Cells were trypsinised and were subject to cell counting, and the fit curve was drawn. Trastuzumab (40 μg/mL) was applied throughout the experiments. Bars show means with SEM. C, The BT474-TR cells were treated with different doses of SU11274 for 5 days. Trastuzumab was added at 40 μg/mL or withdrawn. Cells were trypsinised and were subject to cell counting, and the fit curve was drawn. Bars show means with SEM.

5.2.4 MET and HER3 interaction may be ligand independent

Heregulin (HRG), a putative ligand for HER3 and HER4 has been reported to fully rescue cells from growth inhibition by lapatinib, while HGF, a ligand for MET can partially rescue HER2-positive cells from growth inhibition by lapatinib although the reason why HRG protects the cells from lapatinib is unclear[192]. HRG is a ligand for HER3 and promotes HER2-HER3 dimerisation, which results in an increase of HER3 phosphorylation[39,40]. In my earlier experiments, trastuzumab had been shown to reduce phosphorylation of HER3 in the sensitive cell lines (Figure 5.1C, 5.2). It is hypothesised that exogenous HRG stimulation could protect the cells from trastuzumab treatment by maintaining phosphorylation of HER3. HRG stimulation in the BT474 cells increased phosphorylation of HER3 after 10 minutes but HER3 phosphorylation as well as total HER3 expression were decreased after 5 days possibly as a result of receptor internalisation[55,188] (Figure 5.10A). When parental (trastuzumab sensitive) BT474 cells were treated with trastuzumab and co-stimulated with HRG, HRG protected the cells from a decrease of HER3 phosphorylation by trastuzumab at 60 minutes (Figure 5.10A). The BT474 cells became totally resistant to trastuzumab when they were treated with trastuzumab and HRG, suggesting that HRG protects cells from growth

inhibition by trastuzumab. It is possible that this condition helps to select trastuzumab resistant cells quicker than continuous treatment of trastuzumab more than 8 months (Figure 5.10B).

Figure 5.10

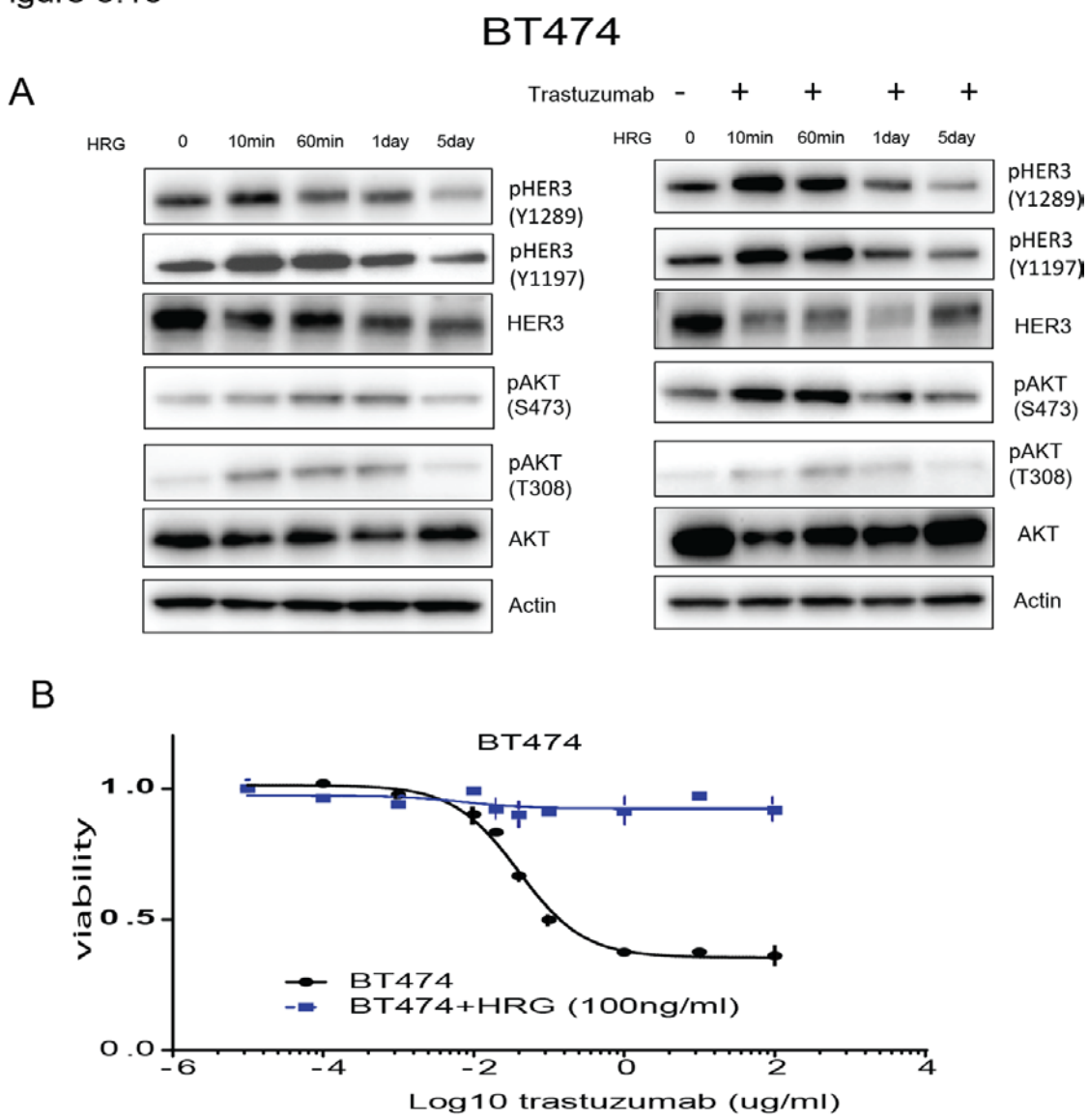

Figure 5.10 The protection of the cells from trastuzumab by maintaining HER3 phosphorylation (pHER3) through heregulin (HRG) stimulation. A, The BT474 cells were stimulated with HRG at 100ng/mL in full serum media for indicated times. Equal amount of proteins were subject to immunoblotting for the indicated proteins and the representative blots are shown (left). Similarly, the BT474 cells were co-treated with HRG and trastuzumab or IgG (40 µg/mL) for indicated durations. Equal amount of proteins were subject to immunoblotting for the indicated proteins and the representative blots are shown (right). B, Equal number of BT474 cells in 96-well plate were treated with either trastuzumab only or trastuzumab with HRG (100 ng/mL) co-stimulation for 5 days in full serum media. Cell viability was determined by resazurin assay and the fit curve was drawn. Bars indicate means and SEM.

It is hypothesised that ligand stimulation may promote MET and HER3 interaction. If MET could catalyse HER3 phosphorylation, activated (HGF-stimulated) MET could induce HER3 phosphorylation. Conversely, if HER3 could induce MET activation, HRG-stimulated activated HER3 could induce phosphorylation of MET. To address this hypothesis, the BT474 cells were stimulated with HGF or HRG. However, HGF stimulation could not increase HER3 phosphorylation level and HRG stimulation had no effect on MET phosphorylation (Figure 5.11A, B). This results indicates that the interaction between MET and HER3 may be ligand independent, and MET upregulation may be enough to induce HER3 phosphorylation.

Figure 5.11

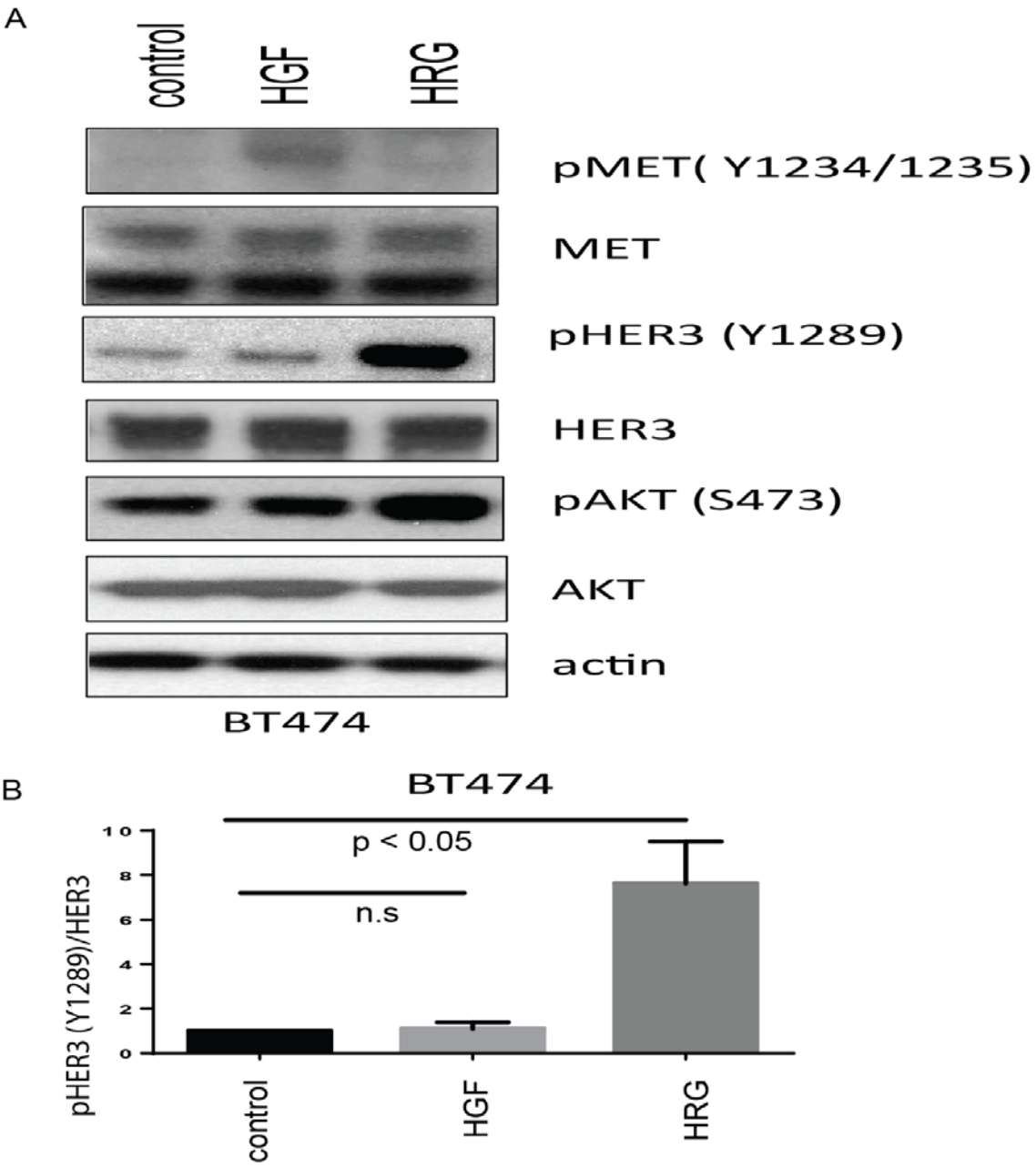

Figure 5.11 An increase of phosphorylation of HER3 by heregulin (HRG) but not HGF. A, The BT474 cells were starved overnight before stimulation with HGF (50 ng/mL) or HRG (100 ng/mL) for 10minutes. Equal amount of proteins were subject to immunoblotting for the indicated proteins and the representative blots are shown. B, Semi-quantification of 3 western blots of phospho-HER3 (pHER3, Y1289) relative to total HER3 level. Bars show means (n = 3) with SEM. One-way ANOVA test with Bonferroni correction was applied.

5.2.5 MET as a biomarker of trastuzumab treatment

The preclinical data implied that MET may contribute to maintain phosphorylation of HER3, possibly by direct ligand independent interaction with HER3. To address whether MET could be a biomarker for HER2-positive breast cancer patients, a method was developed for MET immunohistochemistry. MET antibody titration was firstly performed by using the HCC1954 cells as a strong positive control, Calu3 cells as an intermediate positive control, and UACC732 cells as a weak or negative control (Figure 5.6A, 5.12A). MET expression was assessed in a series of 935 breast cancer samples from the Breast Cancer Campaign tissue bank, including 122 HER2-positive breast tumours, the same data set used for Table 4.5. All the patients in this cohort were early breast cancer and received breast surgery as a primary treatment but did not receive trastuzumab treatment as an adjuvant therapy. MET was detected on the plasma membrane as well as in the cytoplasm (Figure 5.12B).

Since there is no standard cut-off value for MET staining, several cut-off values were examined. Of 122 HER2-positive breast cancer samples, the median IRS score for cytoplasmic MET expression was 3 (range: 0-12). The median

membrane MET expression and median nuclear MET expression were 0 (range 0-12) and 0 (range 0-6), respectively. First, patients were divided into 3 groups by the median cytoplasmic MET expression (low; 0-3, intermediate; 3-6, high; 7-12) (Figure 5.13A). It was found that the survival curves between the intermediate and low MET expression groups were very similar. Although these 3 groups were not statistically different (HR 0.74, p = 0.15), high cytoplasmic MET expression (IRS > 6) had a trend of better progression-free survival. Since IRS score of 6 is also the median of the actual IRS scores 0-12, patients were therefore dichotomised according to this value (IRS > 6) and the progression-free survival was assessed. Patients whose tumours had high cytoplasmic MET had a borderline significance of better progression-free survival than those with low cytoplasmic MET tumour (HR 0.49, p = 0.05) (Figure 5.13B). Since HER2-positive breast cancer is defined as tumours consisting more than 10% HER2-staining with an intensity of 2 or 3[10] (IHC 2+ will require further FISH testing to confirm HER2 gene amplification), this cut-off value was also applied. Patients with positive cytoplasmic MET defined as > 10% MET-positive cells with an intensity of 2 or 3 had a trend to better progression-free survival than those with negative cytoplasmic MET expression (all others) (HR 0.54, p = 0.09) (Figure

5.13). The distant metastasis-free survival was also assessed but there was no statistical difference between cytoplasmic MET positive (IRS > 6) and negative tumours (IRS ≤ 6) [HR 1.19 (95%CI 0.58-2.43), p = 0.63]. High cytoplasmic MET expression (IRS > 6) was significantly associated with better overall survival [HR 0.37 (95%CI 0.15-0.92), *p* = 0.048] (Figure 5.15A). Cause specific overall survival was also assessed, and high cytoplasmic MET expression (IRS > 6) was associated with better cause specific survival (HR; 0.26, 95%CI; 0.08-0.83, *p* = 0.015)

There is also no standard for the cut-off value of membrane MET staining. Therefore, several cut-off values were tested to assess its prognostic value. Since the median membrane MET expression was 0, any membrane MET positivity and negativity were compared. It was shown that any membrane MET positivity had a trend to better progression-free survival (HR 0.73, *p* = 0.19) (Figure 5.14A). Other IRS cut-off values for membrane MET were tested, and all cut-off values [IRS ≥ 2 (n = 44), 3 (n = 27), 4 or more (n = 22)] showed a similar trend, and thus the cut-off point with the strongest p value was selected (IRS ≥ 2 vs. IRS < 2, *p* = 0.08) (Figure 5.14 C). In addition to IRS scoring, the following cut-off value was

tested: more than 10% of positive cells with an intensity of 2-3 *vs.* all others. By using this cut-off value, membrane MET positivity had a trend to association with better progression-free survival (p = 0.05) (Figure 5.14 C). Distant metastasis-free survival was also calculated but membrane MET expression (IRS ≥ 2) was not associated with prognosis [HR 0.66 (95% CI 0.38-1.16), p = 0.15]. High membrane MET expression had a trend to association with good overall survival [HR 0.65 (95%CI 0.38-1.11), p = 0.15] (Figure 5.15B), and also cause specific survival [HR 0.61 (95%CI 0.34-1.11), p = 0.11].

As stated above, the median nuclear MET expression was 0 (range 0-6). Nuclear MET expression (IRS ≥ 1) was identified in 8 patients but nuclear MET expression was not associated with progression-free survival and overall survival [HR 0.87 (95%CI 0.32-2.39), p = 0.79 and HR 0.99 (95%CI 0.36-2.72), p = 0.98, respectively]. Nuclear MET expression were not a prognostic factor for cause specific survival [HR 0.88 (95%CI 0.27-2.81), p = 0.83].

Membrane MET staining (IRS ≥ 2) was detected more frequently in the HER2-positive patients than the HER-negative patients (42.6 % *vs.* 21.4 %, chi-square test; p < 0.05), while cytoplasmic MET staining (IRS > 6) was similar

(11.3% vs. 11.4%, chi-square test; $p = 0.98$). Interestingly, MET expression in the nucleus was also observed in 125 patients (Figure 5.12B). Although the role of nuclear MET expression is unclear, nuclear MET expression (IRS ≥ 1) was found more frequently in HER2-negative tumours than HER2-positive tumours (13.3% *vs.* 6.6%, chi-square test; $p < 0.05$).

The characteristics of the patients according to the cytoplasmic MET expression were summarised in Table 5.1. There were fewer patients with high cytoplasmic MET expression in the node-positive group (5/17 = 29.4% *vs.* 58/105 = 55.2% in node-negative patients, $p = 0.05$). All other factors were similar in these groups. Multivariate analyses including nuclear and cytoplasmic HER3 expression were shown in Table 4.6. Since cytoplasmic MET expression was identified as a good prognostic factor for overall survival ($p = 0.048$) (Figure 5.15A), multivariate analyses including cytoplasmic MET expression and other potential factors were performed, and the results were summarised in Table 5.2. The lymph node status was an independent prognostic factor for progression-free survival and overall survival. Cytoplasmic MET expression was not an independent prognostic factor for progression-free survival (HR 0.55, $p = 0.17$)

and overall survival (HR 0.44, p = 0.09) although there is a possibility that this study could be underpowered due to the relative small number of tumours with high cytoplasmic MET expression.

Figure 5.12

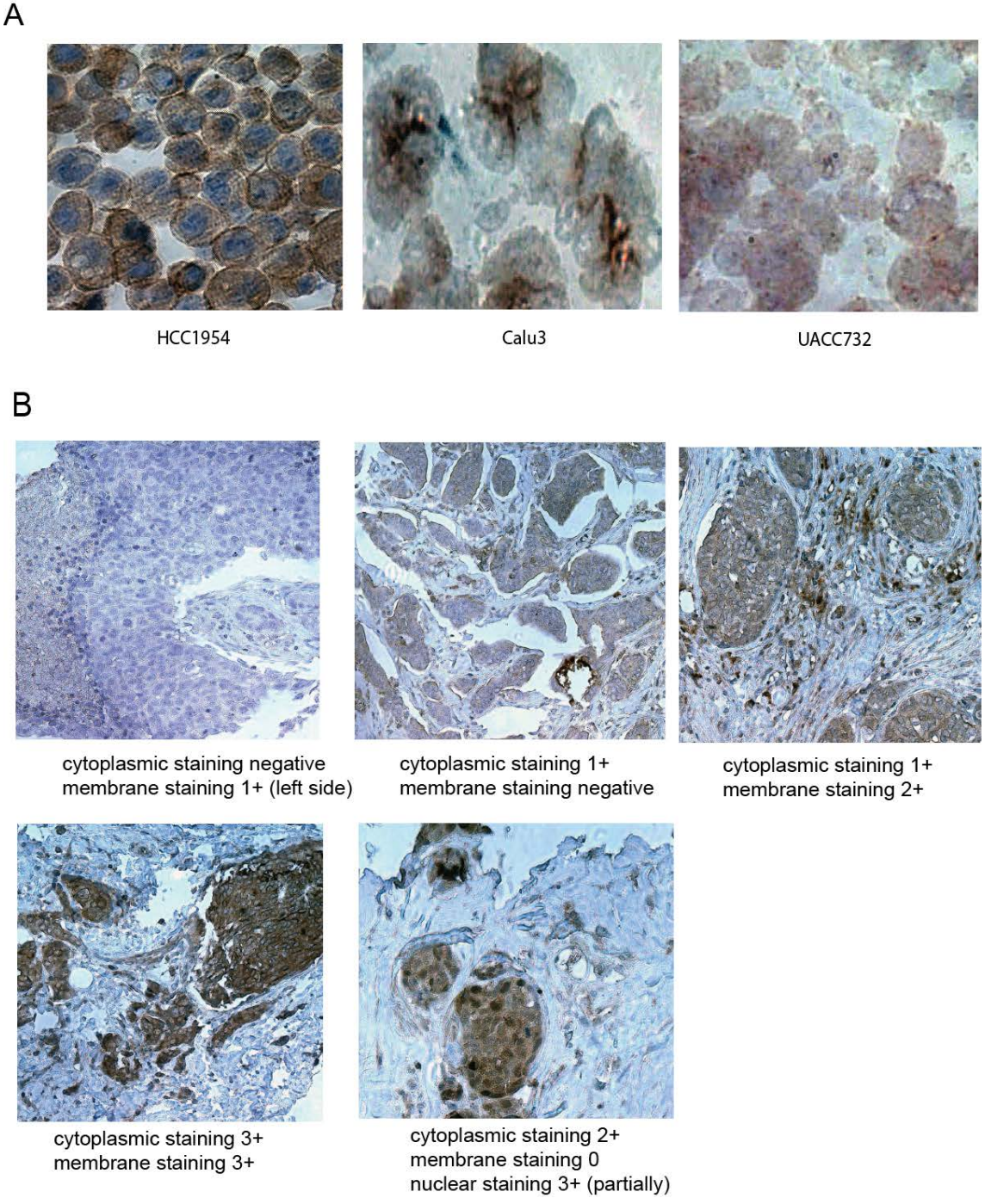

Figure 5.12 Representative MET staining in HER2-positive cell lines (A) and HER2-positive tumours in human tissues (B) (x40).

Figure 5.13

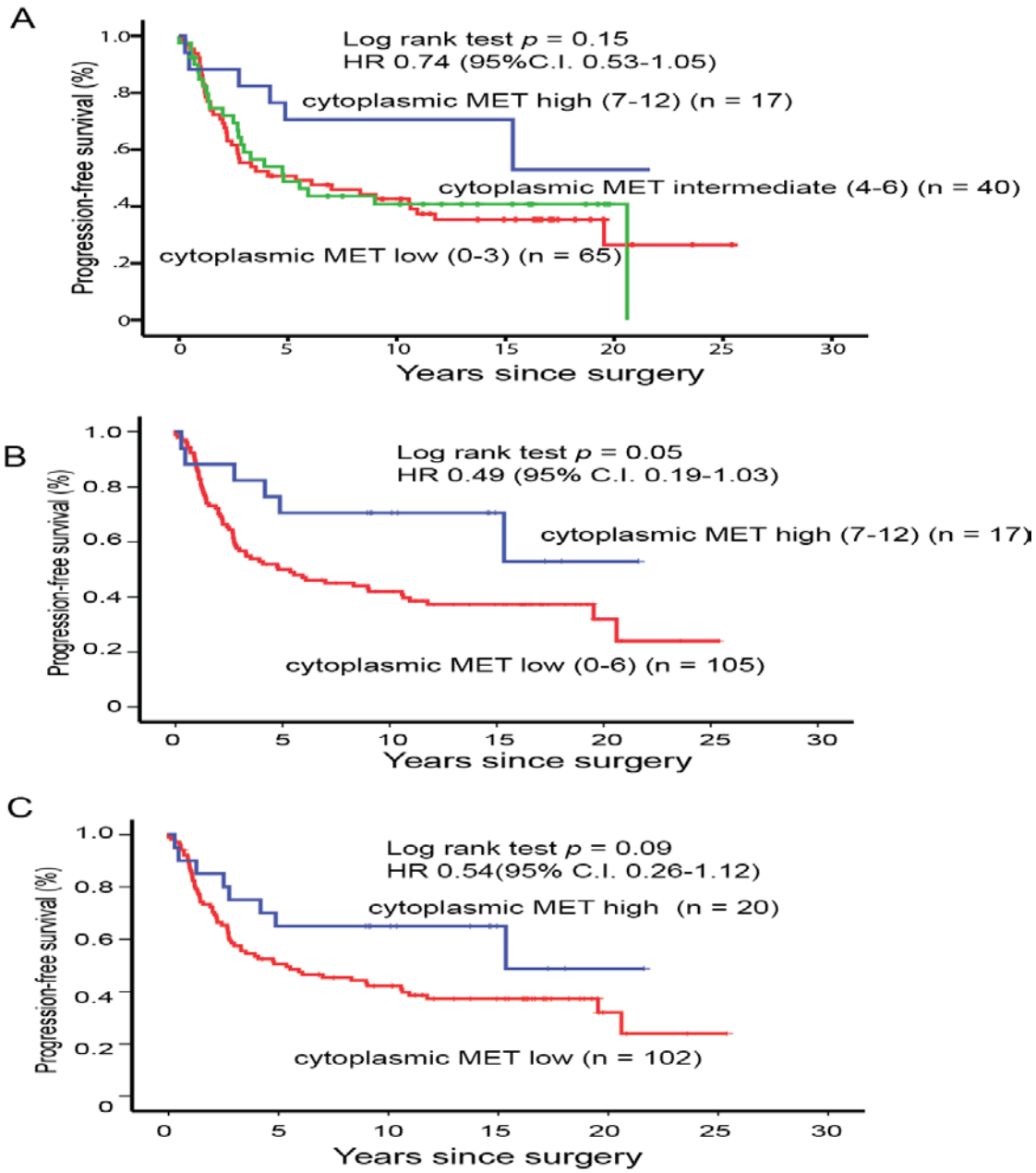

Figure 5.13 Progression-free survival in HER2-positive, trastuzumab non-treated patients according to the cytoplasmic MET expression by different cut-off values. A, Patients were divided into 3 groups according to the immunoreactive scoring system (IRS); low 0-3 (red), intermediate 4-6 (green), and high 7-12 (blue). B, Patients were dichotomised according to the IRS; low 0-6 (red) and high 7-12 (blue). C, Patients were dichotomised by cytoplasmic MET high (more than 10% of positive cells and intensity 2-3) and cytoplasmic MET low expression (all others). HR; hazard ratio, CI; confidence interval.

Figure 5.14

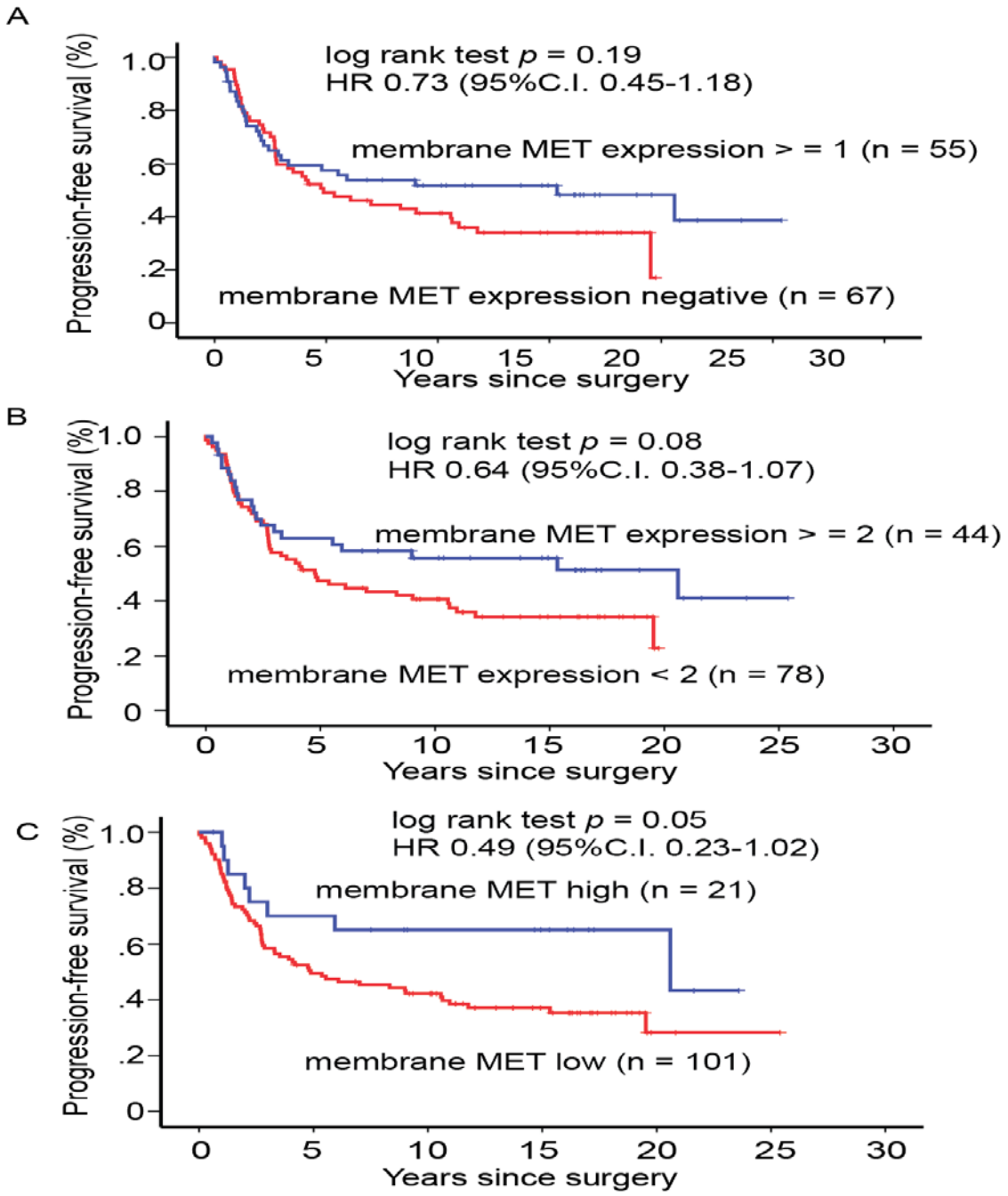

Figure 5.14 Progression-free survival in HER2-positive, trastuzumab non-treated patients according to the membrane MET expression by different cut-off values. A, Patients were dichotomised according to the immunoreactive scoring system (IRS); negative (red) and all others (≥1) (blue). B, Patients were dichotomised according to the IRS; < 2 (red) and ≥ 2 (blue). C, Patients were dichotomised by membrane MET high (more than 10% of positive cells and intensity 2-3) and MET low expression (all others). HR; hazard ratio, CI; confidence interval.

Figure 5.15

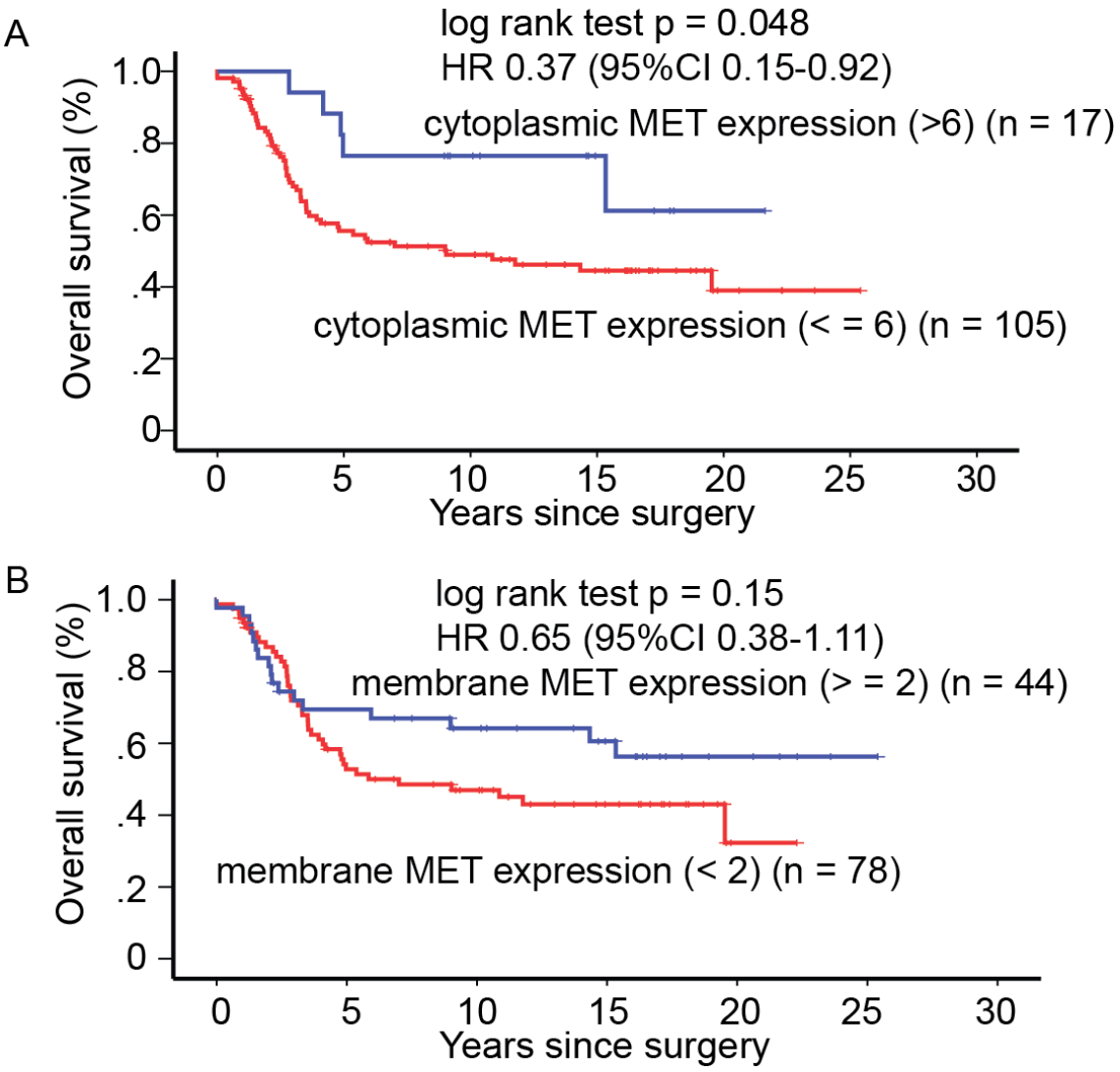

Figure 5.15 Overall survival in HER2-positive, trastuzumab non-treated patients according to the cytoplasmic MET expression (A) and membrane MET expression (B). HR; hazard ratio, CI, confidence interval.

Table 5.1 Characteristics of patients according to cytoplasmic MET expression.

Factor	N	Cytoplasmic MET expression ≤ 6 n (%)	> 6 n (%)	P (chi-square)
Histological type				
Ducutal	109	94 (86)	15 (14)	
Other	13	11 (85)	2 (15)	0.87
Histological grade				
1 or 2	17	15 (88)	2 (12)	
3	105	90 (86)	15 (14)	0.78
ER				
Negative	62	51 (82)	11 (18)	
Positive	60	54 (90)	6 (10)	0.22
PgR				
Negative	78	67 (86)	11 (14)	
Positive	44	38 (86)	6 (14)	0.94
Tumour size (pT)				
≤20 mm	54	43 (80)	11 (20)	
>20mm	68	62 (91)	6 (9)	0.07
Nodal status (N)				
Negative	59	47 (80)	12 (20)	
Positive	63	58 (92)	5 (8)	0.05
Age	53.0 (range 31-71)			0.88*
Tumour diameter (mm)	20 (range 9-80)			0.19*
			* Mann-Whitney test	

Table 5.2 Multivariate analysis for progression-free survival and overall survival.

Variables	Univariate analysis			Multivariate analyis		
	HR	95% C.I.	P value	HR	95% C.I.	P value
Estrogen (positive *vs.* negative)	1.143	0.719-1.819	0.571	0.951	0.534-1.691	0.863
Progesteron (positive *vs.* negative)	1.179	0.734-1.894	0.495	1.137	0.624-2.070	0.676
Lymphnode metastases (positive *vs.* negative)	2.284	1.401-3.723	0.001	2.56	1.508-4.347	0.001
Tumour grade (3 *vs.* 1, 2)	0.812	0.436-1.51	0.52	0.717	0.372-1.382	0.32
Cytoplasmic HER3 (high *vs*. low)	1.158	0.729-1.839	0.535	1.284	0.775-2.127	0.332
Nuclear HER3 (high *vs.* low)	0.641	0.257-1.597	0.339	0.62	0.248-1.553	0.308

5.3 Discussion

5.3.1 HER3 phosphorylation and MET in trastuzumab treatment

In this project, a decrease of HER3 phosphorylation level was shown to be a predictive biomarker for trastuzumab response in a panel of HER2-positive cell lines. After long-term trastuzumab treatment, a recovery of HER3 phosphorylation was observed in 2 cell lines (BT474 and NCI-H2170 cells) after an initial decrease of HER3 phosphorylation in response to trastuzumab. In particular, an increase of MET was also observed in these cell lines after long-term trastuzumab treatment (Figure 5.3, 5.5). In the BT474 resistant cells, MET and HER3 interaction was increased when compared to the parental BT474 cells. This result suggests that MET contributes to maintaining HER3 phosphorylation and protects cells from growth inhibition by trastuzumab. Indeed, MET knockdown led to a decrease of HER3 phosphorylation in 4 cells lines (BT474, BT474-TR, HCC1954, and NCI-H2170-TR cells) (Figure 5.7B) and MET knockdown sensitised the HCC1954 cells to trastuzumab (Figure 5.8A). Furthermore, MET expression tended to be higher in trastuzumab non-responding cells (Figure 5.6B). Taken together, MET is implicated in trastuzumab

resistance. These results implicate that MET could be a predictive biomarker for trastuzumab treatment.

MET gene amplification is found in gefitinib resistant cells and MET inhibitor could recover the sensitivity to gefitinib in the resistant cells[114]. In this report, knockdown of MET decreased HER3 and AKT phosphorylation level in the gefitinib resistant cells. However, the reason why MET knockdown reduced HER3 phosphorylation level is unknown. HER3 and MET interaction was observed in the BT474 cells and the interaction was increased when the cells became resistant to trastuzumab (Figure 5.7C). MET exists as a homodimer and HER3 needs transphosphorylation for maintaining its phosphorylation. It is still uncertain whether MET can form a hybrid dimer with other receptors. In the normal hepatocyte, MET has been suggested to make a hybrid with IGF1R to regulate plasma glucose level[194]. It was reported that a MET inhibitor that inhibited MET phosphorylation could reduce phosphorylation of HER3[115]. These reports support that HER3 can be phosphorylated via direct interaction with MET although crystal structure analysis is necessary to confirm this hypothesis. HER3 is important for HER2-positive cell survival[55,56]. MET knockdown decreased HER3

phosphorylation level and resulted in a decrease of colony formation with or without continuous trastuzumab treatment in the BT474-TR cells (Figure 5.8). These results suggest that HER3 phosphorylation is also important for HER2-positive cell survival. A decrease of HER3 phosphorylation was correlated with trastuzumab sensitivity (Figure 5.2). Therefore, MET could be a factor in predicting trastuzumab response.

HER3 cannot be phosphorylated even with HRG stimulation if there is no HER2[46], and HER3 is catalytically inactive due to the mutation in its kinase domain compared to the other HER receptors[35]. However, HER3 can activate other dimerised partners without HER3 phosphorylation by forming asymmetric kinase dimer[45,195]. Recently, a study has clarified that HER3 kinase domain binds ATP at a similar level to inactivate EGFR and HER4, and thus catalysed HER3 can be transphosphorylated by other partners[196]. If MET can catalyse HER3 and results in its phosphorylation, ligand stimulation would not be necessary since a recent study suggests that ligand stimulation is not always necessary to form heterodimerisation of HER2 and HER3[25]. Ligand stimulation (HGF and HRG) was assessed in this study but the ligands could only increase its own respective

receptor phosphorylation (Figure 5.11), suggesting that the interaction of MET and HER3 may be ligand-independent.

A monoclonal antibody against HER3, SGP1 was used to assess whether HER3 blocking can recover the sensitivity to trastuzumab in the BT474-TR cells (in Chapter 3). SGP1 was raised against HER3 extracellular domain and competes for HRG binding on HER3[172,197]. Although HRG does not promote MET phosphorylation through HER3 (Figure 5.11), SGP1 could reduce colony formation only when co-treated with trastuzumab (Figure 3.16). Previously, SGP1 antibody was shown to have no effect on the growth inhibition of HER3–positive cells, BT483 and T47D[197]. Later, SGP1 antibody was shown to inhibit growth stimulation by HRG in MDA-MD-453 cells. SGP1 and trastuzumab were also found to bind simultaneously to HER3 and HER2 in MDA-MB-453 cells, and SGP1 and trastuzumab co-treatment showed additive effect on the cell growth of the BT474 and MDA-MB-361 cells[172]. There remains uncertainty why the combination of SGP1 and trastuzumab reduced colony formation in the resistant cells since SGP1 did not affect HER3 subcellular localisation (Figure 3.15), HER3 expression[172], and HER3 phosphorylation (preliminary data not shown). Although

the precise mechanism of the combination treatment is unclear, anti-HER2 and anti-HER3 combination directed therapies could be promising.

MET knockdown reduced HER3 phosphorylation and sensitised innate trastuzumab resistant HCC1954 cells to trastuzumab. (Figure 5.8A). MET knockdown reduced phosphorylation of HER3, and thus its downstream signalling affects cell survival. Indeed, MET knockdown reduced the number of colonies by nearly 50% in the BT474-TR cells. It is assumed that the surviving cells may have different signalling pathways so that trastuzumab had no effect on these cells (Figure 5.8B). A anti-MET monoclonal antibody was also assessed whether it can recover the sensitivity to trastuzumab in the BT4747-TR cells. However, the antibody had no effect for cell survival even it reduced MET expression (Figure 5.9). Although MET expression was reduced by the antibody, HER3 phosphorylation examined at different time points was maintained, while total MET knockdown decreased HER3 phosphorylation in 4 different cells (Figure 5.7B). Although significant amount of MET expression was decreased by this monoclonal antibody, it would be possible that HER3 phosphorylation was maintained through residual MET expression. There is also a possibility that MET

monoclonal antibody may induce HRG to maintain HER3 phosphorylation by ligand shedding as seen in trastuzumab treatment[32]. This result may also indicate that reduction of MET expression may not be sufficient to reduce the cell survival and reduction of HER3 phosphorylation may be necessary. Since cytoplasmic MET has been indicate to have signalling role[193], another strategy to inhibit MET signalling was taken. SU11274, a selective MET kinase inhibitor was used for this call. SU11274 has been reported to have synergistic effect with trastuzumab in the parental BT474 and SKBr3 cells[30]. Although the additional effect was not observed in this project, MET kinase inhibitor effectively reduced the cell viability in the BT474-TR cells (Figure 5.9C).

5.3.2 MET as a biomarker in HER2-positive breast cancer

Cytoplasmic, membrane, and nuclear MET expression was assessed in the HER2-positive patients cohort (n = 122). As stated in discussion in chapter 4, this cohort did not receive trastuzumab treatment as an adjuvant therapy because the tumour samples were collected in the pre-trastuzumab era. Therefore the direct link between the preclinical model and clinical result is limited. High cytoplasmic

and membrane MET expression showed a trend to improved progression-free survival in this cohort and high cytoplasmic MET expression was associated with better overall survival (Figure 5.13, 5.14, 5.15). Since MET overexpression sensitises the cells to HGF stimulation or promotes interaction with other receptors ligand independently[95], aberrant MET expression is supposed to be a poor prognostic factor[99,103,104,109] However, there have been several reports suggesting that MET expression was associated with good prognosis in breast cancer[198,199]. These reports evaluated cytoplasmic MET expression using IHC including all breast cancer subtypes. Some other publications reporting MET as a poor prognostic factors have not identified MET as a biomarker in HER2-positive breast cancer subtype[99,104,109]. In these studies, there is a possibility that high MET expression is found in HER2-positive subtype since an association of MET expression and HER2 positivity was reported[99]. In this chapter, membrane MET expression was shown to be associated with HER2 positivity, and nuclear MET expression was shown to be associated with HER2 negativity.

MET gene amplification has been shown to be associated with poor survival in HER2-positive, trastuzumab treated patients[103]. MET gene amplification is

assumed to overexpress MET protein. However, to the best of my knowledge, there seems to be no study to evaluate the prevalence of MET protein overexpression and its clinical implication in HER2-positive breast patients. In addition, MET is internalised by endocytosis and thus exists in the cytoplasm and the nucleus. Furthermore, MET in cytoplasm has been reported to have signalling role[94,193]. Therefore, MET protein expression and its localisation should be evaluated in larger HER2-positive breast cancer samples to further understand its clinical impact. As shown in Chapter 4, HER3 is often co-expressed with HER2 in HER2-positive breast cancer. Therefore, it is interesting to see that HER3 is also co-expressed with MET in HER2-positive breast cancer since HER3 and MET interaction can maintain HER3 phosphorylation during trastuzumab treatment and MET knockdown reduced colony formation in HER2-positive breast cancer cells. HER3 and MET interaction on human tissue samples could be evaluated by using Förster Resonance Energy Transfer (FRET)[200] and proximity ligation assay[82]. Another strategy that could be considered for this purpose is to evaluate HER3 phosphorylation in human tissue samples. However, the detection of phospho-protein in IHC is difficult since immediate fixation is necessary to protect samples from degradation. For this purpose, standard

operating procedures (SOP) should be established for the sample collections. Due to the lack of reliability of phosphoprotein staining in retrospectively collected samples, it is difficult to evaluate phosphorylation of HER3 in these samples.

5.3.3 Study limitations

MET and HER3 interaction could have been determined by additional methods, such as FRET or proximity ligation assay although the success of these assays is highly dependent on suitable antibodies, and a series of optimisation experiments would be required to obtain reliable results. Due to limitation of time and resources, these methods could not be used to validate my findings. It would also be useful to assess the interaction of MET and HER3 in a larger panel of cell lines. To conclude that MET-HER3 interaction is independent of ligand stimulation, FRET or the proximity ligation assay as well as co-immunoprecipitation experiments with HER3 and MET ligand stimulation should be examined in future studies. Furthermore, monoclonal antibody against MET or HER3, or MET tyrosine kinase inhibitor should be examined to see if they disrupt MET-HER3 interaction. In the clinical study, there is a discrepancy

between clinical results and the preclinical model, which could be because the tumour samples were obtained from non-trastuzumab treated patients. Furthermore, it is unclear why cytoplasmic MET expression was associated with favourable outcome. It is proposed that the results on MET expression in patients' survival should be further validated in another data set in the future, preferably in tumour samples from a randomised trial of breast cancer patients treated with or without trastuzumab, e.g. FinHER trials samples as shown in chapter 4 although the samples were not provided by FinHER committee for this part of the project.

CHAPTER 6

CONCLUSIONS AND FUTURE DIRECTIONS

Trastuzumab has been introduced into clinical practice since 1998 but there is no standard biomarker to predict the response except for HER2 positivity. Several proposals have been made for predicting trastuzumab response including PTEN expression, Src activation, PI3K activation, ADAM17 upregulation, IGF1R overexpression, and MET overexpression[26-30,32]. However, none of these markers except for HER2 positivity is currently used in clinical practice. This could be because of several reasons including reproducibility, reliability, and the identification of standard cut-off points of IHC for these markers. Trastuzumab treatment is less toxic compared to conventional chemotherapies, however, 10-30% of the patients develop cardiac toxicity[201]. Furthermore, the response rate to trastuzumab monotherapy is only 10-30 % in HER2-positive patients, and trastuzumab and chemotherapy combination treatment yields about 50-60 % of response[15-21]. It is an important issue to identify responders to trastuzumab before starting treatment so that patients can avoid unnecessary toxicity and treatment. Trastuzumab is known to bind HER2, but it is also known that

trastuzumab does not affect HER2 phosphorylation[25,26,32]. Since HER2 and HER3 are often co-expressed and HER3 is important for HER2-positive cancers[35], it was hypothesised that HER3 could be a biomarker for trastuzumab treatment. Therefore, this project aimed to identify the biomarker(s) in trastuzumab treatment, especially focusing on HER3 subcellular localisation and HER3-MET interaction.

In chapter 3 and 4, HER3 subcellular localisation was assessed based on the hypothesis that HER3 translocation into the nucleus could be associated with trastuzumab response and resistance. HER3 expression in the nucleus was increased when the SKBr3 cells acquired resistance to trastuzumab. In addition, the increased nuclear HER3 expression was not detected by the antibody generated for N-terminus of HER3. Therefore, it was suggested that HER3 may undergo proteolytic cleavage as seen in HER4[118]. Indeed, ADAM17 and γ-secretase inhibitor reduced the nuclear HER3 expression, which corresponded with $HER3_{100kD}$ in the nucleus. Blocking γ-secretase with trastuzumab treatment inhibited colony formation in the SKBr3-TR cells. ADAM17 is known to shed extracellular domain, but there is no known specific cleavage site that ADAM17

can recognise[152]. It is also controversial whether the γ-secretase complex recognises the specific sequence for cleavage[161,162]. Therefore, it is difficult to predict specific cleavage site for truncated HER3 by these proteases. To identify the cleavage site of HER3, it is necessary to perform Mass Spectrometry in the future. In addition, it should be assessed whether the mutated cleavage site could block the nuclear HER3 translocation into the nucleus. It would also be interesting to see whether introducing mutated cleavage site of HER3 into the innate and acquired resistant cells could re-sensitise the cells to trastuzumab.

In this study, the frequency of nuclear HER3 in human HER2-positive breast cancer varied between 8.9-37% in the different cohorts of patient samples. There is a possibility that there are missing cases of nuclear HER3 in this study due to the fixation problem since the protocol used for tissue fixation could vary between different institutes, and some tumours may have degenerated nuclear protein. To ensure minimal protein degradation in tumours, the samples should be collected and fixed immediately. It is recommended that the methods of collection should be stated in the standard operating procedure including the time from the samples collected by biopsy or excision to the fixation, the fixation time as well as fixation

reagent used since all these factors will affect sample condition for IHC results[202]. However, these details are not always stated or followed during sample collection for some of the biobanks or clinical trials. This may result in variation in the tissue quality. In this study, all the IHC samples were evaluated by the same two persons. However, since IHC scoring may be subjective, it is recommended that a universal scoring system (IRS in this study) for judging nuclear HER3 positivity should be used in future studies. In addition, the cut-off values used for HER3 and MET staining in this project need to be further refined. Although nuclear HER3 was associated with poor progression-free survival and overall survival for both trastuzumab treated and non-treated patients in FinHER trials, the results need to be further validated in another data set from a randomised controlled trial which compared trastuzumab and non-trastuzumab treatment for HER2-positive breast cancer patients. It would be interesting to plan a prospective clinical trial using nuclear HER3 as a biomarker in the future. Stratifying HER2-positive breast cancer patients by nuclear HER3 to assess trastuzumab response, or designing 2x2 trial to apply trastuzumab or alternative treatment according to nuclear HER3 status would be warranted to translate this result to the bedside.

In chapter 5, MET expression in HER2-positive cell lines in relation with HER3 phosphorylation was assessed. It is known that HER3 phosphorylation is reduced by trastuzumab treatment[25]. Previously, our laboratory found that HER3 phosphorylation recovers when cells become resistant to trastuzumab after long exposure to trastuzumab[32]. MET has been found to be overexpressed during trastuzumab treatment and contributes to trastuzumab resistance[30]. Furthermore, HER3 and MET co-expression in Chinese hamster ovary (CHO) cells results in HER3 phosphorylation, which is not reduced by gefitinib or lapatinib treatment[114]. Therefore, it was hypothesised that HER3 phosphorylation in the trastuzumab resistant cells could be maintained through MET overexpression, and MET overexpression could be an indicator of trastuzumab response. HER3 phosphorylation was decreased by trastuzumab treatment mainly in the sensitive cell lines, and high MET expression was observed mainly in the resistant cell lines (Figure 5.2, 5.6B). MET expression was increased in acquired-trastuzumab resistant BT474 and NCI-H2170 cells. These findings suggest that MET could be a factor for trastuzumab resistance due to the maintenance of HER3 phosphorylation. Indeed, MET knockdown reduced HER3 phosphorylation in several cell lines and MET-HER3 interaction was increased in the BT474-TR cells

as shown by the immunoprecipitation method. However, it is recommended that this interaction should be further assessed using other more precise methodologies including FRET or proximity ligation assay in the future. Furthermore, it should be assessed whether ligand stimulation promotes MET and HER3 interaction. Ideally, crystal structure analysis is warranted to confirm HER3-MET heterodimerisation.

Preclinical results in chapter 5 and previous publication indicate that high MET expression could be a prognostic or predictive marker for HER2-positive, trastuzumab treated breast cancer patients[30]. Although the samples used to stain for MET expression in this project were all non-trastuzumab treated samples, high MET expression (cytoplasm) was associated with good prognosis. Since there is no standard cut-off value for MET IHC staining, several cut-off values were assessed. In the future, MET IHC scoring and the cut-off points should be further refined and validated in another data set. If MET expression is confirmed to be a good prognostic marker for HER2-positive breast cancer patients in the future, careful selection of patients for MET-directed therapy would be necessary since MET-positive tumours could be a more non-aggressive phenotype in HER2-

positive cancer cells. Although the clinical impact of MET expression is still unclear, it is possible that MET could be a target only when tumours have acquired resistance to trastuzumab.

It is also necessary to clarify MET localisation and its clinical impact. Membrane and cytoplasmic MET expression was assessed in this project and both of them were associated with good prognosis. However, the clinical significance of nuclear MET expression is unclear due to low prevalence of nuclear positivity and a small sample size. Nuclear MET expression was found to be more prevalent in non HER2-positive breast cancer samples. Thus, it would be interesting to clarify its clinical impact in non HER2-positive breast cancer, especially triple-negative breast cancer since there is no available targeted therapy for this subtype. Although MET tyrosine kinase inhibitors and monoclonal antibodies have been tested in various clinical trials for different cancers, the results have not been very promising and none of the inhibitors is approved for clinical use in any cancer at present. In addition, its clinical use as monotherapy or in combination with other agents in breast cancer remains to be determined.

Furthermore, as shown in this study and other studies, MET expression as a prognostic and predictive biomarker remains unclear and controversial.

Concluding remarks

In this study, nuclear HER3 was identified in innate and acquired trastuzumab resistant cell lines and mouse xenograft tumours. It was found that induction of nuclear HER3 was mediated by ADAM17 and γ-secretase. Nuclear HER3 was found to be increased after neoadjuvant trastuzumab and docetaxel combination therapy for HER2-positive breast cancer patients. Nuclear HER3 was also a poor prognostic marker for HER2-positive breast cancer patients participating in FinHER trial. The role of MET was also studied and it was shown to interact with HER3 to maintain HER3 phosphorylation in response to trastuzumab treatment and resistance. However, higher MET expression was associated with good prognosis in HER2-positive breast cancer patients who were not treated with trastuzumab. Although MET upregulation is implicated in trastuzumab resistance in preclinical models, the clinical significance of MET expression in HER2-positive breast cancer patients remains unclear. Overall, this study has proposed novel

resistance mechanisms to trastuzumab in HER2 positive breast cancer. However, the clinical significance of nuclear HER3 and MET expression should be further validated in future studies.

BIBLIOGRAPHY

1. Siegel, R., Ma, J., Zou, Z. & Jemal, A. Cancer statistics, 2014. *CA Cancer J Clin* **64**, 9-29 (2014).
2. DeSantis, C., Ma, J., Bryan, L. & Jemal, A. Breast cancer statistics, 2013. *CA Cancer J Clin* **64**, 52-62 (2014).
3. Weigelt, B. & Reis-Filho, J.S. Histological and molecular types of breast cancer: is there a unifying taxonomy? *Nat Rev Clin Oncol* **6**, 718-730 (2009).
4. Senkus, E.*, et al.* Primary breast cancer: ESMO clinical practice guidelines for diagnosis, treatment and follow-up. *Ann Oncol* **24 Suppl 6**, vi7-23 (2013).
5. Perou, C.M.*, et al.* Molecular portraits of human breast tumours. *Nature* **406**, 747-752 (2000).
6. Sorlie, T.*, et al.* Gene expression patterns of breast carcinomas distinguish tumor subclasses with clinical implications. *Proc Natl Acad Sci U S A* **98**, 10869-10874 (2001).
7. Prat, A.*, et al.* Molecular characterization of basal-like and non-basal-like triple-negative breast cancer. *Oncologist* **18**, 123-133 (2013).
8. Rakha, E., Ellis, I. & Reis-Filho, J. Are triple-negative and basal-like breast cancer synonymous? *Clin Cancer Res* **14**, 618; author reply 618-619 (2008).
9. Perou, C.M. Molecular stratification of triple-negative breast cancers. *Oncologist* **15 Suppl 5**, 39-48 (2010).
10. Wolff, A.C.*, et al.* Recommendations for human epidermal growth factor receptor 2 testing in breast cancer: american society of clinical oncology/college of american pathologists clinical practice guideline update. *J Clin Oncol* **31**, 3997-4013 (2013).
11. Giordano, S.H.*, et al.* Systemic therapy for patients with advanced human epidermal growth factor receptor 2-positive breast cancer: american society of clinical oncology clinical practice guideline. *J Clin Oncol* (2014).
12. Slamon, D.J.*, et al.* Use of chemotherapy plus a monoclonal antibody against HER2 for metastatic breast cancer that overexpresses HER2. *N Engl J Med* **344**, 783-792 (2001).
13. Swain, S.M.*, et al.* Pertuzumab, trastuzumab, and docetaxel for HER2-positive metastatic breast cancer (CLEOPATRA study): overall survival results from a randomised, double-blind, placebo-controlled, phase 3 study. *Lancet Oncol* **14**, 461-471 (2013).

14. Cho, H.S.*, et al.* Structure of the extracellular region of HER2 alone and in complex with the Herceptin Fab. *Nature* **421**, 756-760 (2003).
15. Baselga, J.*, et al.* Phase II study of weekly intravenous recombinant humanized anti-p185HER2 monoclonal antibody in patients with HER2/neu-overexpressing metastatic breast cancer. *J Clin Oncol* **14**, 737-744 (1996).
16. Inoue, K.*, et al.* Randomized phase III trial of trastuzumab monotherapy followed by trastuzumab plus docetaxel versus trastuzumab plus docetaxel as first-line therapy in patients with HER2-positive metastatic breast cancer: the JO17360 Trial Group. *Breast Cancer Res Treat* **119**, 127-136 (2010).
17. Seidman, A.D.*, et al.* Weekly trastuzumab and paclitaxel therapy for metastatic breast cancer with analysis of efficacy by HER2 immunophenotype and gene amplification. *J Clin Oncol* **19**, 2587-2595 (2001).
18. Vogel, C.L.*, et al.* Efficacy and safety of trastuzumab as a single agent in first-line treatment of HER2-overexpressing metastatic breast cancer. *J Clin Oncol* **20**, 719-726 (2002).
19. Robert, N.*, et al.* Randomized phase III study of trastuzumab, paclitaxel, and carboplatin compared with trastuzumab and paclitaxel in women with HER-2-overexpressing metastatic breast cancer. *J Clin Oncol* **24**, 2786-2792 (2006).
20. Buzdar, A.U.*, et al.* Significantly higher pathologic complete remission rate after neoadjuvant therapy with trastuzumab, paclitaxel, and epirubicin chemotherapy: results of a randomized trial in human epidermal growth factor receptor 2-positive operable breast cancer. *J Clin Oncol* **23**, 3676-3685 (2005).
21. Baselga, J.*, et al.* Lapatinib with trastuzumab for HER2-positive early breast cancer (NeoALTTO): a randomised, open-label, multicentre, phase 3 trial. *Lancet* **379**, 633-640 (2012).
22. Clynes, R.A., Towers, T.L., Presta, L.G. & Ravetch, J.V. Inhibitory Fc receptors modulate in vivo cytotoxicity against tumor targets. *Nat Med* **6**, 443-446 (2000).
23. Yakes, F.M.*, et al.* Herceptin-induced inhibition of phosphatidylinositol-3 kinase and Akt Is required for antibody-mediated effects on p27, cyclin D1, and antitumor action. *Cancer Res* **62**, 4132-4141 (2002).
24. Nahta, R., Takahashi, T., Ueno, N.T., Hung, M.C. & Esteva, F.J. P27(kip1) down-regulation is associated with trastuzumab resistance in breast cancer cells. *Cancer Res* **64**, 3981-3986 (2004).

25. Junttila, T.T.*, et al.* Ligand-independent HER2/HER3/PI3K complex is disrupted by trastuzumab and is effectively inhibited by the PI3K inhibitor GDC-0941. *Cancer Cell* **15**, 429-440 (2009).
26. Nagata, Y.*, et al.* PTEN activation contributes to tumor inhibition by trastuzumab, and loss of PTEN predicts trastuzumab resistance in patients. *Cancer Cell* **6**, 117-127 (2004).
27. Berns, K.*, et al.* A functional genetic approach identifies the PI3K pathway as a major determinant of trastuzumab resistance in breast cancer. *Cancer Cell* **12**, 395-402 (2007).
28. Zhang, S.*, et al.* Combating trastuzumab resistance by targeting SRC, a common node downstream of multiple resistance pathways. *Nat Med* **17**, 461-469 (2011).
29. Lu, Y., Zi, X., Zhao, Y., Mascarenhas, D. & Pollak, M. Insulin-like growth factor-I receptor signaling and resistance to trastuzumab (Herceptin). *J Natl Cancer Inst* **93**, 1852-1857 (2001).
30. Shattuck, D.L., Miller, J.K., Carraway, K.L., 3rd & Sweeney, C. Met receptor contributes to trastuzumab resistance of Her2-overexpressing breast cancer cells. *Cancer Res* **68**, 1471-1477 (2008).
31. Tse, C., Gauchez, A.S., Jacot, W. & Lamy, P.J. HER2 shedding and serum HER2 extracellular domain: biology and clinical utility in breast cancer. *Cancer Treat Rev* **38**, 133-142 (2012).
32. Gijsen, M.*, et al.* HER2 phosphorylation is maintained by a PKB negative feedback loop in response to anti-HER2 herceptin in breast cancer. *PLoS Biol* **8**, e1000563 (2010).
33. Feldinger, K.*, et al.* ADAM10 mediates trastuzumab resistance and is correlated with survival in HER2 positive breast cancer. *Oncotarget* **in press**(2014).
34. Hynes, N.E. & Lane, H.A. ERBB receptors and cancer: the complexity of targeted inhibitors. *Nat Rev Cancer* **5**, 341-354 (2005).
35. Baselga, J. & Swain, S.M. Novel anticancer targets: revisiting ERBB2 and discovering ERBB3. *Nat Rev Cancer* **9**, 463-475 (2009).
36. Ogiso, H.*, et al.* Crystal structure of the complex of human epidermal growth factor and receptor extracellular domains. *Cell* **110**, 775-787 (2002).
37. Burgess, A.W.*, et al.* An open-and-shut case? Recent insights into the activation of EGF/ErbB receptors. *Mol Cell* **12**, 541-552 (2003).
38. Harari, D. & Yarden, Y. Molecular mechanisms underlying ErbB2/HER2 action in breast cancer. *Oncogene* **19**, 6102-6114 (2000).

39. Holmes, W.E.*, et al.* Identification of heregulin, a specific activator of p185erbB2. *Science* **256**, 1205-1210 (1992).
40. Agus, D.B.*, et al.* Targeting ligand-activated ErbB2 signaling inhibits breast and prostate tumor growth. *Cancer Cell* **2**, 127-137 (2002).
41. Olayioye, M.A., Neve, R.M., Lane, H.A. & Hynes, N.E. The ErbB signaling network: receptor heterodimerization in development and cancer. *Embo Journal* **19**, 3159-3167 (2000).
42. Lemmon, M.A. & Schlessinger, J. Cell signaling by receptor tyrosine kinases. *Cell* **141**, 1117-1134 (2010).
43. Ushiro, H. & Cohen, S. Identification of phosphotyrosine as a product of epidermal growth factor-activated protein kinase in A-431 cell membranes. *J Biol Chem* **255**, 8363-8365 (1980).
44. Yarden, Y. & Sliwkowski, M.X. Untangling the ErbB signalling network. *Nat Rev Mol Cell Biol* **2**, 127-137 (2001).
45. Zhang, X., Gureasko, J., Shen, K., Cole, P.A. & Kuriyan, J. An allosteric mechanism for activation of the kinase domain of epidermal growth factor receptor. *Cell* **125**, 1137-1149 (2006).
46. Berger, M.B., Mendrola, J.M. & Lemmon, M.A. ErbB3/HER3 does not homodimerize upon neuregulin binding at the cell surface. *FEBS Lett* **569**, 332-336 (2004).
47. Yu, X., Sharma, K.D., Takahashi, T., Iwamoto, R. & Mekada, E. Ligand-independent dimer formation of epidermal growth factor receptor (EGFR) is a step separable from ligand-induced EGFR signaling. *Mol Biol Cell* **13**, 2547-2557 (2002).
48. Alvarado, D., Klein, D.E. & Lemmon, M.A. Structural basis for negative cooperativity in growth factor binding to an EGF receptor. *Cell* **142**, 568-579 (2010).
49. Liu, P.*, et al.* A single ligand is sufficient to activate EGFR dimers. *Proc Natl Acad Sci U S A* **109**, 10861-10866 (2012).
50. Prigent, S.A.*, et al.* Expression of the c-erbB-3 protein in normal human adult and fetal tissues. *Oncogene* **7**, 1273-1278 (1992).
51. Yano, S.*, et al.* Distribution and function of EGFR in human tissue and the effect of EGFR tyrosine kinase inhibition. *Anticancer Res* **23**, 3639-3650 (2003).
52. Press, M.F., Cordon-Cardo, C. & Slamon, D.J. Expression of the HER-2/neu proto-oncogene in normal human adult and fetal tissues. *Oncogene* **5**, 953-962 (1990).

53. Lahlou, H., Muller, T., Sanguin-Gendreau, V., Birchmeier, C. & Muller, W.J. Uncoupling of PI3K from ErbB3 impairs mammary gland development but does not impact on ErbB2-induced mammary tumorigenesis. *Cancer Res* **72**, 3080-3090 (2012).
54. Riethmacher, D.*, et al.* Severe neuropathies in mice with targeted mutations in the ErbB3 receptor. *Nature* **389**, 725-730 (1997).
55. Pinkas-Kramarski, R.*, et al.* Diversification of Neu differentiation factor and epidermal growth factor signaling by combinatorial receptor interactions. *EMBO J* **15**, 2452-2467 (1996).
56. Lee-Hoeflich, S.T.*, et al.* A central role for HER3 in HER2-amplified breast cancer: implications for targeted therapy. *Cancer Res* **68**, 5878-5887 (2008).
57. Jaiswal, B.S.*, et al.* Oncogenic ERBB3 mutations in human cancers. *Cancer Cell* **23**, 603-617 (2013).
58. Soltoff, S.P., Carraway, K.L., 3rd, Prigent, S.A., Gullick, W.G. & Cantley, L.C. ErbB3 is involved in activation of phosphatidylinositol 3-kinase by epidermal growth factor. *Mol Cell Biol* **14**, 3550-3558 (1994).
59. Kim, H.H., Sierke, S.L. & Koland, J.G. Epidermal growth factor-dependent association of phosphatidylinositol 3-kinase with the erbB3 gene product. *J Biol Chem* **269**, 24747-24755 (1994).
60. Smirnova, T.*, et al.* Phosphoinositide 3-kinase signaling is critical for ErbB3-driven breast cancer cell motility and metastasis. *Oncogene* **31**, 706-715 (2012).
61. Ciardiello, F.*, et al.* Differential expression of epidermal growth factor-related proteins in human colorectal tumors. *Proc Natl Acad Sci U S A* **88**, 7792-7796 (1991).
62. Earp, H.S., Dawson, T.L., Li, X. & Yu, H. Heterodimerization and functional interaction between EGF receptor family members: a new signaling paradigm with implications for breast cancer research. *Breast Cancer Res Treat* **35**, 115-132 (1995).
63. Krahn, G.*, et al.* Coexpression patterns of EGFR, HER2, HER3 and HER4 in non-melanoma skin cancer. *Eur J Cancer* **37**, 251-259 (2001).
64. Memon, A.A.*, et al.* Expression of HER3, HER4 and their ligand heregulin-4 is associated with better survival in bladder cancer patients. *Br J Cancer* **91**, 2034-2041 (2004).
65. Lee, C.M.*, et al.* Correlation between human epidermal growth factor receptor family (EGFR, HER2, HER3, HER4), phosphorylated Akt (P-Akt), and clinical

outcomes after radiation therapy in carcinoma of the cervix. *Gynecol Oncol* **99**, 415-421 (2005).

66. Tanner, B.*, et al.* ErbB-3 predicts survival in ovarian cancer. *J Clin Oncol* **24**, 4317-4323 (2006).
67. Wei, Q.*, et al.* EGFR, HER2, and HER3 expression in laryngeal primary tumors and corresponding metastases. *Ann Surg Oncol* **15**, 1193-1201 (2008).
68. Wei, Q.*, et al.* EGFR, HER2 and HER3 expression in esophageal primary tumours and corresponding metastases. *Int J Oncol* **31**, 493-499 (2007).
69. Hayashi, M.*, et al.* High expression of HER3 is associated with a decreased survival in gastric cancer. *Clin Cancer Res* **14**, 7843-7849 (2008).
70. Sun, M.*, et al.* HER family receptor abnormalities in lung cancer brain metastases and corresponding primary tumors. *Clin Cancer Res* **15**, 4829-4837 (2009).
71. Ho-Pun-Cheung, A.*, et al.* EGFR and HER3 mRNA expression levels predict distant metastases in locally advanced rectal cancer. *Int J Cancer* **128**, 2938-2946 (2011).
72. Trocme, E.*, et al.* Nuclear HER3 is associated with favorable overall survival in uveal melanoma. *Int J Cancer* **130**, 1120-1127 (2012).
73. Takikita, M.*, et al.* Membranous expression of Her3 is associated with a decreased survival in head and neck squamous cell carcinoma. *J Transl Med* **9**, 126 (2011).
74. Begnami, M.D.*, et al.* Prognostic implications of altered human epidermal growth factor receptors (HERs) in gastric carcinomas: HER2 and HER3 are predictors of poor outcome. *J Clin Oncol* **29**, 3030-3036 (2011).
75. Hirakawa, T.*, et al.* HER3 overexpression as an independent indicator of poor prognosis for patients with curatively resected pancreatic cancer. *Oncology* **81**, 192-198 (2011).
76. Yoon, H.H.*, et al.* HER-2/neu gene amplification in relation to expression of HER2 and HER3 proteins in patients with esophageal adenocarcinoma. *Cancer* **120**, 415-424 (2014).
77. Ocana, A.*, et al.* HER3 overexpression and survival in solid tumors: a meta-analysis. *J Natl Cancer Inst* **105**, 266-273 (2013).
78. Park, Y.H.*, et al.* Role of HER3 expression and PTEN loss in patients with HER2-overexpressing metastatic breast cancer (MBC) who received taxane plus trastuzumab treatment. *Br J Cancer* **110**, 384-391 (2014).

79. Bae, S.Y.*, et al.* HER3 status by immunohistochemistry is correlated with poor prognosis in hormone receptor-negative breast cancer patients. *Breast Cancer Res Treat* **139**, 741-750 (2013).
80. Witton, C.J., Reeves, J.R., Going, J.J., Cooke, T.G. & Bartlett, J.M. Expression of the HER1-4 family of receptor tyrosine kinases in breast cancer. *J Pathol* **200**, 290-297 (2003).
81. Sassen, A.*, et al.* Cytogenetic analysis of HER1/EGFR, HER2, HER3 and HER4 in 278 breast cancer patients. *Breast Cancer Res* **10**, R2 (2008).
82. Barros, F.F.*, et al.* Characterisation of HER heterodimers in breast cancer using in situ proximity ligation assay. *Breast Cancer Res Treat* **144**, 273-285 (2014).
83. Chandarlapaty, S.*, et al.* AKT inhibition relieves feedback suppression of receptor tyrosine kinase expression and activity. *Cancer Cell* **19**, 58-71 (2011).
84. Chakrabarty, A., Sanchez, V., Kuba, M.G., Rinehart, C. & Arteaga, C.L. Feedback upregulation of HER3 (ErbB3) expression and activity attenuates antitumor effect of PI3K inhibitors. *Proc Natl Acad Sci U S A* **109**, 2718-2723 (2012).
85. Garrett, J.T.*, et al.* Transcriptional and posttranslational up-regulation of HER3 (ErbB3) compensates for inhibition of the HER2 tyrosine kinase. *Proc Natl Acad Sci U S A* **108**, 5021-5026 (2011).
86. Montero-Conde, C.*, et al.* Relief of feedback inhibition of HER3 transcription by RAF and MEK inhibitors attenuates their antitumor effects in BRAF-mutant thyroid carcinomas. *Cancer Discov* **3**, 520-533 (2013).
87. Fattore, L.*, et al.* Activation of an early feedback survival loop involving phospho-ErbB3 is a general response of melanoma cells to RAF/MEK inhibition and is abrogated by anti-ErbB3 antibodies. *J Transl Med* **11**, 180 (2013).
88. Abel, E.V.*, et al.* Melanoma adapts to RAF/MEK inhibitors through FOXD3-mediated upregulation of ERBB3. *J Clin Invest* **123**, 2155-2168 (2013).
89. Narayan, M.*, et al.* Trastuzumab-induced HER reprogramming in "resistant" breast carcinoma cells. *Cancer Res* **69**, 2191-2194 (2009).
90. Chakrabarty, A.*, et al.* Trastuzumab-resistant cells rely on a HER2-PI3K-FoxO-survivin axis and are sensitive to PI3K inhibitors. *Cancer Res* **73**, 1190-1200 (2013).
91. Huang, X.*, et al.* Heterotrimerization of the growth factor receptors erbB2, erbB3, and insulin-like growth factor-i receptor in breast cancer cells resistant to herceptin. *Cancer Res* **70**, 1204-1214 (2010).

92. Dai, R.*, et al.* Disturbance of Ca2+ homeostasis converts pro-Met into non-canonical tyrosine kinase p190MetNC in response to endoplasmic reticulum stress in MHCC97 cells. *J Biol Chem* **287**, 14586-14597 (2012).
93. Gherardi, E., Birchmeier, W., Birchmeier, C. & Vande Woude, G. Targeting MET in cancer: rationale and progress. *Nat Rev Cancer* **12**, 89-103 (2012).
94. Joffre, C.*, et al.* A direct role for Met endocytosis in tumorigenesis. *Nat Cell Biol* **13**, 827-837 (2011).
95. Gentile, A., Trusolino, L. & Comoglio, P.M. The Met tyrosine kinase receptor in development and cancer. *Cancer Metastasis Rev* **27**, 85-94 (2008).
96. Birchmeier, C. & Gherardi, E. Developmental roles of HGF/SF and its receptor, the c-Met tyrosine kinase. *Trends Cell Biol* **8**, 404-410 (1998).
97. Boccaccio, C. & Comoglio, P.M. Invasive growth: a MET-driven genetic programme for cancer and stem cells. *Nat Rev Cancer* **6**, 637-645 (2006).
98. Prat, A. & Perou, C.M. Mammary development meets cancer genomics. *Nat Med* **15**, 842-844 (2009).
99. Ho-Yen, C.M.*, et al.* C-Met in invasive breast cancer: is there a relationship with the basal-like subtype? *Cancer* **120**, 163-171 (2014).
100. Tuck, A.B., Park, M., Sterns, E.E., Boag, A. & Elliott, B.E. Coexpression of hepatocyte growth factor and receptor (Met) in human breast carcinoma. *Am J Pathol* **148**, 225-232 (1996).
101. Ivan, M., Bond, J.A., Prat, M., Comoglio, P.M. & Wynford-Thomas, D. Activated ras and ret oncogenes induce over-expression of c-met (hepatocyte growth factor receptor) in human thyroid epithelial cells. *Oncogene* **14**, 2417-2423 (1997).
102. Di Renzo, M.F.*, et al.* Somatic mutations of the MET oncogene are selected during metastatic spread of human HNSC carcinomas. *Oncogene* **19**, 1547-1555 (2000).
103. Minuti, G.*, et al.* Increased MET and HGF gene copy numbers are associated with trastuzumab failure in HER2-positive metastatic breast cancer. *Br J Cancer* **107**, 793-799 (2012).
104. Raghav, K.P.*, et al.* cMET and phospho-cMET protein levels in breast cancers and survival outcomes. *Clin Cancer Res* **18**, 2269-2277 (2012).
105. Peng, Z.*, et al.* Prognostic significance of MET amplification and expression in gastric cancer: a systematic review with meta-analysis. *PLoS One* **9**, e84502 (2014).

106. Yamashita, Y.*, et al.* Met is the most frequently amplified gene in endometriosis-associated ovarian clear cell adenocarcinoma and correlates with worsened prognosis. *PLoS One* **8**, e57724 (2013).
107. Gibney, G.T.*, et al.* c-Met is a prognostic marker and potential therapeutic target in clear cell renal cell carcinoma. *Ann Oncol* **24**, 343-349 (2013).
108. Miyamoto, M.*, et al.* Prognostic significance of overexpression of c-Met oncoprotein in cholangiocarcinoma. *Br J Cancer* **105**, 131-138 (2011).
109. Ponzo, M.G.*, et al.* Met induces mammary tumors with diverse histologies and is associated with poor outcome and human basal breast cancer. *Proc Natl Acad Sci U S A* **106**, 12903-12908 (2009).
110. Kong, D.S.*, et al.* Prognostic significance of c-Met expression in glioblastomas. *Cancer* **115**, 140-148 (2009).
111. Sawada, K.*, et al.* c-Met overexpression is a prognostic factor in ovarian cancer and an effective target for inhibition of peritoneal dissemination and invasion. *Cancer Res* **67**, 1670-1679 (2007).
112. Cheng, T.L.*, et al.* Overexpression of circulating c-met messenger RNA is significantly correlated with nodal stage and early recurrence in non-small cell lung cancer. *Chest* **128**, 1453-1460 (2005).
113. Cheng, H.L.*, et al.* Overexpression of c-met as a prognostic indicator for transitional cell carcinoma of the urinary bladder: a comparison with p53 nuclear accumulation. *J Clin Oncol* **20**, 1544-1550 (2002).
114. Engelman, J.A.*, et al.* MET amplification leads to gefitinib resistance in lung cancer by activating ERBB3 signaling. *Science* **316**, 1039-1043 (2007).
115. Liu, X.*, et al.* A novel kinase inhibitor, INCB28060, blocks c-MET-dependent signaling, neoplastic activities, and cross-talk with EGFR and HER-3. *Clin Cancer Res* **17**, 7127-7138 (2011).
116. Turke, A.B.*, et al.* Preexistence and clonal selection of MET amplification in EGFR mutant NSCLC. *Cancer Cell* **17**, 77-88 (2010).
117. Lin, S.Y.*, et al.* Nuclear localization of EGF receptor and its potential new role as a transcription factor. *Nature Cell Biology* **3**, 802-808 (2001).
118. Ni, C.Y., Murphy, M.P., Golde, T.E. & Carpenter, G. gamma-Secretase cleavage and nuclear localization of ErbB-4 receptor tyrosine kinase. *Science* **294**, 2179-2181 (2001).

119. Offterdinger, M., Schofer, C., Weipoltshammer, K. & Grunt, T.W. c-erbB-3: a nuclear protein in mammary epithelial cells. *Journal of Cell Biology* **157**, 929-939 (2002).
120. Wang, S.C.*, et al.* Binding at and transactivation of the COX-2 promoter by nuclear tyrosine kinase receptor ErbB-2. *Cancer Cell* **6**, 251-261 (2004).
121. Wang, S.C. & Hung, M.C. Nuclear translocation of the epidermal growth factor receptor family membrane tyrosine kinase receptors. *Clin Cancer Res* **15**, 6484-6489 (2009).
122. Marti, U.*, et al.* Localization of epidermal growth factor receptor in hepatocyte nuclei. *Hepatology* **13**, 15-20 (1991).
123. Lin, S.Y.*, et al.* Nuclear localization of EGF receptor and its potential new role as a transcription factor. *Nat Cell Biol* **3**, 802-808 (2001).
124. Wang, S.C.*, et al.* Binding at and transactivation of the COX-2 promoter by nuclear tyrosine kinase receptor ErbB-2. *Cancer Cell* **6**, 251-261 (2004).
125. Offterdinger, M., Schofer, C., Weipoltshammer, K. & Grunt, T.W. c-erbB-3: a nuclear protein in mammary epithelial cells. *J Cell Biol* **157**, 929-939 (2002).
126. Gupta, R.A. & Dubois, R.N. Colorectal cancer prevention and treatment by inhibition of cyclooxygenase-2. *Nat Rev Cancer* **1**, 11-21 (2001).
127. Naresh, A.*, et al.* The HER4/4ICD estrogen receptor coactivator and BH3-only protein is an effector of tamoxifen-induced apoptosis. *Cancer Res* **68**, 6387-6395 (2008).
128. Williams, C.C.*, et al.* The ERBB4/HER4 receptor tyrosine kinase regulates gene expression by functioning as a STAT5A nuclear chaperone. *J Cell Biol* **167**, 469-478 (2004).
129. Adilakshmi, T., Ness-Myers, J., Madrid-Aliste, C., Fiser, A. & Tapinos, N. A nuclear variant of ErbB3 receptor tyrosine kinase regulates ezrin distribution and Schwann cell myelination. *J Neurosci* **31**, 5106-5119 (2011).
130. Lee, H. & Maihle, N.J. Isolation and characterization of four alternate c-erbB3 transcripts expressed in ovarian carcinoma-derived cell lines and normal human tissues. *Oncogene* **16**, 3243-3252 (1998).
131. Srinivasan, R.*, et al.* Intracellular expression of the truncated extracellular domain of c-erbB-3/HER3. *Cell Signal* **13**, 321-330 (2001).
132. Andrique, L.*, et al.* ErbB3(80 kDa), a nuclear variant of the ErbB3 receptor, binds to the Cyclin D1 promoter to activate cell proliferation but is negatively controlled by p14ARF. *Cell Signal* **24**, 1074-1085 (2012).

133. Thor, A.D., Edgerton, S.M. & Jones, F.E. Subcellular localization of the HER4 intracellular domain, 4ICD, identifies distinct prognostic outcomes for breast cancer patients. *Am J Pathol* **175**, 1802-1809 (2009).
134. Nafi, S.N.M.*, et al.* Nuclear HER4 mediates acquired resistance to trastuzumab and is associated with poor outcome in HER2 positive breast cancer. *Oncotarget* **in press**(2014).
135. Lo, H.W.*, et al.* Novel prognostic value of nuclear epidermal growth factor receptor in breast cancer. *Cancer Res* **65**, 338-348 (2005).
136. Xia, W.*, et al.* Nuclear expression of epidermal growth factor receptor is a novel prognostic value in patients with ovarian cancer. *Mol Carcinog* **48**, 610-617 (2009).
137. Traynor, A.M.*, et al.* Nuclear EGFR protein expression predicts poor survival in early stage non-small cell lung cancer. *Lung Cancer* **81**, 138-141 (2013).
138. Schillaci, R.*, et al.* Clinical relevance of ErbB-2/HER2 nuclear expression in breast cancer. *BMC Cancer* **12**, 74 (2012).
139. Dillon, M.F.*, et al.* Cyclooxygenase-2 predicts adverse effects of tamoxifen: a possible mechanism of role for nuclear HER2 in breast cancer patients. *Endocr Relat Cancer* **15**, 745-753 (2008).
140. Koumakpayi, I.H.*, et al.* Expression and nuclear localization of ErbB3 in prostate cancer. *Clin Cancer Res* **12**, 2730-2737 (2006).
141. Cheng, C.J.*, et al.* Bone microenvironment and androgen status modulate subcellular localization of ErbB3 in prostate cancer cells. *Mol Cancer Res* **5**, 675-684 (2007).
142. Li, W., Park, J.W., Nuijens, A., Sliwkowski, M.X. & Keller, G.A. Heregulin is rapidly translocated to the nucleus and its transport is correlated with c-myc induction in breast cancer cells. *Oncogene* **12**, 2473-2477 (1996).
143. Raabe, T.D., Deadwyler, G., Varga, J.W. & Devries, G.H. Localization of neuregulin isoforms and erbB receptors in myelinating glial cells. *Glia* **45**, 197-207 (2004).
144. Menendez, J.A. & Lupu, R. Transphosphorylation of kinase-dead HER3 and breast cancer progression: a new standpoint or an old concept revisited? *Breast Cancer Res* **9**, 111 (2007).
145. Levallet, G.*, et al.* Plasma cell membrane localization of c-MET predicts longer survival in patients with malignant mesothelioma: a series of 157 cases from the MESOPATH Group. *J Thorac Oncol* **7**, 599-606 (2012).

146. Gomes, D.A.*, et al.* c-Met must translocate to the nucleus to initiate calcium signals. *J Biol Chem* **283**, 4344-4351 (2008).
147. Pozner-Moulis, S., Pappas, D.J. & Rimm, D.L. Met, the hepatocyte growth factor receptor, localizes to the nucleus in cells at low density. *Cancer Res* **66**, 7976-7982 (2006).
148. Brusevold, I.J., Soland, T.M., Khuu, C., Christoffersen, T. & Bryne, M. Nuclear and cytoplasmic expression of Met in oral squamous cell carcinoma and in an organotypic oral cancer model. *Eur J Oral Sci* **118**, 342-349 (2010).
149. Blobel, C.P. ADAMs: key components in EGFR signalling and development. *Nat Rev Mol Cell Biol* **6**, 32-43 (2005).
150. Gooz, M. ADAM-17: the enzyme that does it all. *Crit Rev Biochem Mol Biol* **45**, 146-169 (2010).
151. Edwards, D.R., Handsley, M.M. & Pennington, C.J. The ADAM metalloproteinases. *Mol Aspects Med* **29**, 258-289 (2008).
152. Arribas, J. & Esselens, C. ADAM17 as a therapeutic target in multiple diseases. *Curr Pharm Des* **15**, 2319-2335 (2009).
153. Elenius, K.*, et al.* A novel juxtamembrane domain isoform of HER4/ErbB4. Isoform-specific tissue distribution and differential processing in response to phorbol ester. *J Biol Chem* **272**, 26761-26768 (1997).
154. Schlessinger, J. & Lemmon, M.A. Nuclear signaling by receptor tyrosine kinases: the first robin of spring. *Cell* **127**, 45-48 (2006).
155. Zhou, B.B.*, et al.* Targeting ADAM-mediated ligand cleavage to inhibit HER3 and EGFR pathways in non-small cell lung cancer. *Cancer Cell* **10**, 39-50 (2006).
156. Newton, R.C.*, et al.* Clinical benefit of INCB7839, a potent and selective ADAM inhibitor, in combination with trastuzumab in patients with metastatic HER2+breast cancer. *Journal of Clinical Oncology* **28**(2010).
157. Zhou, S., Zhou, H., Walian, P.J. & Jap, B.K. CD147 is a regulatory subunit of the gamma-secretase complex in Alzheimer's disease amyloid beta-peptide production. *Proc Natl Acad Sci U S A* **102**, 7499-7504 (2005).
158. Zhang, Z.*, et al.* Presenilins are required for gamma-secretase cleavage of beta-APP and transmembrane cleavage of Notch-1. *Nat Cell Biol* **2**, 463-465 (2000).
159. Lammich, S.*, et al.* Presenilin-dependent intramembrane proteolysis of CD44 leads to the liberation of its intracellular domain and the secretion of an Abeta-like peptide. *J Biol Chem* **277**, 44754-44759 (2002).

160. Yu, G., *et al.* Nicastrin modulates presenilin-mediated notch/glp-1 signal transduction and betaAPP processing. *Nature* **407**, 48-54 (2000).
161. Struhl, G. & Adachi, A. Requirements for presenilin-dependent cleavage of notch and other transmembrane proteins. *Mol Cell* **6**, 625-636 (2000).
162. Vidal, G.A., Naresh, A., Marrero, L. & Jones, F.E. Presenilin-dependent gamma-secretase processing regulates multiple ERBB4/HER4 activities. *J Biol Chem* **280**, 19777-19783 (2005).
163. Steiner, H., *et al.* PEN-2 is an integral component of the gamma-secretase complex required for coordinated expression of presenilin and nicastrin. *J Biol Chem* **277**, 39062-39065 (2002).
164. Takasugi, N., *et al.* The role of presenilin cofactors in the gamma-secretase complex. *Nature* **422**, 438-441 (2003).
165. Francis, R., *et al.* aph-1 and pen-2 are required for Notch pathway signaling, gamma-secretase cleavage of betaAPP, and presenilin protein accumulation. *Dev Cell* **3**, 85-97 (2002).
166. Luo, W.J., *et al.* PEN-2 and APH-1 coordinately regulate proteolytic processing of presenilin 1. *J Biol Chem* **278**, 7850-7854 (2003).
167. Seo, S.J., *et al.* PEN-2 overexpression induces gamma-secretase protein and its activity with amyloid beta-42 production. *Neurochem Res* **32**, 1016-1023 (2007).
168. Sheng, Q., *et al.* An activated ErbB3/NRG1 autocrine loop supports in vivo proliferation in ovarian cancer cells. *Cancer Cell* **17**, 298-310 (2010).
169. Garner, A.P., *et al.* An antibody that locks HER3 in the inactive conformation inhibits tumor growth driven by HER2 or neuregulin. *Cancer Res* **73**, 6024-6035 (2013).
170. Schoeberl, B., *et al.* An ErbB3 antibody, MM-121, is active in cancers with ligand-dependent activation. *Cancer Res* **70**, 2485-2494 (2010).
171. Garrett, J.T., *et al.* Combination of antibody that inhibits ligand-independent HER3 dimerization and a p110alpha inhibitor potently blocks PI3K signaling and growth of HER2+ breast cancers. *Cancer Res* **73**, 6013-6023 (2013).
172. Blackburn, E., *et al.* A monoclonal antibody to the human HER3 receptor inhibits Neuregulin 1-beta binding and co-operates with Herceptin in inhibiting the growth of breast cancer derived cell lines. *Breast Cancer Res Treat* **134**, 53-59 (2012).
173. Garrett, J.T., Sutton, C.R., Kuba, M.G., Cook, R.S. & Arteaga, C.L. Dual blockade of HER2 in HER2-overexpressing tumor cells does not completely eliminate HER3 function. *Clin Cancer Res* **19**, 610-619 (2013).

174. Hickinson, D.M.*, et al.* AZD8931, an equipotent, reversible inhibitor of signaling by epidermal growth factor receptor, ERBB2 (HER2), and ERBB3: a unique agent for simultaneous ERBB receptor blockade in cancer. *Clin Cancer Res* **16**, 1159-1169 (2010).
175. LoRusso, P.*, et al.* Phase I study of U3-1287, a fully human anti-HER3 monoclonal antibody, in patients with advanced solid tumors. *Clin Cancer Res* **19**, 3078-3087 (2013).
176. Wakui, H.*, et al.* Phase 1 and dose-finding study of patritumab (U3-1287), a human monoclonal antibody targeting HER3, in Japanese patients with advanced solid tumors. *Cancer Chemother Pharmacol* **73**, 511-516 (2014).
177. Sharma, N. & Adjei, A.A. In the clinic: ongoing clinical trials evaluating c-MET-inhibiting drugs. *Ther Adv Med Oncol* **3**, S37-50 (2011).
178. Spigel, D.R.*, et al.* Treatment rationale study design for the MetLung trial: a randomized, double-blind phase III study of onartuzumab (MetMAb) in combination with erlotinib versus erlotinib alone in patients who have received standard chemotherapy for stage IIIB or IV MET-positive non-dmall-cell lung cancer. *Clinical Lung Cancer* **13**, 500-504 (2012).
179. Spigel, D.R.*, et al.* Randomized phase II trial of Onartuzumab in combination with erlotinib in patients with advanced non-small-cell lung cancer. *J Clin Oncol* **31**, 4105-4114 (2013).
180. Koeppen, H.*, et al.* Biomarker analyses from a placebo-controlled phase II study evaluating erlotinib+/-onartuzumab in advanced non-small cell lung cancer: MET expression levels are predictive of patient benefit. *Clin Cancer Res* **20**, 4488-4498 (2014).
181. Comoglio, P.M., Giordano, S. & Trusolino, L. Drug development of MET inhibitors: targeting oncogene addiction and expedience. *Nat Rev Drug Discov* **7**, 504-516 (2008).
182. Adjei, A.A., Schwartz, B. & Garmey, E. Early clinical development of ARQ 197, a selective, non-ATP-competitive inhibitor targeting MET tyrosine kinase for the treatment of advanced cancers. *Oncologist* **16**, 788-799 (2011).
183. Sequist, L.V.*, et al.* Randomized phase II study of erlotinib plus tivantinib versus erlotinib plus placebo in previously treated non-small-cell lung cancer. *J Clin Oncol* **29**, 3307-3315 (2011).

184. Santoro, A.*, et al.* Tivantinib for second-line treatment of advanced hepatocellular carcinoma: a randomised, placebo-controlled phase 2 study. *Lancet Oncol* **14**, 55-63 (2013).
185. O'Brien, N.A.*, et al.* Targeting PI3K/mTOR overcomes resistance to HER2-targeted therapy independent of feedback activation of AKT. *Clin Cancer Res* **20**, 3507-3520 (2014).
186. O'Brien, N.A.*, et al.* Activated phosphoinositide 3-kinase/AKT signaling confers resistance to trastuzumab but not lapatinib. *Mol Cancer Ther* **9**, 1489-1502 (2010).
187. Remmele, W. & Stegner, H.E. [Recommendation for uniform definition of an immunoreactive score (IRS) for immunohistochemical estrogen receptor detection (ER-ICA) in breast cancer tissue]. *Pathologe* **8**, 138-140 (1987).
188. Baulida, J., Kraus, M.H., Alimandi, M., Di Fiore, P.P. & Carpenter, G. All ErbB receptors other than the epidermal growth factor receptor are endocytosis impaired. *J Biol Chem* **271**, 5251-5257 (1996).
189. Joensuu, H.*, et al.* Adjuvant docetaxel or vinorelbine with or without trastuzumab for breast cancer. *N Engl J Med* **354**, 809-820 (2006).
190. Goss, P.E.*, et al.* Adjuvant lapatinib for women with early-stage HER2-positive breast cancer: a randomised, controlled, phase 3 trial. *Lancet Oncol* **14**, 88-96 (2013).
191. Piccart-Gebhart, M. First results from the phase III ALTTO trial (BIG 2-06; NCCTG [Alliance] N063D) comparing one year of anti-HER2 therapy with lapatinib alone (L), trastuzumab alone (T), their sequence (T→L), or their combination (T+L) in the adjuvant treatment of HER2-positive early breast cancer (EBC). *J Clin Oncol* **32**, LBA4 (2014).
192. Wilson, T.R.*, et al.* Widespread potential for growth-factor-driven resistance to anticancer kinase inhibitors. *Nature* **487**, 505-509 (2012).
193. Menard, L., Parker, P.J. & Kermorgant, S. Receptor tyrosine kinase c-Met controls the cytoskeleton from different endosomes via different pathways. *Nat Commun* **5**, 3907 (2014).
194. Fafalios, A.*, et al.* A hepatocyte growth factor receptor (Met)-insulin receptor hybrid governs hepatic glucose metabolism. *Nat Med* **17**, 1577-1584 (2011).
195. Jura, N., Shan, Y., Cao, X., Shaw, D.E. & Kuriyan, J. Structural analysis of the catalytically inactive kinase domain of the human EGF receptor 3. *Proc Natl Acad Sci U S A* **106**, 21608-21613 (2009).

196. Shi, F., Telesco, S.E., Liu, Y., Radhakrishnan, R. & Lemmon, M.A. ErbB3/HER3 intracellular domain is competent to bind ATP and catalyze autophosphorylation. *Proc Natl Acad Sci U S A* **107**, 7692-7697 (2010).
197. Rajkumar, T. & Gullick, W.J. A monoclonal antibody to the human c-erbB3 protein stimulates the anchorage-independent growth of breast cancer cell lines. *Br J Cancer* **70**, 459-465 (1994).
198. Gisterek, I.*, et al.* Prognostic role of c-met expression in breast cancer patients. *Rep Pract Oncol Radiother* **16**, 173-177 (2011).
199. Nakopoulou, L.*, et al.* c-met tyrosine kinase receptor expression is associated with abnormal beta-catenin expression and favourable prognostic factors in invasive breast carcinoma. *Histopathology* **36**, 313-325 (2000).
200. Waterhouse, B.R.*, et al.* Assessment of EGFR/HER2 dimerization by FRET-FLIM utilizing Alexa-conjugated secondary antibodies in relation to targeted therapies in cancers. *Oncotarget* **2**, 728-736 (2011).
201. Cardinale, D.*, et al.* Trastuzumab-induced cardiotoxicity: clinical and prognostic implications of troponin I evaluation. *J Clin Oncol* **28**, 3910-3916 (2010).
202. De Marzo, A.M., Fedor, H.H., Gage, W.R. & Rubin, M.A. Inadequate formalin fixation decreases reliability of p27 immunohistochemical staining: probing optimal fixation time using high-density tissue microarrays. *Hum Pathol* **33**, 756-760 (2002).

APPENDIX

List of Presentations

1. **Kenji Hashimoto**, Valentine Macaulay, Anthony Kong. *HER3 activation by MET contributes to trastuzumab resistance in HER2-positive breast cancer.* Poster presentation at the AACR annual meeting in April 2014, San Diego

2. **Kenji Hashimoto**, Ioannis Roxanis, Daniele Generali, Daniele Andreis, Carla Strina, Mariarosa Cappelletti**,** Valentine Macaulay, Anthony Kong. *Investigating the role of nuclear HER3 in relation to trastuzumab treatment and resistance in HER2-positive breast cancer.* Poster presentation at the San Antonio Breast Cancer Symposium in December 2013, San Antonio